SYNTHESIS AND OPTIMIZATION OF TIME MODULATED ANTENNA ARRAY

A Thesis

Submitted in Partial Fulfilment for the Award of Degree of

Doctor of Philosophy

By

RUCHI

(Registration Number: 951106005)

Under the Guidance of

Dr. BANANI BASU

Assistant Professor,
Department of ECE,
NIT Silchar,
Assam- 788010.

ELECTRONICS AND COMMUNICATION ENGINEERING DEPARTMENT
THAPAR UNIVERSITY
PATIALA 147004, INDIA

(March-2017)

Declaration

I, **Ruchi**, hereby declare that the thesis, entitled **"SYNTHESIS AND OPTIMIZATION OF TIME MODULATED ANTENNA ARRAY"**, submitted to the **Thapar University**, in partial fulfillment of the requirements for the award of the Degree of Doctor of Philosophy in Electronics and communication Engineering is a record of original and independent research work done by me during the period 2012-2017, under the supervision and guidance of **Dr. Banani Basu**. The work contained in this thesis has not been previously submitted to meet the requirements for a degree or diploma at this or any other higher education institution.

(Ruchi)

(Registration Number: 951106005)

Certificate

This is to certify that the thesis entitled "Synthesis and optimization of time modulated antenna arrays" submitted by Ms. Ruchi to Electronics and Communication Engineering Department, Thapar University, Patiala for the award of degree of Doctor of Philosophy is a report of original work carried out under my supervision and guidance. The matter presented in the thesis has not been presented for any other degree.

Banani Basu

Date:

Assistant Professor
Department of Electronics and Communication Engineering
National Institute of Technology, Silchar
Silchar, Assam, India

Assistant Professor
Dept. of Electronics & Commn. Engg.
National Institute of Technology Silchar
Cachar, Assam-788010

Acknowledgements

Above all, it is all the grace of god that I got opportunity to pursue the doctoral degree. It would not have been possible to write this doctoral thesis without the help and support of the kind people around me. I would like to acknowledge all the people associated directly and indirectly in completion of thesis work.

I would like to express my deepest respect and most sincere gratitude to my supervisor, **Dr**. **Banani Basu** for providing me an opportunity to work under her guidance. She has been an incredible mentor for me. Her dedication for research is always a leading source of energy for me. I am thankful for her constant encouragement, intellectual generosity and valuable contribution of her time throughout this research work. It has been a great honour and privilege to work under her inspiring guidance.

I greatly acknowledge Director, Thapar University, Patiala and Dr. O.P.Pandey, Dean (Research and sponsored projects), Thapar University, Patiala for giving necessary approvals and support to complete this research work.

I am thankful to Dr. Alpana Aggarwal, HOD, Electronics and Communication Engineering Department, Thapar University and Dr. Rajesh Khanna, Professor, Electronics and Communication Engineering Department, Thapar University, Patiala for motivation and inspiration that triggered me for the thesis work. I acknowledge my profound thanks to Dr. Arnab Nandi, Assistant Professor, Department of Electronics and Communication Engineering, NIT Silchar for his valuable suggestions and help in completion of my research work.

I would like to thank Doctoral Committee for their valuable suggestions and encouragement to carry thesis work in right directions. Their enlightening guidance has enabled me to think, explore and experience new ways to look at the work.

I would also like to thank all of my friends who supported me in writing, and incented me to strive towards my goal. I am thankful to Dr. Nitin Saluja, Assistant Director Research, Chitkara University for the fruitful research related discussions.

A special thanks to my family. I would like to thank my husband, Gurpreet Singh, my beloved daughter, Baani and son, Ishmeet, for all the sacrifices and great patience at all times. My mother-in law and father-in law have given me their unequivocal support throughout, as always, for which my mere expression of thanks likewise does not suffice. I also express my sincere gratitude to my parents, brothers and sisters for their ceaseless love and firm support.

(**Ruchi)**

Abstract

The thesis designed time modulated antenna arrays using optimization techniques. Conventional antenna arrays use complex feed network with expensive phase shifters to meet the demand of radiation pattern with specific requirements. Time modulation in antenna arrays produces asymmetric radiation pattern with low or ultra-low side lobe level without the use of phase shifters. Time modulated antenna arrays (TMAAs) provides an additional control parameter "time" to achieve the desired amplitude and phase excitation. TMAAs equipped with RF switches are turned on/off using predetermined switching sequences. The switching sequence of RF switches can easily and accurately be calculated and tuned to produce pattern with desired radiation characteristics. Due to ON/OFF switching harmonics or sidebands are generated in TMAAs causing power wastage.

The dissertation studied different optimization techniques to design time modulated antenna arrays. It discussed various radiation parameters followed by the mathematical analysis of the TMAA.

The thesis simulated TMAAs of half wave dipoles to obtain desired radiation performances. It designed TMAAs using artificial bee colony (ABC) and particle swarm optimization (PSO) and obtained broad side radiation pattern with fixed sidelobe level (SLL) and first null beam width (FNBW) constraining side band level (SBL). It simulated scanned beam pattern with fixed SLL and FNBW using progressive phase shift between array elements.

The dissertation designed a TMAA where each element of the array was controlled by radio frequency (RF) switches and excited with a common complex time exponential signal with unit amplitude at the switching frequency resulting in relative amplitude weight and phase difference between the elements at the central frequency without phase shifters. The design applied ABC to compute the switching intervals and produced cosecant squared and scanned beam patterns at the fundamental frequency with reduced side band radiations.

Owing to the beneficial properties of printed antennas, the thesis discussed TMAA designs consisted of printed dipoles for achieving patterns with different radiation characteristics. It simulated a printed dipole with microstrip balun in Computer simulation technology (CST).

After investigating the parametric optimization of ground plane of printed dipole, the thesis designed a single band TMAA and a dual band TMAA of two printed dipoles with different ground planes to demonstrate beam steering without using phase shifters. It designed single band and wide dual band printed power dividers to feed the TMAAs. The elements of TMAAs, coupled with PIN diode RF switches, used a common complex exponential excitation signal and modified the timing sequences of RF switches to create phase and amplitude variations. The timings of RF switches were controlled by a micro-controller based circuit. The phase difference among the antenna elements steered the beam in different directions. In dual band TMAA, SLL and SBL at both the resonating frequencies were reduced to increase the dynamic efficiency of the array using differential evolution (DE).

The thesis also designed an 8-element TMAA of printed dipoles to obtain a radiation pattern with a specified SLL and SBL for a fixed half power beam width (HPBW). The design used 1:8 printed power divider to feed the array. Enhanced charged system search (ECSS) optimization was used to compute the timing sequence of the array and desired radiation pattern was obtained with increase in directivity.

The optimization programs were written in matlab. The printed TMAA designs were simulated in CST and measured using network analyzer and spectrum analyzer and radiation pattern was characterized in anechoic chamber.

Table of Contents

List of Figures

List of Tables

Abbreviations

ABC	Artificial bee colony
CPLD	Complex programmable logic device
CST	Computer simulation technology
DE	Differential evolution
ECSS	Enhanced charge system search
EM	Electromagnetic
FNBW	First null beam width
GA	Genetic algorithm
HPBW	Half power beam width
MPA	Microstrip patch antenna
PSO	Particle swarm optimization
SLL	Sidelobe level
SBL	Sideband level
SBR	Sideband radiations
TMAA	Time modulated antenna array
TMLA	Time modulated linear array

Chapter1
Introduction

1.1 Overview

The rapid advancement in the field of mobile and wireless communication demands growth in many technical areas. In modern communication systems antennas are very important components. Antennas are the devices capable of transferring a signal to waves which propagate through space and can be received by another antenna. Conventional antenna element emits signal in every direction and suffers from low directivity. Antenna arrays are widely used in communication systems for producing electronically controlled highly directive radiation pattern. The antenna arrays are widely used for conventional beam scanning, beam steering, and adaptive beam forming applications by adapting the excitation amplitude and phase distribution. The limitations associated with the array antenna to produce radiation patterns with diverse stringent designing constraints are cost, size, power consumption and high complexity. Time modulation applied to linear antenna array is a technique to modify the excitations of the individual array element by periodically modulating the switching sequences of the RF switches coupled to each antenna. A variety of optimization techniques have been applied to synthesize desired radiation pattern using time modulated antenna arrays (TMAA). Printed antenna owing to variety of beneficial properties including light weight, low profile, and low cost has become explosively popular and widely investigated in recent articles. Design of various beam forming networks using printed dipoles are the current research interest for generating patterns with stringent radiation requirements.

1.2 Antenna Array

A single-element antenna has a broad radiation pattern with low directivity but to fulfill the demand of long distance communication antenna pattern must be highly directive. It can be accomplished by increasing the electrical size of the antenna. Forming an assembly of radiating elements in an electrical and geometrical configuration may increase the size of the antenna. Fields from multiple radiating elements add constructively or in phases in the desired direction and null in the remaining space. This gives directive patterns and the new antenna created by multi-elements is referred as an antenna array [1]. Antenna elements

have practical application when used singly but to fulfill some specific demands of radiation pattern, antenna arrays are widely used. The antenna array can be used to:

- boost the overall gain
- offer diversity reception
- cancel out interference from a specific set of directions
- "steer" the array so that it is most responsive in a particular direction
- find out the direction of arrival of the received signals
- to increase the Signal to Interference Plus Noise Ratio (SINR)

The importance and effectiveness of an antenna array lies in its capability to find out or modify the received or transmitted power as a function of the arrival angle. The shape of the radiation pattern of an array can be controlled by changing

- the relative physical positioning of the elements
- the relative electrical excitation amplitudes
- the relative electrical excitation phases

This provides us a freedom to select (or design) a certain desired array pattern from an array, without altering its physical dimensions. Different types of antenna array are:

- Conventional Antenna Array
- Switching Antenna Array
- Time Modulated Antenna Array

Conventional arrays use the large dynamic range ratio of their amplitude excitations for achieving certain patterns with some particular necessities, such as low side lobe level (SLL), high directive gain, null placement etc. The excitations are calculated using conventional techniques like Dolph-chebyshev and Taylor [2-3]. Higher insertion loss and quantization errors are the main limitations of the phase shifters used in phased arrays to manage phase excitations of each element. Non-Uniformly placed arrays show excellent performance with respect to gain and SLL, but contain many elements to achieve this. With larger aperture lengths the complexity of the feed networks rapidly grows.

Problem of large dynamic range ratio of amplitude excitations of conventional antennas is overcome by thinning of periodic arrays to achieve a desired amplitude density across the aperture. Antenna elements are excited through a set of radio frequency (RF) switches.

Thinning of array means switching off some elements to produce desired pattern which is much simpler than the conventional arrays and thereby reduces the complexity of the beam forming network. Pattern reconfiguration is achieved by just changing the on-off sequence of the RF switches.

Time Modulated Antenna Arrays consists of simple on-off switching of antenna elements in a preset sequence to produce radiation pattern with very low SLL. As compared to conventional antenna arrays, a fourth dimension "time" is introduced into the design of TMAA, and this time factor used for tapering the amplitude excitation distribution can be adjusted very easily and precisely. Although having more flexibility for the design, TMAAs produce undesired harmonics spaced at multiples of the time modulation frequency causing energy losses. In some applications side bands may not be desirable and needs to be suppressed to enhance array efficiency. However, sidebands are not always harmful to the TMAA. Harmonic patterns may be exploited to configure simple direction finding system with active null scanning capabilities. A simultaneous scan operation can be achieved where the beams at different sidebands are used to point at different directions. Such strategies allow generating and shaping of harmonic patterns and thereby utilizing the sideband radiations (SBR).

1.3 Printed Antennas

There has been huge advancement in the field of antenna after the invention of microwave components during the World War II which lead to the design of waveguide horn, slot, reflector, open ended waveguide and lens antenna [1]. However, those antennas were high profile, less reliable, costly, difficult to integrate with transmitter and receiver, large in size. The limitations were overcome with the introduction of planar antennas in 1960s. In 1969 Gallergo [4] proposed printed dipole antenna on high dielectric substrate. Microstrip antennas (MPA) got popular in the era of 1970-1980 and used for wide range of applications like satellite, mobile communication, aircraft antenna etc. MPAs dominate the conventional wire antennas due to various advantages like small size, conformal nature, ease of integration as well as fabrication [5]. However MPA suffers from the problem of less bandwidth and surface wave excitation [6]. Various method are discussed in literature to achieve the wideband with MPA by applying different techniques like slot cut in the patch[7-10], multilayer structure [11-12] , aperture coupled feed[13-15] , fractal shaped patch[16] , shaped and reduced ground plane [17-19]. In article [17] the V shaped ground

printed dipole antenna with microstrip balun is presented. Coupling between the dipole and balun is reduced to broaden the impedance bandwidth by extending the ground plane in V shape.

1.4 Objectives of Thesis

The main objective of the thesis is to synthesize antenna arrays using time modulation and different optimization techniques. It provides an overview of various optimization algorithms and time modulated antenna array. Dissertation presents TMAAs consisting of actual sources like wired and printed dipoles for different applications. The main objectives of the thesis are outlined as follows:

- Synthesis of TMAAs with improved performance by reducing the shift of the radiated power in the sidebands and enhancement of the directivity at the centre frequency.

16-element TMAAs of half wave dipoles are designed to generate broadside and scanned beam pattern. The timing sequences controlling the RF switches are optimized using PSO and ABC to reduce the SLL and SBL. Also an 8-element printed TMAA consisted of printed dipole array, power divider, PIN diode RF switches and CPLD is fabricated and tested. To get the desired radiation pattern ECSS optimization technique is used to get optimum timing sequences for RF switches.

- Synthesis of shaped or multiple beams in presence of interference signal

16-element TMAA of half wave dipoles is designed and simulated to generate cosecant squared beam pattern for radar application. Each element of the array is excited with the continuous complex exponential signal to achieve relative phase variation between the elements.

- Designing appropriate time sequences to synthesize sideband radiation for some specific applications like electronic beam steering, direction of arrival finding, null placement etc.

Two TMAAs of printed dipoles with V and U shapes grounds are fabricated for beam steering application. The timing sequence of the TMAA with U shaped ground is optimized using DE algorithm to increase the dynamic efficiency of the array. Beam steering is realized at both the central frequencies as well as at their sidebands in dual band TMAA.

1.5 Analysis Tools

Time modulated antenna arrays are designed and simulated using EM simulation software CST Microwave studio. The thesis also introduces the application of several optimization techniques like Particle swarm optimization (PSO), Artificial Bee Colony (ABC) algorithm, Differential Evolution (DE) and Enhanced charged system search (ECSS) optimization to synthesize the radiation characteristics of the designed TMAAs. The optimization program is written in MATLAB 7 and runs on a computer with windows operating system. The hardware of the fabricated TMAA is measured using network analyzer and spectrum analyzer in anechoic chamber.

1.6 Organization of Thesis

Based on the objectives defined above, the aim of the thesis is synthesis and optimization of TMAAs. TMAAs of different sizes are considered for synthesizing problems. Different Optimization techniques have been implemented to achieve the desired radiation pattern. TMAAs have been designed using various optimization techniques for different applications like sideband suppression, beam steering and beam shaping etc. The comparison between simulated and fabricated results is presented for different designs of TMAAs. The TMAAs consist of printed antennas are also covered in the thesis. The contents of each chapter are briefly described as under:

Chapter1

The **Chapter 1** provides a brief overview of the antenna, different antenna arrays and evolution of printed antennas. It comprises of the objectives of the thesis and analysis tools. Remainder of the discussion includes the organization of the thesis. This chapter is concluded with the publication details.

Chapter2

In **Chapter 2,** study of different optimization techniques have been included. Literature survey and algorithms of conventional optimization strategies like particle swarm optimization (PSO), differential evolution (DE), artificial bee colony (ABC) and Enhanced charged system search (ECSS) algorithms have been included in the chapter. All these algorithms will be applied to solve various electromagnetic examples considered in the dissertation.

Chapter3

Starting with the basic antenna parameters, the analysis of TMAA has been described in detail in chapter 3. It calculates the directivity, sideband power and dynamic efficiency of the TMAA. The literature survey covers TMAA of isotropic elements, wired antenna elements, printed antenna elements. It studies the effect of different dimensions on antennae design and motivates the study of different methods to enhance the bandwidth of printed antennas. It also includes the different optimization algorithms used for optimization of TMAAs for different applications like SLL reduction, sideband suppression, beam steering, beam shaping, direction finding etc. The literature survey of TMAA with different geometrical configurations and different time schemes has also been included.

Chapter 4

Chapter 4 includes the synthesis of TMAA for beam forming using optimization techniques. This chapter elaborates five designing examples to achieve the desired radiation characteristics. First example synthesizes broad side radiation pattern with fixed SLL and first null beam width (FNBW) while in the second one, by applying progressive phase shifts between array elements, the scanned beam pattern is generated with fixed SLL and FNBW using ABC optimization approach. A method based on the PSO algorithm is used to decrease the SBR losses while SLL is suppressed significantly at the centre frequency in a TMAA of wired dipole antennas. A common complex time exponential signal is utilized in the next examples to generate shaped and scanned beam patterns at central frequency without phase shifters. The designed cosecant squared pattern antenna finds application in Radars.

Chapter 5

Design and fabrication of TMAAs for achieving patterns with different radiation characteristics are presented in this chapter. TMAAs are designed and tested to demonstrate the beam steering without phase shifters. At first instance TMAA consisting of two printed dipoles with V shaped ground using quarter wavelength microstrip balun is designed at 2.45 GHz. Further the U-shaped ground structure is proposed to design TMAA with improved bandwidth characteristics at 2.45GHz and 5.8GHz. In all the fabricated TMAAs, each dipole is connected to the power divider and a RF switch. Three power dividers have also been designed and fabricated. A 1:2 power divider is designed for TMAA operating at 2.45GHz. A wide band power divider ranging from 2.1 GHz to 7GHz is designed to cover both the resonating frequencies of TMAA operated at 2.45 GHz and 5.8 GHz. For eight-

element TMAA 1:8 power divider is designed at 2.45 GHz operating frequency. The time sequences controlling the RF switches connected to the elements of TMAA with U-shaped ground are optimized using DE to increase the dynamic efficiency of the array. An eight element TMAA of printed dipoles with microstrip balun is designed and reported to get the radiation performance with desired SLL and HPBW using ECSS optimization. Comparison of measured and simulated results is presented here.

Chapter 6

A summary of the research works analysis to achieve all the objectives is presented in Chapter 6. The chapter discusses the contribution and limitations of the current work and suggests ideas and directions for future research.

1.7 Catalogue of Definitions

The definitions of phrases most frequently used in the literature are enlisted in this section. The phrases are used in order to characterize the radiation patterns using different antenna arrays.

Isotropic Antenna

An isotropic antenna is a hypothetical lossless antenna which radiates and receives equally well in all direction. However it is ideal and not physically realizable.

Antenna Array

Arrangement of multiple antennas in some geometrical configuration to obtain a given radiation pattern

Linear Array

A configuration of antenna elements placed along a straight line

Time Modulated Antenna Array

A configuration of antenna elements equipped with RF switches to time modulate the excitation distribution

Radiation Pattern

A graphical representation of distribution of antenna radiation in space

Half power beam width

Angle between two directions in which the radiation intensity is one half of the maximum value (or 3dB below the maximum on the decibel plot) of the beam

First null beam width

Angular width between the first nulls on either side of the main beam

Side lobe level

A radiation lobe in any direction other than the direction of intended radiation

Directivity

The ratio of the radiation intensity in a given direction from the antenna to the radiation intensity averaged over all the directions.

1.8 Published work

Work published during the duration of the doctoral program follows:

1.8.1 Journal Article

1. **Ruchi**, Arnab Nandi and Banani Basu, "Design Of Beam Forming Network For Time Modulated Linear Array With Artificial Bees Colony Algorithm", International Journal of Numerical Modelling: Electronic Networks, Devices and Fields, vol. 28, no.5, pp. 508-521, 2015.

2. **Ruchi Gahley**, Banani Basu, "A Time Modulated Printed Dipole Antenna Array for Beam Steering Application", International Journal of Antennas and Propagation, DOI: 10.1155/2017/3687293, 2017.

1.8.2 Conference Proceeding

1. **Ruchi**, Arnab Nandi and Banani Basu, "Synthesis Of Broadside And Scanned Beam Pattern With Time Modulated Antenna Array Using Artificial Bees Colony Algorithm", Microwave and RF Conference, 2013 IEEE MTT-S International, 14-16 December 2013, DOI: 10.1109/IMaRC.2013.6777745

Chapter2

Study of Optimization Algorithms

2.1 Introduction

Optimization process finds the optimum solution from a range of choices which fulfills the desired objective. Optimization techniques play a vital role in the field of engineering, operational research, information science, management and related areas. Optimization of complex real world problems is a challenging task owing to its stringent mathematical characteristics. As a result, extensive researches have been conducted over last few decades to develop optimization approaches for finding solution of the various engineering and real world problems.

The chapter provides overview of the various optimization algorithms that have been applied to electromagnetic problems considered in the dissertation.

2.2 Review of Optimization Techniques

Over the last few decades, the use of various optimization techniques is on rise to find the solution of different engineering problems with diverse constrains. A numerical optimization algorithm based on the annealing process of metallurgy is known as simulated annealing [20-24]. Simulated annealing is a metaheuristic approach that prevents converging in weak local minima. Annealing permits an uphill move and relaxes the greedy criterion. These moves potentially allow a parameter vector to reach out of a local minimum. These methods use the concept of improvement in overall exploration by learning from the single exploring experiences of a population of agents. Through this way Holland [25] pioneered a new idea on evolutionary search algorithm and gave a new solution to the nonlinear optimization problem. Encouraged by the natural adaptations of the biological species Holland reproduced the Darwinian theory of evolution in the most popular and well known algorithm known as Genetic Algorithm (GA). Realization of biological crossovers and mutations of chromosomes is used in the algorithm [26] is presented by Goldberg and Dejong to improve the quality of the solutions over iterations.

To solve the non linear optimization issues; Eberhart and Kennedy [27-30] proposed a novel optimization approach known as Particle Swarm Optimization (PSO) inspired by the cooperative conduct of mass of birds, seeds and boids method of Craig Reynolds and socio-cognition.

In literature [31] with some improvement in the conventional PSO a new algorithm known as multi-grouped particle swarm optimization (MGPSO) is proposed for solving optimization issues of multi-modal electromagnetic problems to achieve convergence more easily as compared to the conventional PSO. Whereas to increase the convergence rate and to prevent premature convergence [32] a mixed global optimization approach combining PSO with a modified Broyden-Fletcher-Goldfarb-Shanno (BFGS) method is presented for optimization of multimodal functions. In article [33] the authors proposed an orthogonal learning (OL) technique for PSO which finds much important information. This OL technique converges very fastly to global optima with higher solution quality, and more robustness. The general PSO algorithm is not so much suitable for optimization problems that are time sensitive and software-based applications like smart beam forming of thinned array antennas. So to overcome these problems a new algorithm based on the alterations in the velocity computation of PSO algorithm is proposed [34].

A novel two-subpopulation particle swarm organization (TSPSO) to get better performance in terms of the best possible solution within a realistic number of generations is presented in article [35]. The ratio of individual knowledge and group knowledge is different in every subpopulation swarm. If the proportion of individual knowledge is greater than the group knowledge, the particle swarm searches globally, whereas, if the proportion of group knowledge is greater than individual knowledge, the particle swarm searches the local area fully. In literature [36] robust particle swarm optimization (RPSO) is proposed and applied to mathematical function and a realistic electromagnetic problem.

Article [37] presented PSO based on Fission Bootstrap Particle Filter algorithm with the advantage that it avoids particle degradation caused by premature of the PSO. A new optimization algorithm called multi frequency vibration PSO [38] is presented for optimization of six standard trial functions and direct shape optimization of an airfoil in transonic flow. In literature [39] PSO with multiple adaptive methods (PSO-MAM) was proposed, which was verified to be successful for diverse functions with different properties. In a group of social animal, the older leader gives chance to the other members to become leader as the older member are no longer capable to handle leadership due to age. So in article [40] a new algorithm called Aging leader and challengers-PSO (ALC-PSO) is proposed which transplanted the aging mechanism to PSO .The algorithm is experimentally validated on 17 benchmark functions. In [41] global convergence Kalman PSO (GKPSO) algorithm is proposed and verified for various standard problems. This

proposed algorithm finds out the best possible point by the PSO algorithm and at each iteration kalman correction mechanism is applied to correct the optimum location till searched. To improve the performance of existing PSO technique a new PSO algorithm facilitated with some new parameters known as neighborhood re-dispatch (NR) technique is presented to design an ultra wideband antenna [42].

In article [43] particle swarm optimization-expectation maximization (PSO-EM) algorithm is proposed to solve the parameter estimation problem. The proposed algorithm is based on the normal compositional model (NCM). To prevent premature convergence and produce competitive solutions the authors in [44] proposed scatter learning PSO algorithm (SLPSOA) specially used for multi-modal issues. The effectiveness of the proposed algorithm is verified by testing this algorithm on a set of 16 benchmark functions. After comparing with the six different PSO algorithms, the SLPSOA is found more efficient. In [45] PSO is applied in space application and implemented to solve multiple dipole modeling (MDM) problems in spacecrafts.

During the same time, Price and Storn [46-47] proposed a new algorithm called differential evolution (DE) based on the differential operator which replaced the conventional crossover and mutation operators in GA. During the last few years, various differential evolution motivated strategies have been introduced to solve optimization problems. Using new base vector selection during the mutation process in conventional DE, a new algorithm named as multi-guiders non-dominated ranking differential evolution algorithm (MG-NRDE) is developed for multi objective electromagnetic optimization problems [48].

Article [49] presents a new improved self-adaptive multi-operators differential evolution SAMODE .This new DE algorithm makes use of mixing of various mutation operators and is able to converge faster to save the computational time. The proposed algorithm is verified by taking a variety of complex real world problems. For global optimization of electromagnetic devices the authors proposed another improved DE algorithm by implementing a new mutation criterion DE/λ-best/1 which increases the performance of global optimization [50]. A bi-objective approach based on the DE algorithm named as MOBiDE is used to solve various multi-modal optimization issues [51]. Literature [52] proposed a novel hybrid algorithm based on artificial bee colony (ABC) algorithm and differential evolution (DE) algorithm called ABC-DE for pattern synthesis in antennas. Also for the pattern optimization of the linear aperiodic arrays, a modified differential

evolution (DE) based on harmony search algorithm is proposed in [53]. Article [54] proposed ranking-based mutation operators for the DE algorithm. The algorithm is experimentally verified through the benchmark functions and five real-world problems. Literature [55] discussed a multi-population-based adaptive DE with Brownian and Quantum individuals (DDEBQ) to solve dynamic optimization problems. Article [56] shows the application of DE to resolve port selection problem in multi-beam antenna satellite communication system. In [57] authors proposed an adaptive parameter controlling non-dominated ranking differential evolution (A-NRDE) algorithm for multi-objective optimal design of electromagnetic problems while in [58] a newly dynamic Taylor Kriging (DTK) is developed and combined with a multi-objective DE algorithm to acquire a numerically competent multi-objective optimization approach. The success of the proposed DTK and multi-objective optimization approach is demonstrated through applications to analytic examples. DE and GA have been successfully implemented for the synthesis of linear arrays in articles [59-61]. Firefly Algorithm (FFA) optimization and collective Animal Behavior (CAB) are used in the synthesis of linear arrays to obtain hyper beam [62-63].

A preliminary study of ABC was intended to assess the performance of ABC on the commonly used set of numerical standard test functions and to compare it with that of other state-of-the-art evolutionary algorithms [64-65]. The ABC algorithm is so successful and encouraged researchers to expand the utility of the algorithm in other areas. For example, Akay et al. [66] used ABC to solve problems of integer programming while in [67] Ho et al. applied an ABC algorithm in an inverse electromagnetic problem. A novel approach based on ABC [68] is applied to solve a routing and wavelength assignment problem. Literature [69] studied the usage of ABC in electronic circuit design and tested its performance on the design of a complementary metal–oxide– semiconductor inverter considering transient performance. Akdagli et al. [70] obtained a novel expression for resonant length to compute the resonant frequency of C-shaped compact microstrip antennas using ABC. Furthermore, ABC is used to obtain simple formulas for calculating resonant frequencies of C and H-shaped compact microstrip antennas by Toktas et al. [71]. Rao and Pawar presented a new idea for edge enhancement using hybridized smoothening filters and introduced a promising technique of obtaining the best hybrid filter using ABC [72]. Taspinar et al. [73] proposed a partial transmit sequence (PTS) based on ABC to reduce the computational complexity of PTS in the multicarrier code division multiple

access systems. Article [74] discussed a method for the synthesis of a scanned and broadside linear array antenna based on ABC.

A meta-heuristic algorithm, named Enhanced charged system Search (ECSS) optimization algorithm, is proposed in 2010 by Kaveh and Talatahari [75]. ECSS algorithm is based on two principles: Coulombs law from physics and Newtonian law from mechanics. ECSS has been efficiently applied to find configurations of optimum design structures [76] with advantages that it neither needs the gradient information nor the continuity of the search space. Application of charged system search (CSS) method in many benchmarks and engineering functions are presented in [76]. ECSS differs from Charged System Search CSS on utilizing the continuous space- time search which increases the speed of convergence.

2.3 Particle Swarm Optimization

In PSO terminology, each member of the swarm is called "particle" or "agent" and the total number of the particles S composing the swarm is termed as "population size". It is observed from the experience that for most of the problems the sufficient size of population lies between 24 and 50. The act of particles is same as bees i.e. all the particles in the swarm move in search of best solution in D-dimensional search space. During the search process they update their velocities according to the already found their own best positions and that of their neighboring particles that are in search of better positions. In the D-dimension search space, every particle of population is taken as a point. The position of each particle is represented as $a_i = (a_{i1}, a_{i2}, \ldots, a_{iD})$ where $i = 1, \ldots, S$. The value of "cost function" f, a mathematical function related to the problem determines the performance of each particle, depends on the position coordinates $f = f(a_i) = f(a_{i1}, a_{i2}, \ldots, a_{iN})$. The minimization of value of cost function indicates improvement in the particle position. The determined best previous position (pbest position) is denoted by $p_i = (p_{i1}, p_{i2}, \ldots, p_{iN})$. The change of a_i is $\Delta a_i = v_i \Delta t$, where Δt is the time interval, $v_i = (v_{i1}, v_{i2}, \ldots, v_{iN})$ is the velocity of the *i-th* particle and v_{in} $(n = 1, \ldots, N)$ are the velocity coordinates. The new velocity is calculated as follows. Assuming $\Delta t = 1$, the position change becomes $\Delta a_i = v_i$. After a time step the new position of *i-th* particle is given by Eq. (2.1)

$$a_i(t+1) = a_i(t) + v_i(t+1) \tag{2.1}$$

$$If \quad a_i(t+1) > U_n \quad or \quad a_i(t+1) < L_n$$

$$then \quad a_i(t+1) = L_n + rand_i^t(U_n - L_n) \tag{2.2}$$

Un and Ln are the upper and lower boundary limitation for each solution a_i in their respective (*n-th*) dimension so that $L_n \leq a_{in} \leq U_n$ ($n = 1, \ldots, N$). The difference between upper and lower bounds known as "dynamic range" of the *n-th* dimension is denoted as $R_n = U_n - L_n$.

There are two types of neighborhoods studied in Particle swarms, namely "Gbest" and "Lbest". In the Gbest type of neighborhood, the best position searched by any particle is called "Gbest position" and each particle attracts towards this "Gbest position" represented as G= $(G_1, G_2, \ldots, G_N)$ and corresponds to the minimum value of cost function found by the swarm so far $f_{min} = f(G) = f(G_1, G_2, \ldots, G_N)$. Every particle does the comparison of performance with that of other particles of the population and tries to be very best. In the Lbest neighborhood, each (*i-th*) particle is attracted towards the best position searched by its J_i neighbors. This position is called as "Lbest position" represented as $L_i = (L_{i1}, L_{i2}, \ldots, L_{iN})$ and corresponds to the minimum value of cost function found so far by the J_i neighbors of the *i-th* particle $f_{min,i} = f(L_i) = f(L_{i1}, l_{i2}, \ldots, l_{iN})$.Converging on optimum solution is more rapid in case of Gbest neighborhood but it suffers from the convergence of local optima.

As discussed above, each particle in the swarm gets affected by its own conduct and by the acts of their neighbors.

As per the Gbest neighborhood model , the velocity of the *i-th* particle after a time step is given by

$$v_i(t+1) = \omega * v_i(t) + c_1 * rand(t) * \left(p_i(t) - a_i(t)\right) + c_2 * rand(t) * (G(t) - a_i(t)) \tag{2.3}$$

According to the Lbest model, the velocity of the *i-th* particle after a time step is given by

$$v_i(t+1) = \omega * v_i(t) + c_1 * rand(t) * \left(p_i(t) - a_i(t)\right) + c_2 * rand(t) * (L_i(t) - a_i(t)) \tag{2.4}$$

$$V_i(t+1) = Min(V_{\max}^d, \max(V_{\min}^d, V_i(t))) \tag{2.5}$$

Here ω is the called "inertia weight", c_1 and c_2 are positive acceleration coefficients called respectively "cognitive coefficient" and "social coefficient", and rand (t) generates random numbers between 0 and 1. The value of the inertia weight ω usually set between 0 and 1 controls the influence of previous velocity on the current velocity. The ω with bigger value enables global exploration whereas a smaller value of ω makes it for local exploration.

Thus the number of iterations to find the optimum depends on the right choice of ω. It is easy to understand that the changes in the velocity are stochastic and an unwanted consequence is that the particle's trajectory can spread out into wider and wider cycles through the problem space, finally approaching infinity. Eq. (2.5) has been introduced to clamp the velocity along each dimension to $(V_{\max}^{d}, V_{\min}^{d})$ if they attempt to cross the desired area of concern. These clipping techniques are sometimes required to prevent particles from explosion. The selection of a value for $V_{\max}^{d}$ depends on the problem. For example, the particle will be trapped if a step bigger than $V_{\max}^{d}$ is required to escape a local optimum. However, in approaching an optimum it is better to take smaller steps. In our problem the maximum velocity is set to half the upper limit of the dynamic range of the search ($V_{\max}^{d}$ = $0.5\, X_{\max}^{d}$) and the minimum velocity is set to $-0.5\, X_{\max}^{d}$.

Using the theory described above, the steps involved with standard PSO (Lbest model) are as follows.

Initialization

Step-1: Three counters are initialized. Counter t is initialized for time steps, counter D is initialized for dimensions, and counter i is initialized to count the particles.

Step-2: random numbers are set.

Step-3: values of D, S, J_i, ω, c_1,c_2, t_{max} (total number of iterations) and the values of L_n, U_n, $V_{max,,d}$ for $d = 1, \ldots, D$ are set.

Step-4: the particle positions a_i $(i = 1, \ldots, S)$ within the search space are randomly initialized, so that $L_n \leq a_{in} \leq U_n$ $(n = 1, \ldots, N)$.

Step-5: within the specified bound, the particle velocities v_i for $i = 1, \ldots, S$ are initialized.

Step-6: value of cost function $f(a_i)$ *for* $i = 1, \ldots, S$. is evaluated.

Step-7: Set $p_i = a_i$ and $f(p_i) = f(a_i)$ for $i = 1, \ldots, S$ (the first position of each particle is considered as pbest position).

Step-8: Find f_{min} among $f(p_i)$ $(i = 1, \ldots, S)$. The position that corresponds to f_{min} is the Gbest position, so that $f_{min} = f(G)$.

Optimization

Step-1: Find randomly J_i neighbors of each *i-th* particle.

Step-2: Find the particle that gives the minimum cost value $f_{min,i}$ among the J_i neighbors of each (*i-th*) particle. The position of this particle is the Lbest position L_i in the neighborhood of the *i-th* particle, so that $f_{min,i} = f(L_i)$.

Step-3: according to above expression, particle velocities v_i $(i = 1, \ldots, S)$ are updated.

Step-4: particle positions a_i $(i = 1, \ldots, S)$ are updated and are checked whether it is within the specified range or not.

Step-5: cost value $f(x_i)$ $(i = 1, \ldots, S)$ for all the particles is calculated.

Step-6: For each (*i-th*) particle, if $f(a_i) < f(p_i)$ $(i = 1, \ldots S)$ then $p_i = a_i$ (the new position becomes pbest position of the *i-th* particle).

Step-7: For each (*i-th*) particle, if $f(p_i) < f(g)$ $(i = 1, \ldots, S)$ then $G = p_i$ (the pbest position with the minimum cost value in the swarm becomes Gbest position).

Step-8: the counter t is incremented by 1.

Step-9: If $t < t_{max}$ and $f(G)$ was improved then go to Step-2. If $t < t_{max}$ and $f(G)$ was not improved then go to Step-1 of initialization part .

2.4 Differential Evolution

DE algorithm consists of following basic steps- Initialization, mutation, crossover, selection and termination.

1. **Initialization of Population**: DE searches for a global optimum within a continuous search space of dimension D. Generate K D–dimensional population of target vectors for each generation G.

$$\vec{A}_{i,G} = \left[a^1_{i,G}, a^2_{i,G}, a^3_{i,G}, \ldots\ldots, a^D_{i,G}\right] \qquad \text{Where } i=1,2,3,\ldots\ldots K \qquad (2.6)$$

Target vectors with better results may be found in a definite region of search space with maximum and minimum bounds in each dimension as

$$\vec{A}_{\max} = \left[a^1_{\max}, a^2_{\max}, \ldots\ldots, a^D_{\max}\right] \text{and } \vec{A}_{\min} = \left[a^1_{\min}, a^2_{\min}, \ldots\ldots, a^D_{\min}\right] \qquad (2.7)$$

The j^{th} component of the i^{th} vector is initialized as

$$a_{i,0}^{j} = a_{\min}^{j} + rand_{i}^{j}(0,1).(a_{\max}^{j} - a_{\min}^{j}), \qquad j \in \{1,2,3,.....D\} \tag{2.8}$$

Where $rand_{i}^{j}(0,1)$ is a uniformly distributed random number lying between 0 and 1.

2. **Mutation:** After initialization, s a donor vector $\vec{M}_{i,G}$ corresponding to best population member $\vec{A}_{best,G}$ in the current generation is created through mutation.

$$\vec{M}_{i,G} = \vec{A}_{best,G} + F \cdot \left(\vec{A}_{r_1^i,G} - \vec{A}_{r_2^i,G} \right) \tag{2.9}$$

The indices r_1^i and r_2^i are mutually exclusive integers randomly chosen from the range (1,2,…..K).. The F is called scaling factor which will be tuned by the value of fitness function generated by each vector. $\vec{A}_{best,G}$ is the best individual vector with minimum fitness value in the population at generation G.

3. **Crossover:** In crossover operation the donor vector mixes its components with the target vector $\vec{A}_{i,G}$ to obtain the trial vector of the same index denoted as $\vec{T}_{i,G} = \left[t_{i,G}^{1}, t_{i,G}^{2}, t_{i,G}^{3}, \ldots\ldots, t_{i,G}^{D}\right]$.The trial vector created is:

$$t_{i,G}^{j} = \begin{cases} m_{i,G}^{j} & if\ (rand_{i}^{j}(0,1) \le CR\ or\ j = j_{rand}) \\ a_{i,G}^{j} & otherwise \end{cases} \tag{2.10}$$

where *CR* is the crossover rate in the range (0,1) and $j_{rand} \in [1,2,\ldots\ldots,D]$ is a randomly chosen index which differentiate trial vector $\vec{T}_{i,G}$ from its corresponding target vector $\vec{A}_{i,G}$.

4. **Selection:** Selection is introduced to find out which of the target or trial vectors survives to the next generation. If the fitness value of the trial vector is equal to or less than that of the corresponding target vector then the trial vector is selected for next generation otherwise the target vector is selected for next generation.

5. **Termination:** If termination condition is not satisfied go to mutation Step, otherwise terminate.

2.5 Artificial Bee Colony Optimization

Karaboga et al. developed ABC to be a stochastic class of optimization algorithm that is successfully used to resolve various real-world problems.

ABC is basically aimed at producing computational intelligence by exploiting the natural behavior of real honey bees in food foraging.

Following are the control parameters in the ABC:

1. Number of food sources which is equal to the number of employed or onlooker bees (SN)
2. Limit. Limit is a predetermined number of cycles. If a position cannot be improved further, the food source is assumed to be abandoned.
3. Maximum cycle number (MCN)

STEP1. Initialize SN number of possible solutions randomly, where each solution is a D (dimensions of optimization parameters) dimensional vector

$$x_i^j = x_{\min}^j + rand(0,1)(x_{\max}^j - x_{\min}^j) \tag{2.11}$$

Where $x_{\min}^j$ and $x_{\max}^j$ are the lower and upper bound of the parameter j.

STEP2. Evaluate the population.

Probability value p_i associated with the source is calculated using the expression

$$p_i = \frac{fit_i}{\sum_{n=1}^{SN} fit_n} \tag{2.12}$$

Fit is the fitness value associated with every solution, which is determined using

$$fit = \begin{cases} \dfrac{1}{1+J_i} & J_i \geq 0 \\ 1+abs(J_i) & J_i < 0 \end{cases} \tag{2.13}$$

Where J_i is the cost value of the corresponding cost function. The solution with minimum cost has greater probability value.

STEP3. Produce new solutions in the neighborhood of the older one using

$$v_{ij} = x_{ij} + \varphi_{ij}(x_{ij} - x_{kj}) \tag{2.14}$$

Where $k \{1, 2,..., SN\}$, $j \{1, 2,...,D\}$ and $k \neq i$, φ_{ij} is a random number between -1 to 1.

STEP4. Compute the fitness values related with that solution.

STEP5. Apply the greedy selection process between old and candidate one.

STEP6. Find out the abandoned solution for the scout and replace it with a new randomly produced solution using the same

$$x_i^j = x_{\min}^j + rand(0,1)(x_{\max}^j - x_{\min}^j) \quad (2.15)$$

Where $x_{\min}^j$ and $x_{\max}^j$ are the lower and upper bound of the parameter j.

STEP7. Memorize the best solution obtained so far.

STEP8. Repeat the process until cycle=MCN

2.6 Enhanced Charged System Search Algorithm

In ECSS terminology every agent is called a Charge Particle (CP). The amount of charge on each CP depends on its fitness value. The effect of electric field of CPs on other CPs is based on their fitness value and their separation. The amount of resultant force on each CP is determined by coulombs law while the quality of movement of each CP due to applied force is determined by Newtonian law. A storage device called as charged memory (CM) is used to save the best CP vectors with their related fitness values. Following the continuous space-time search, the new positions of each CP are used to find the movement of other CPs before an iteration is completed.

In ECSS each solution candidate containing a number of decision variables $\vec{C}_i = \{c_{i,j}\}$is considered as a CP. The main steps of the algorithm are:

Level1. **Initialization**

(a) Initialize the array of the N number of CPs with random positions and their associative velocities. The magnitude of charge on *i-th* CP depends on its fitness value and described in Eq. (2.16)

$$q_i = \frac{fit_i - fit_{worst}}{fit_{best} - fit_{worst}} \quad \text{for } i = 1,2,\ldots\ldots N \quad (2.16)$$

fit_i is fitness value of the *i-th* CP ; fit_{best} and fit_{worst} are the best and worst fitness values found so far for all the CPs. The separation distance between the two CPs is-

$$d_{ij} = \frac{\left\| \overrightarrow{C_i} - \overrightarrow{C_j} \right\|}{\left\| (\overrightarrow{C_i} + \vec{C}_j)/2 - \vec{C}_{best} \right\| + \xi} \tag{2.17}$$

$\overrightarrow{C_i}$ and $\overrightarrow{C_j}$ are positions of *i-th* and *j-th* CP respectively ; $\vec{C}_{best}$ is Position of the best CP found so far ; ξ is small positive number to avoid singularities.

(b) The initial positions of CPs are determined randomly in the search space as

$$c_{i,j}^{(0)} = c_{i,\min} + rand.(c_{i,\max} - c_{i,\min}) \quad \text{for i=1,2,……..n} \tag{2.18}$$

$c_{i,j}^{(0)}$ determines initial value of the i-th variable for the j-th CP ; $c_{i,min}$ *and* $c_{i,max}$ are the minimum and maximum allowable values for the i-th variable; n is the number of variables.

(c) Initial velocity of CPs are $v_{i,j}^{(0)} = 0 \quad \forall \quad i, j = 1,2,..n$

(d) Generate the CM to save the CPs with best Fitness.

Level 2. **Search**

(a) Each CP acts as a source of the field. A CP can attract another CP if its fitness value is better than the other CP. The probability of moving each CP towards the other CP is

$$p_{ij} = \begin{cases} 1 & \dfrac{fit_i - fit_{best}}{fit_j - fit_i} > rand \quad or \quad fit_j > fit_i \\ 0 & else \end{cases} \tag{2.19}$$

Considering each CP as a charged sphere of radius ‘a’ having uniform volume charge density the resultant force acting on a CP is calculated using coulombs law as

$$\overrightarrow{F_j} = q_j \sum_{i,i\neq j} \left(\frac{q_i}{a^3} d_{ij} . i_1 + \frac{q_i}{d_{ij}^2} . i_2 \right) \times p_{ij} (\overrightarrow{C_i} - \overrightarrow{C_j}) \quad \left| \begin{array}{c} j = 1,2,....., N \\ i = 1, i_2 = 0 \Leftrightarrow d_{ij} < a \\ i = 0, i_2 = 1 \Leftrightarrow d_{ij} \geq a \end{array} \right. \tag{2.20}$$

New position and new velocity of each CP is determined using Newtonian law utilizing recent location of the previous CPs as-

$$\vec{C}_{j,new} = rand_{j1} . k_a . \frac{\overrightarrow{F_j}}{m_j} . \Delta t^2 + rand_{j2} . k_v . \vec{V}_{j,recent} . \Delta t + \vec{C}_{j,recent} \tag{2.21}$$

$$\vec{V}_{j,new} = \frac{\vec{C}_{j,new} - \vec{C}_{j,recent}}{\Delta t} \tag{2.22}$$

$rand_{j1}$ and $rand_{j,2}$ are two random numbers uniformly distributed in the range (0,1) ;m_j is mass of the j-th CP and equals to q_j; Δt is time step; k_a and k_v are acceleration coefficient and velocity coefficient to control the influence of recent velocity defined as- $k_a=0.5(1+iter/iter(max))$; $k_v=0.5(1-iter/ iter(max))$ where iter and iter(max) are the actual and maximum number of iterations.

The new fitness value is calculated using new position and velocity of each CP.

Level3.**Source Updating**

CM is updated by including better CP vectors and excluding the worst CP vectors.

Level4.**Terminating Criterion Control**

Steps in level 2 and level 3 are repeated until a terminating criterion is satisfied.

2.7 Conclusion

The conventional optimization strategies like particle swarm optimization (PSO), differential evolution (DE), artificial bee colony (ABC) and Enhanced charged system search (ECSS) are described in this chapter. All these algorithms will be applied to solve various electromagnetic examples considered in the thesis.

Chapter-3

Study of Time Modulated Antenna Arrays

3.1 Introduction

Modern wireless communication systems demand antenna array with improved radiation characteristics. It is a challenging task to calculate the large dynamic ranges of amplitude excitations and the phase differences between each element of array to meet the radiation requirement. By applying a suitable optimization algorithm the amplitude and phase excitations for achieving a particular radiation pattern of predefined specifications can be achieved. In conventional arrays a complicated electronic circuit is required to achieve the amplitude excitations of large dynamic range ratio and these excitations are influenced by systematic and random errors. Moreover the phase shifters used in the conventional arrays have the limitations of cost, size, power consumption and high complexity. Thus hardware of the conventional arrays is costly and complex to implement the amplitude excitations distribution in practice. To overcome the problem of hardware complexity of conventional arrays the concept of time modulation in antenna array is introduced to produce pattern with low or ultra low side lobe level.

This chapter presents the overview of the various researches done in the field of TMAA followed by the mathematical analysis of the TMAA in detail.

3.2 Review of Time Modulated Antenna Arrays

A lot of work is presented by the various authors for synthesizing the time modulated antenna arrays. In this context many optimization techniques are also adopted by the various researchers

Shanks and bickmore in late 1950s proposed the concept of time modulation in antenna array to produce pattern with low or ultra low side lobe level [77]. Kummer et al. applied time modulation concept in antenna arrays and realized a radiation pattern with ultralow SLL in an 8-element linear array of slotted waveguides [78]. In article [79] the sideband level in 32-element TMAA is appreciably reduced by computing amplitude excitations and the switching time sequence of individual array element using DE. The achieved SLL is ≤ -50 dB at centre frequency, and the maximum SBL is approximately -32 dB.

Yang et al. implemented the time modulation concept in planar antenna arrays in square and circular geometrical configuration to obtain radiation pattern with extremely low SLL

[80]. The article applies combination of Tseng-Cheng approach and discrete Taylor distribution in TMAA for obtaining low SLL radiation pattern with reduction in SBR while reducing the dynamic range ratio with DE algorithm. Yang in the same year [81] presented a strategy for synthesizing the radiation performance of linear antenna arrays with two types of bi-directional phase centre motion (BPCM). In 2007, Tenant et al. [82] presented the direction finding application of TMAA. In this work the time modulation technique is applied to the signal received by the each element of the array to obtain a phase modulated output signal. The modulation index of the output signal is dependent on the angle of received signal direction. The angular response at the first sideband of the switching frequency exhibits a null at broadside and the beam is scanned in different angle. Therefore electronic null steering is obtained without the use of phase shifters.

In 2008 Yang presented another time scheme Variable aperture Size (VAS) time scheme [83] to simulate TM printed dipole linear arrays at central frequency and sideband frequency. Some of the applications require suppression of sideband radiations to increase the effectiveness of the antenna array. Power wasted due to SBR is examined carefully in article [84]. A dynamic efficiency coefficient is also proposed in this work which can be used as an optimization function for the optimization of TMAA. Yang proposed Finite Difference Time domain (FDTD) method of simulation of TMAAs and analyzed TMAAs using this method with two switching schemes namely, the variable aperture sizes (VAS) and C-scheme BPCM [85].

TMLAs with VAS timing scheme are applied into airborne pulse Doppler (PD) radar to reduce average power losses using DE. The observations show that unlike the conventional arrays the waveform of the transmitted and received signal by proposed TMLA is no longer a rectangular pulse train. Also the average transmitted power loss is less than 3 dB at SLL equals to-40 dB [86].

In the same year Li et al. proposed an electronic beam steering technique without using phase shifters based on BPSK modulated signals arriving from different directions [87]. DE algorithm has been used to boost up the gain and reduce the SLLs at both the centre frequency and the first harmonic simultaneously. The author proposed another additional control “switch –on instants” in synthesis of the time-modulated linear arrays [88]. Shaped beam patterns are desired in many applications like in radars and wireless communications. Li and Yang presented flat-top beam and cosecant-squared beam patterns in TMAA with

semicircular boundary using DE [89]. In the same year the author [90] used PSO to minimize the power losses associated to the SBR while synthesizing a fixed SLL pattern at the carrier frequency. Basu and Mahanti proposed a TMLA for beam reconfiguration with modified PSO to generate two different beam pairs, one pencil-pencil beam pair and another pencil-flat-top beam pair in the horizontal plane having a prefixed SLL [91]. For achieving a comparative evaluation various metaheuristic approaches like DE, gravitational search algorithm (GSA) and ABC are also employed.

The various optimization algorithms presented above by various authors are applied for the single objective. In article [92] the author proposes a new optimization strategy named as Multi-Objective (MO) MOEA/D-DE (Decomposition based MOEA with Differential Evolution operator) for designing TMLAs with ultra low maximum SLL, maximum SBL and FNBW. It is concluded that MO approach is more flexible as compared to single-objective techniques. Another multi-objective problem is presented in [93] where optimization used is adaptive that is to manage beam steering as well as SLL at the first sideband. For multi-objective designing problem Basu and Mahanti proposed two optimization techniques, namely Fire fly algorithm (FFA) and ABC for broad side arrays and steerable linear arrays. The work was aimed to achieve radiation pattern with minimum SLL for particular HPBW and FNBW [94]. Proposed optimization technique is applied to six sets of antenna configurations to verify the usefulness of the proposed algorithms in the field of antenna and it is seen that the angular widths of the main beams are inversely related to the length of the array and for a given length array, HPBW and FNBW both increase as the SLL decreases. So there is always a tradeoff between these conflicting design specifications. It is also seen that the performance of FFA is better than ABC in terms of convergence and cost minimization.

In 2011 a lot of work is done to minimize sideband radiations. Dependency of SBR on the shifting of time pulses is fully exploited using PSO [95]. Both SLL reduction and SR minimization issues have been addressed. It is concluded that the pulse-shift methodology works effectively. In [96] sidebands levels and power losses in harmonics is reduced by tapering the array using power divider and the development of efficient TMAAs demands appropriate power dividers [97-98].

However, sidebands are not always harmful to the TMAA. Harmonic patterns may be utilized to construct a direction finding system. In [99] multi beams are achieved by means

of harmonics using PSO and synthesis of broadside sum and difference patterns, flat-top and narrow beam patterns, and steered multi-beams have been done. The multiple beams can be used in multiband applications to handle different communications from different directions. The designed shaped patterns can be used in adaptive systems to sustain trustworthy wireless links in the presence of jammers or interference signals or to properly tackle different needs of service. The total power radiated in sidebands is examined in literature [100] and it is observed that the total sideband power depends on pulse durations and pulse positions.

Another practical approach of reducing SLL and SBR in TMLA is proposed in [101]. In the proposed technique the time modulation period is divided into many time steps with uneven lengths. DE algorithm is applied to compute the switch-on/off times of each time steps of 16 elements linear array of printed dipoles to achieve the designing goals. Each element is coupled to a high speed single pole single throw (SPST) RF switch and the switches are controlled by CPLD. But the TMLA based on SPST usually have lesser gain due to SBR and power absorption of the off-state SPST switches. So to improve the gain with stable directivity ZHU et. Al presented a novel topology of TMLA using single pole double throw (SPDT) switches [102] and it is observed that, the proposed TMLA has improved gain and a more stable instantaneous directivity with fewer switches. In article [103] author presented RF characterization of Microwave devices

The radiation performance of TMLA has been reconfigured by changing the pulse timing sequence of RF switches used to modify the static excitations of the element of arrays [104]. A two-channel 16-element TMLA configured for use in an adaptive beam forming system is presented by Tong and Tennant [105]. Adaptive beam forming is achieved by TMLA consisting of switching network of multi-throw switches to provide several independent array output channels. In another work Tong and Tennant proposed another technique to suppress the sidebands without using any optimization algorithm. The technique uses fixed bandwidth of the array elements as band pass filters to minimize the out-of-band sidebands [106].

Sometimes the received signal cannot be retrieved so correctly due to the variation in the gain of antenna. The desired radiation pattern is obtained at impinging signal frequency by optimizing the switching sequence used to obtain the main beam with stable instantaneous directivity [107]. The proposed work overcomes the problem of spreading desired signal

power into the sidebands generated as a consequence of time modulation. In literature [108] Contiguous partition method (CPM) is used to optimize the mono pulse antennas used in TMLA to generate the patterns required to approximate the target position and movement. Independent sets of static excitations have been applied to produce the sum beam. Array elements are grouped into sub-arrays that are time modulated using RF switches to get the difference beams have.

A new DE optimization algorithm, sub populated differential evolution (sub DE), is used with time modulation technique in circular antenna array for null synthesis. This new approach is compared with DE on embedded microprocessor in terms of power, time consumption and memory requirement. It is observed that sub DE can converge to better solutions more speedily than conventional DE and also it can capably work on a Raspberry Pi (RP) embedded system having restricted resources [109].

Further for synthesis of TMAA Yang et al. proposed a new hybrid optimization algorithm ABC-DE. This novel ABC-DE algorithm overcomes the limitation of easily falling into the local most favorable solution and possesses a better convergence rate. The author verified the effectiveness of the proposed ABC-DE optimization algorithm by designing TMAs with different arrays structures to realize low equal-ripple SLL pattern, deep null level pattern, multiple-beams patterns and satellite footprint pattern [110].

DIRECTION finding systems are widely used in wireless communication, sensor network and military applications. The authors proposed a simple and low cost S-band direction finding TMAA using discrete fourier transform technique [111]. It has been proven [112-113] that at the central frequency, the power content of the beam obtained in a TMAA does not depend upon the shapes of the pulses; rather it is related to the area of the timing pulses [84]. So pulse shaping has been used as an additional degree of choice in TMAAs design. Trapezoidal and time-domain raised cosine (TDRC) pulses shapes of the modulating waveform have been used to check the radiation performance of the TMAA. The pulse shaping technique makes the use of TMAAs in various applications within communications and radar [114].

Masotti *et al.* presented a technique to simulate electromagnetic problems using full-wave description of the linear radiating sub-network, on the circuit-level description of the nonlinearities, and of their combination [115]. A lot of new pioneering work in the field of TMAA is done by the various authors in the year 2014. In [116] the TMAA is used to

implement sidelobe blanking (SLB). Typical SLB techniques use two beams but this technique permits SLB uses a single beam former which is simpler, less complex and less costly than conventional methods. Authors presented and simulated an optimized TMAA of 32 elements to verify the proposed technique.

EUZIÈRE *et al.* presented the use of sparse time-modulated arrays (STMAs) in radar applications in article [117]. STMA is proposed using improved version of Schelkunoff Multi Diagrams (SMD) and Genetic Algorithm (GA) optimization. SMD does not depend on a switching method, but on a continuous weighting of the array elements and permits modification of the coefficients along the length of array. Many examples are presented by the authors which shows the application of STMA in radars to achieve low SLL, constant main lobe or interference rejection with a 1-bit coding of the element weighting coefficients.

The total power radiated in harmonics in TMAAs and time-modulated volumetric arrays was studied in [118-119]. A closed form equation is presented and the total SBR formulation is extended to conformal arrays. An example of tetrahedron array is presented to verify the proposed equation. A general representation is also presented to calculate sideband power.

In article [118] an inequality is derived based on DE to suppress all SBLs at the same time to a SBL bound while a failure correction approach is presented in [119] for retaining the original pattern features at the time of failure at the array elements characterized by short on-times. TMAAs for beam forming, null synthesis, direction finding are presented in articles [120-125] TMAA also finds application in cognitive radio [121] and for secure communication [125].

3.3 Antenna Theory

Half -wavelength dipole antenna is the most widely used antenna owing to its simplicity, high gain and reasonable length [1]. A dipole antenna consists of a conductive wire rod split in the middle, and the two sections are separated by an insulator. RF signal is applied to dipole at the center, between the two conductors to obtain a sinusoidal current distribution with its maxima at the middle. A simple half-wavelength wired dipole fed at the center is shown with its current distribution in figure 3.1.

The fields from the half-wave dipole antenna are given by [1]:

$$E_\theta = \frac{j\eta I_0 e^{-jkr}\cos(\frac{\pi\cos\theta}{2})}{2\pi r\sin\theta} \tag{3.1}$$

Where η is the intrinsic impedance of the medium, $k = 2\pi/\lambda$ is wave number where λ is the wavelength.

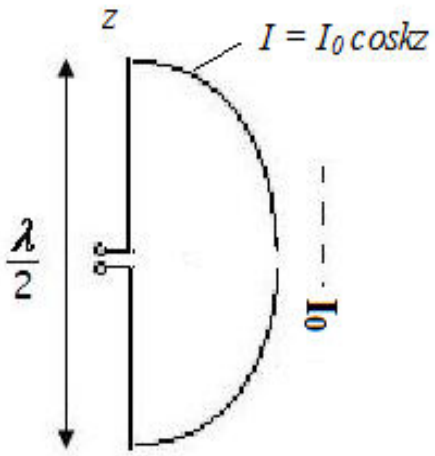

Figure 3.1 Half –wavelength dipole with current distribution

The average power density of the half-wave dipole is given by:

$$W_{av} = \eta\frac{|I_0|^2}{8\pi^2 r^2}\sin^3\theta \tag{3.2}$$

The radiation intensity of half-wave dipole is given as:

$$U = r^2 W_{av} = \eta\frac{|I_0|^2}{8\pi^2}\sin^3\theta \tag{3.3}$$

Total power radiated by the dipole is given as:

$$P_{rad} = \eta\frac{|I_0|^2}{4\pi}\int_0^\pi \frac{\cos^2(\frac{\pi}{2})}{\sin\theta}d\theta \tag{3.4}$$

The maximum directivity of half wave dipole is:

$$D_0 = 4\pi\frac{U_{\max}}{P_{rad}} = 4\pi\frac{U|_{\theta=\pi/2}}{P_{rad}} \approx 1.643 \tag{3.5}$$

The radiation pattern of half-wave dipole with unity excitation is shown in figure.3.2. As shown in figure 3.2 the radiation pattern of a single element is relatively wide with low value of directivity. Antenna elements have practical application when used singly but they are widely used as array to fulfill some specific demands of radiation pattern. The relative physical positioning of the elements and their relative electrical excitations are two parameters that can be used to exercise control over the shape of the radiation pattern of an array.

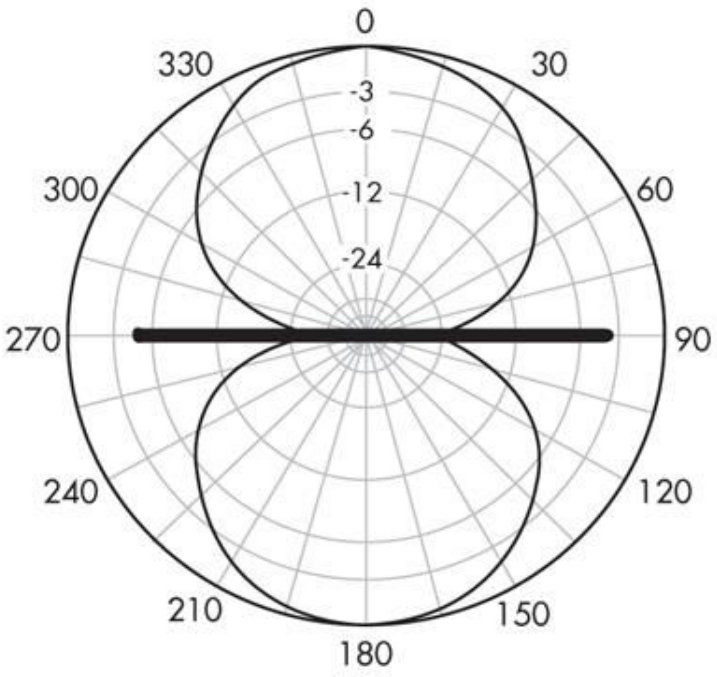

Figure 3.2 Radiation pattern of half wave dipole

To differentiate the radiation of a single dipole with that of an array, an *N*-element linear array of equally spaced parallel dipoles with element spacing *d* as shown in figure3.3 is considered. All the elements have identical amplitudes I_n with a progressive phase shift of β between the elements.

The corresponding field pattern of the array is given by –

$$AF(\theta) = \sum_{n=1}^{N} I_n \, e^{\, j(n-1)(kd\cos\theta+\beta)} \tag{3.6}$$

Where $k=2\,\pi/\lambda$ is the wave number and θ is the angle measured from axis of the array.

For very small values of β, the Eq. (3.6) reduces to Eq. (3.7) considering unity excitation

$$AF \approx \left[\frac{\sin(\frac{N}{2} kd\cos\theta)}{(\frac{N}{2} kd\cos\theta)} \right] \tag{3.7}$$

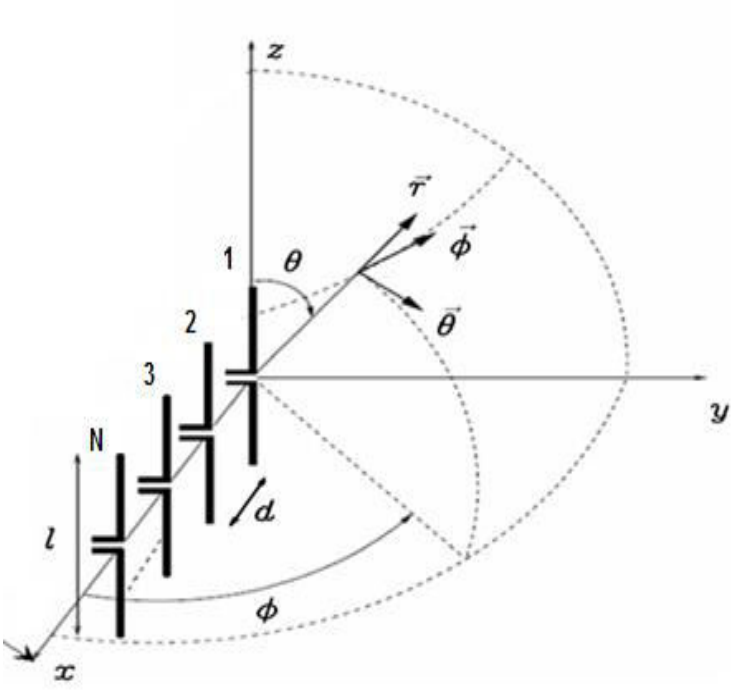

Figure 3.3 Array of N-element half wave dipoles

The radiation intensity of the array is-

$$U(\theta) = \left[(AF)_n\right]^2 = \left[\frac{\sin(\frac{N}{2} kd\cos\theta)}{(\frac{N}{2} kd\cos\theta)} \right]^2 \tag{3.8}$$

For broadside array, $U_{max}=1$ at $\theta=90°$. The average intensity U_o is defined as-

$$U_o = \frac{1}{4\pi} P_{rad} = \frac{1}{2} \int_0^{\pi} \left[\frac{\sin(\frac{N}{2} kd\cos\theta)}{(\frac{N}{2} kd\cos\theta)} \right]^2 \sin\theta \, d\theta \approx \frac{\pi}{Nkd} \tag{3.9}$$

The directivity of the array of N elements is given by-

$$D_o = \frac{U_{\max}}{U_o} \approx \frac{Nkd}{\pi} \tag{3.10}$$

If the number of elements are eight then the directivity of the array for the element spacing $d=\lambda/2$ according to Eq. (3.10) becomes very large as compared to the directivity of the single dipole. The radiation pattern of a uniformly excited array is shown in figure 3.4. The different lobes of a radiation pattern are shown in figure 3.5.

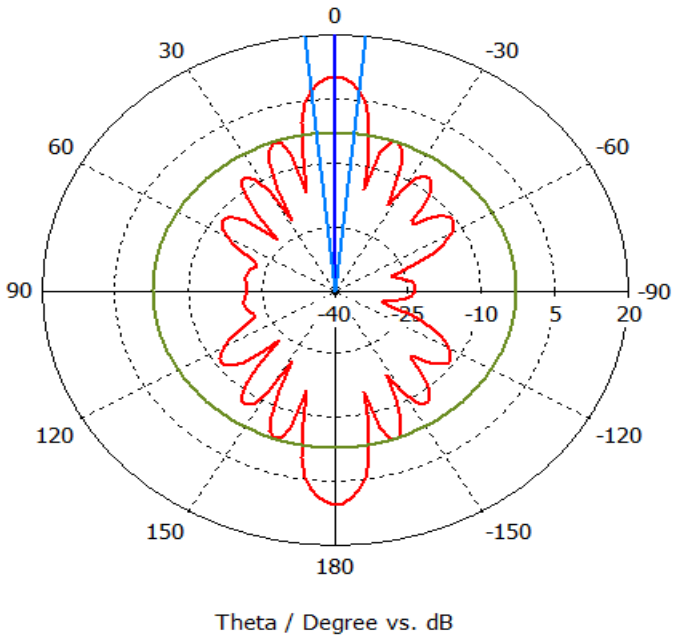

Figure 3.4 Radiation pattern of the 8-element uniformly excited array

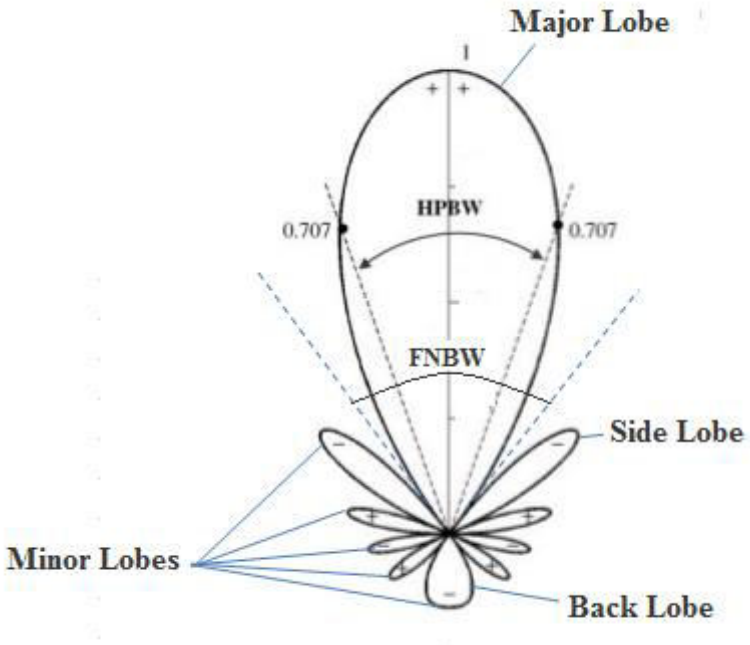

Figure 3.5 Radiation pattern with different lobes

Due to the rapid development of the modern wireless technology, demand of high performance antenna arrays with stringent requirements, such as broadband, higher directivity, low or ultra-low SLL, etc. has been increasing day by day.

The pattern with desired performance can be obtained by modifying the excitation and inter-element separation of the elements of the array .The conventional arrays using phase shifters are used to get the required excitation distribution but it is very complex to realize in practice. Moreover the obtained pattern has fixed performance characteristics. To change the radiation pattern of the array dynamically, switching ON-OFF the array elements is a good option providing control on amplitude excitation but it is less efficient as compared to excitation modification.

The introduction of an additional parameter "**time**" into the conventional antenna arrays makes it possible to exercise more control on the radiation performance of the array with simple feed network and the array is known as time modulated antenna arrays.

3.4 Analysis of Time Modulated Antenna Array

Let us consider an *N*-element linear array of equally spaced parallel dipoles with element spacing *d* as shown in figure 3.6. The corresponding array factor is given by

$$AF(\theta,t) = e^{j2\pi f_0 t}\sum_{n=0}^{N-1} I_n(t)e^{jnk'} \tag{3.11}$$

Where f_0 is the central frequency, $k' = \frac{2\pi}{\lambda_0} d\cos\theta$, λ_0 is the corresponding wavelength, θ is the angle measured from the axis of the array. Each element of TMAA is fed by a common excitation signal from the power divider through RF switches. The ON-OFF sequences of RF all the RF switches are controlled using a CPLD. The structure of TMAA with feed network is shown in figure 3.7.

The time modulated excitation for n-th element is given by

$$I_n(t) = E_n S_n(t) \quad n = 0,1,....N-1 \tag{3.12}$$

E_n is the static excitation of n-th element, the time switching function $S_n(t)$ for n-th element (shown in figure 3.8) is given by

$$S_n(t) = \begin{cases} 1 & t_{0n} \le t \le t_{0n} + \tau_n \\ 0 & otherwise \end{cases} \quad (3.13)$$

Where t_{on} is the switch on time instance and τ_n is the duration of switch on time of n-th element. Due to the periodicity of $S_n(t)$, the space and frequency response of Eq.(3.11) can be obtained by decomposing it into Fourier series given in Eq.(3.14) shown in figure 3.9.

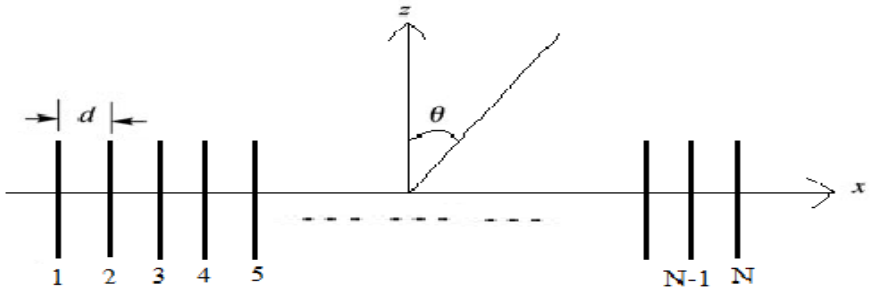

Figure 3.6 Geometry of equally spaced N-element linear array

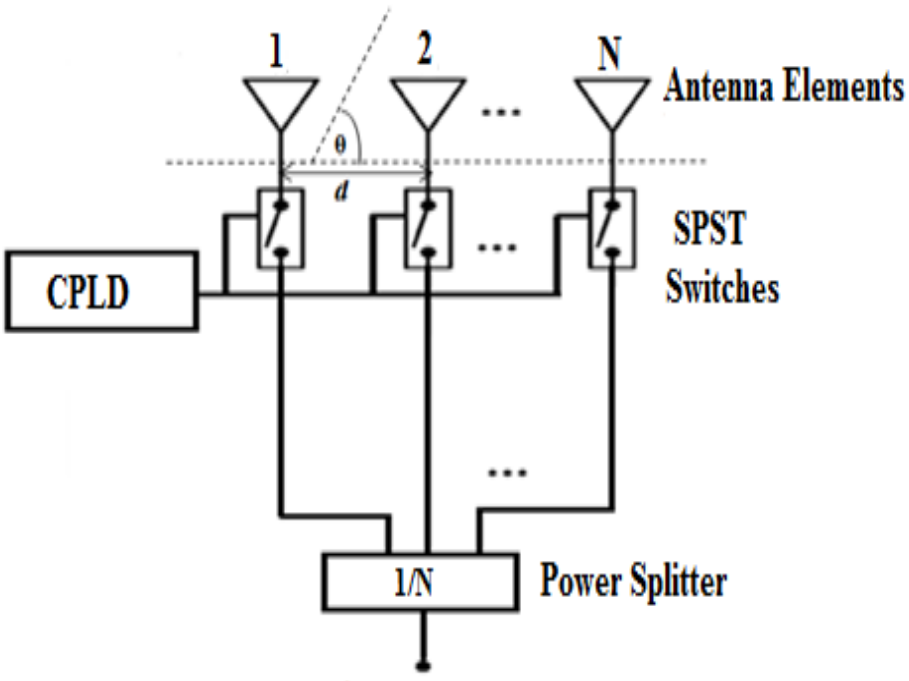

Figure 3.7 TMAA with feed network

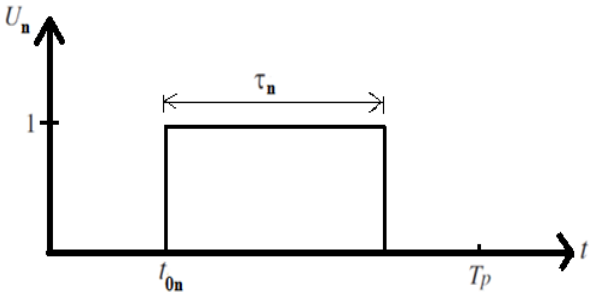

Figure 3.8 Time switching function

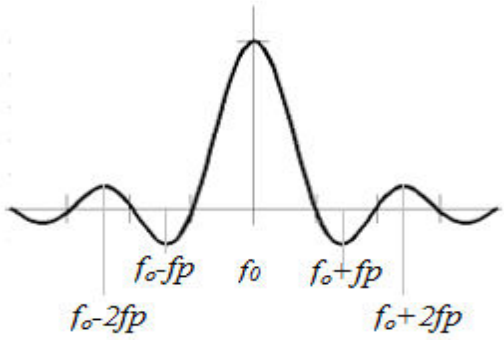

Figure 3.9 Frequency response after time modulation

It is seen from the frequency bands that signal is not only radiated at the fundamental frequency but also at the harmonics of modulating frequency m*f_p=m/Tp (m=0, $\pm1,\pm2,.....,\pm\infty$), where T_p is the total time modulation period.

$$AF_m(\theta,t) = e^{j2\pi(f_0+mf_p)t}\sum_{n=0}^{N-1}\beta_{mn}e^{jnk'} \quad \text{m=0,}\pm1,\pm2,.....,\pm\infty \tag{3.14}$$

where $\beta_{mn} = \dfrac{1}{Tp}\int_0^{Tp} E_n S_n(t) e^{-j2\pi mf_p t}$

$$\beta_{mn} = E_n f_p \tau_n \frac{\sin(m\pi f_p \tau_n)}{m\pi f_p \tau_n} e^{-jm\pi f_p(2t_{0n}+\tau_n)} \tag{3.15}$$

The complex amplitude coefficients centre frequency f_0 *(m=0),* at first sideband frequency f_o+fp *(m=1)* and the second sideband frequency f_o+2fp *(m=2)* are given as follows:

$$\beta_{0n} = E_n f_p \tau_n \tag{3.16}$$

$$\beta_{1n} = E_n f_p \tau_n \frac{\sin(\pi f_p \tau_n)}{\pi f_p \tau_n} e^{-j\pi f_p (2t_{0n}+\tau_n)} \tag{3.17}$$

$$\beta_{2n} = E_n f_p \tau_n \frac{\sin(2\pi f_p \tau_n)}{2\pi f_p \tau_n} e^{-j2\pi f_p (2t_{0n}+\tau_n)} \tag{3.18}$$

The array factor in Eq. (3.14) can be re-written in frequency domain as-

$$AF_m(\theta, f) = e^{j2\pi(f_0+mf_p)t} \sum_{m=+\infty}^{m=-\infty} \sum_{n=0}^{N-1} \beta_{mn} e^{jnk'} \tag{3.19}$$

At centre frequency and first two sidebands the Eq. (3.19) become as-

$$AF_0(\theta, f) = e^{j2\pi f_0 t} \sum_{n=0}^{N-1} E_n f_p \tau_n e^{jnk'} \tag{3.20}$$

$$AF_1(\theta, f) = e^{j2\pi(f_0+fp)t} \sum_{n=0}^{N-1} E_n f_p \tau_n \frac{\sin(\pi f_p \tau_n)}{\pi f_p \tau_n} e^{-j\pi f_p (2t_{0n}+\tau_n)} e^{jnk'} \tag{3.21}$$

$$AF_2(\theta, f) = e^{j2\pi(f_0+2fp)t} \sum_{n=0}^{N-1} E_n f_p \tau_n \frac{\sin(2\pi f_p \tau_n)}{2\pi f_p \tau_n} e^{-j2\pi f_p (2t_{0n}+\tau_n)} e^{jnk'} \tag{3.22}$$

The Esq. (3.16), (3.17) and (3.18) show the expressions for complex amplitudes at centre frequency as well as at sidebands and these can be used to synthesize the desired radiation pattern.

The directivity of the array is given as-

D=Radiation Intensity in Direction (θ_0, ϕ_0) / Average Radiation intensity

The directivity of the TMAA becomes-

$$D(TMAA) = \frac{\left|AF_0(\theta_0, \phi_0)\right|^2}{(1/4\pi) \sum_{m=-\infty}^{m=+\infty} \int_0^{2\pi} \int_0^{\pi} \left|AF_m(\theta, \phi)\right|^2 \sin\theta \, d\theta \, d\phi} \tag{3.23}$$

The power radiated by the TMAA at the centre frequency is given by the following equation-

$$P_0 = \int_0^{2\pi} \int_0^{\pi} \left|AF_0(\theta,\phi)\right|^2 \sin\theta \, d\theta \, d\phi \tag{3.24}$$

The power radiated by the TMAA at the sideband frequency is given by the following equation

$$P_{SR} = \sum_{\substack{m=-\infty \\ m\neq 0}}^{m=\infty} \int_0^{2\pi} \int_0^{\pi} \left|AF_m(\theta,\phi)\right|^2 \sin\theta \, d\theta \, d\phi \tag{3.25}$$

Dynamic efficiency (η_d) of the array is defined as-

$$\eta_d = \frac{Power\ radiated\ at\ centre\ \ frequency}{Sum\ of\ \ Power\ radiated\ at\ centre\ \ frequency\ and\ at\ sideband\ \ frequencie\ s} \tag{3.26}$$

$$\eta_d = \mathrm{P_0} / (\mathrm{P_0} + \mathrm{P_{SR}}) \tag{3.27}$$

Thus, the dynamic efficiency of the TMAA is as -

$$\eta_d(TMAA) = \frac{1}{1 + \left(\sum_{\substack{m=-\infty \\ m\neq 0}}^{m=\infty} \int_0^{2\pi} \int_0^{\pi} \left|AF_m(\theta,\phi)\right|^2 \sin\theta \, d\theta \, d\phi \Big/ \int_0^{2\pi} \int_0^{\pi} \left|AF_0(\theta,\phi)\right|^2 \sin\theta \, d\theta \, d\phi \right)} \tag{3.28}$$

3.5 Conclusion

The chapter discusses the analysis of TMAA to provide a more flexible and accurate way of obtaining the desired beam patterns with low or ultra-low sidelobe level. It calculates the switch ON-time duration of each antenna element for obtaining the desired current excitation distribution like conventional antenna array. Since we are using On-OFF switching the system excites sideband power radiation causing sideband power losses. The chapter efficiently calculates the directivity, sideband power losses and dynamic efficiency of the array. In the following chapters we will apply the optimization techniques to obtain the desired radiation pattern minimizing the sideband radiations.

Chapter - 4

Beam-Forming with Sideband Suppression using Time Modulated Antenna Arrays

4.1 Introduction

TMAAs are widely used in military and commercial applications including radar systems and wireless communication for convenient beam scanning, beam shaping and adaptive beam forming. As compared to conventional antenna arrays, TMAAs controlled by on-off timings of RF switches are used to taper the excitation distribution of array elements but suffer from high sideband radiation losses at multiples of the modulation frequency. The sideband signals need to be suppressed to improve the efficiency of the array. The chapter focuses on beam formation with and without using phase shifters in TMAA.

4.2 Review

The TMAA faces an inherent challenge because of the radiation at unwanted harmonics at multiples of the switching frequency [77] [84] [90]. Different stochastic optimization algorithms are proposed to suppress the sideband radiation while synthesizing desired patterns is reported in [79] [90] [92] [101]. Existing literatures present various innovative approaches for synthesis of TMAA using Artificial bee colony algorithm (ABC) [94], particle swarm optimization (PSO) [90], multi-objective optimization approach [92] and differential evolution (DE) algorithm [79][101]. Li and Yang applied DE to obtain flat-top beam and cosecant-squared beam patterns in time-modulated semicircular arrays [89].

In the chapter five designing instances have been investigated. First example synthesizes broad side radiation pattern with fixed SLL and FNBW while in second one by applying progressive phase shifts between array elements, the scanned beam pattern is generated with fixed SLL and FNBW. A common complex time exponential signal is utilized in the next examples to generate shaped and scanned beam patterns without phase shifters.

4.3 Design of TMAA for Broadside and Scanned Beam Pattern Using ABC

The thesis considered time modulated linear array consisted of 16 half wavelength ($\lambda/2$) dipole antennas with $\lambda/2$ spacing at 3GHz operating frequency (f_0). The array is excited with the rectangular pulses having 1MHz pulse repetition frequency (fp). The problem will

synthesize radiation pattern with desired SLL and SBL. According to the design objective we form fitness function as given in Eq. 4.1.

$$Fitness = \begin{cases} (SLL_o - SLL_d)^2_{f=f_0} + (SLL_o - SLL_d)^2_{f=f_o+f_p} \\ + (SLL_o - SLL_d)^2_{f=f_0-f_p} \quad if \quad FNBW_o \le FNBW_d \\ 10^2 \quad otherwise \end{cases} \tag{4.1}$$

Where SLL_o - Obtained SLL, SLL_d -Desired SLL, $FNBW_o$ - Obtained FNBW and $FNBW_d$ –Desired FNBW.

4.3.1 Design of broadside beam pattern

ABC is applied to find the ON/OFF time duration of the switching pulses in order to achieve the designing goal. ABC algorithm is written in matlab. While optimization of τ_n using ABC, 20 independent runs are carried out and best optimal calculated time sequence is shown in figure 4.1.

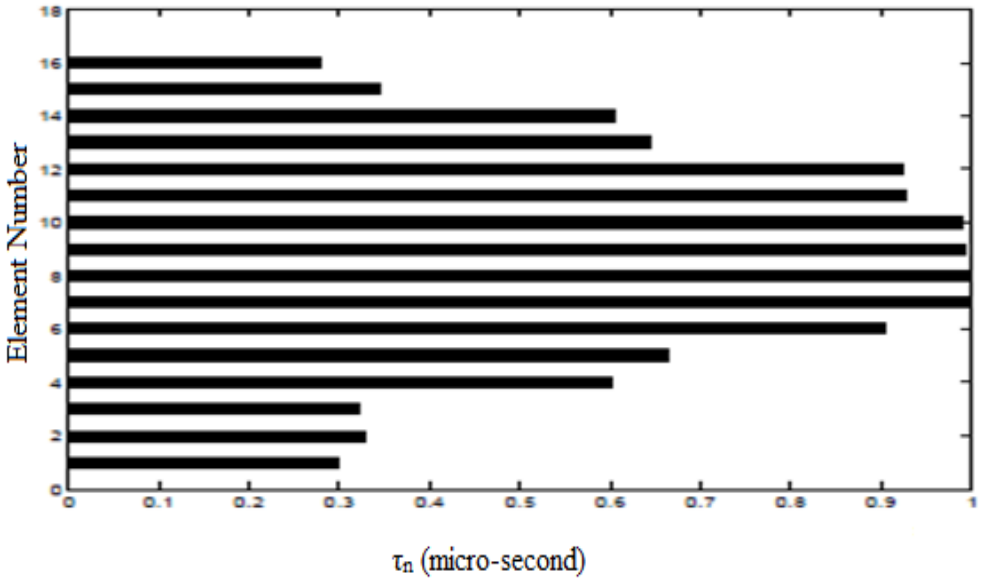

Figure 4.1 Optimized switch-on time duration (τ_n) of 16-element TMAA for broadside pattern

The radiation pattern obtained with the calculated timing sequences is shown in figure 4.2. It is observed that the obtained SLL= -28dB and FNBW=22°at f_o. The obtained sideband level at frequency f_0+f_p and f_0-f_p is -34.78dB which is approximately -7 dB lower than that of the pattern obtained at centre frequency f_0. The simulation is done in matlab and the

results in terms of desired and obtained values of SLL, FNBW at centre frequency and relative level of sidebands respectively are shown in Table4.1.

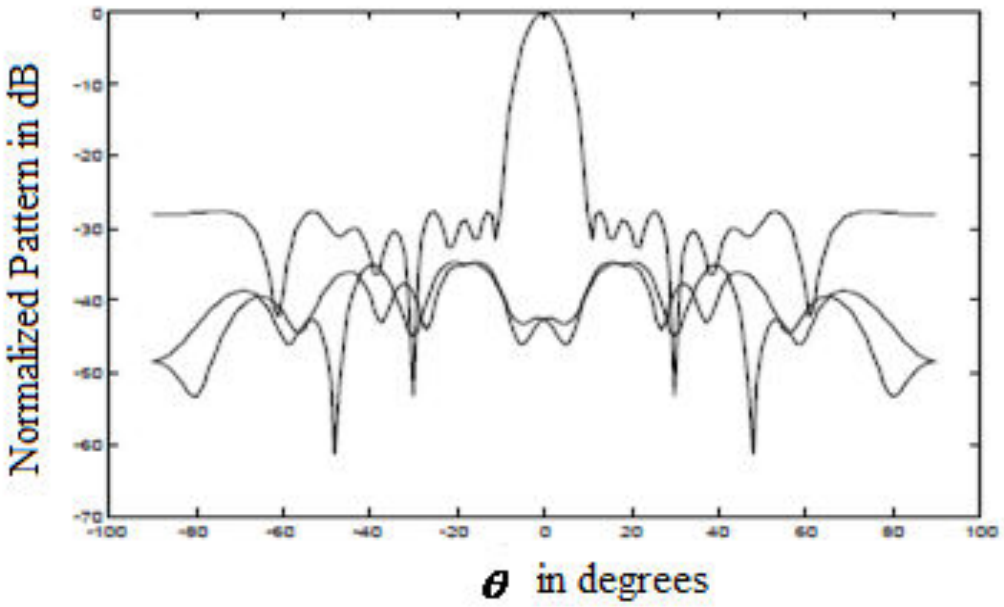

Figure 4.2 Radiation pattern of 16-element TMAA for broadside pattern

Table 4.1 Desired and obtained results for 16-element TMAA for broadside beam pattern

Design Parameters	Side Lobe Level (dB)		FNBW (degrees)	
	Desired	Obtained	Desired	Obtained
f_o=3GHz	-28	-27.68	22	22
f_o+f_p=3.001GHz	-35	-34.78	NA	
f_o-f_p=2.999GHz	-35	-34.78	NA	

4.3.2 Design of Scanned beam pattern

ABC optimization technique is used here to compute the time sequence τ_n of all the elements of the TMAA to generate scanned pattern at f_0 with specific SLL and FNBW using progressive phase difference between elements as well as to keep maximum SBR below a predefined level. Figure 4.3 shows the calculated time sequences in order to obtain the desired scanned beam radiation pattern. 1.57 radian phase difference between two consecutive elements is applied to steer the beam at 60°.

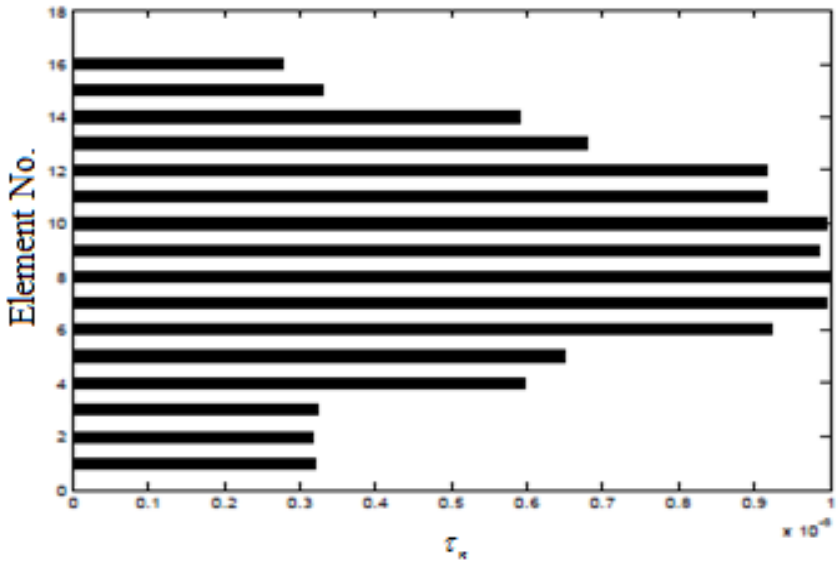

Figure 4.3 Optimized switch-on time duration (τ_n) for scanned beam pattern

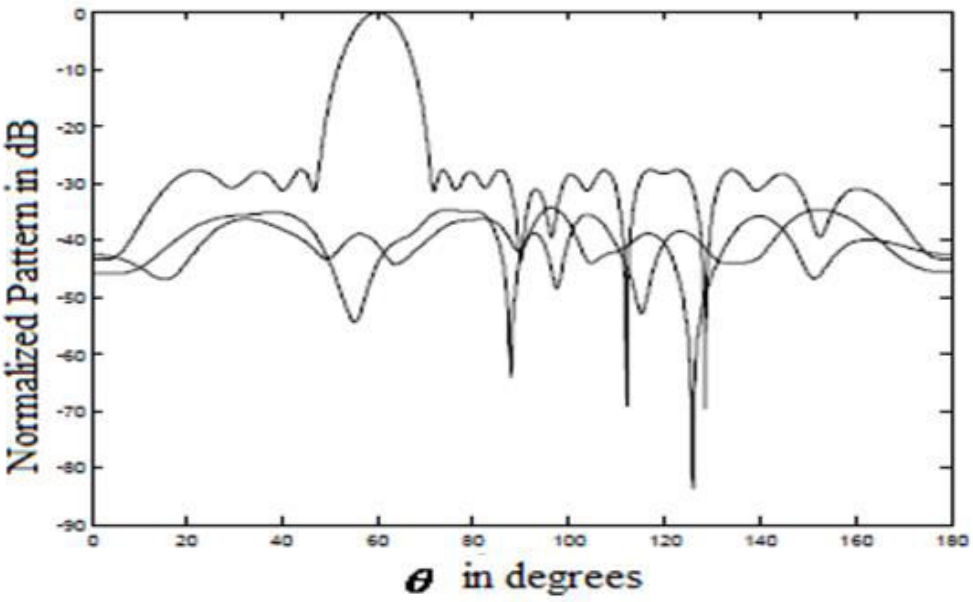

Figure 4.4 Radiation pattern of TMAA for scanned beam pattern

The radiation pattern obtained is shown in figure 4.4 which shows that the main beam is steered at 60°. It is observed that the obtained SLL= -28dB and FNBW=25°at f_o. The obtained Sideband level at frequency f_0+f_p and f_0-f_p is -34.68dB which is approximately -7 dB lower than that of the pattern obtained at centre frequency f_0. The simulated results in terms of desired and obtained values of SLL, FNBW at centre frequency and relative SBL respectively are shown in Table4.2.

Table 4.2 Desired and obtained results for 16-element TMAA for scanned beam Pattern

Design Parameters	Side Lobe Level (dB)		FNBW (degrees)	
	Desired	Obtained	Desired	Obtained
f_o=3GHz	-28	-27.62	25	25
f_o+f_p=3.001GHz	-35	-34.68	NA	
f_o-f_p=2.999GHz	-35	-34.68	NA	

4.4 Design of TMAA of Wired Dipoles for Beam Forming with Sideband Suppression using PSO

A TMAA of 16-element wired dipoles is designed and simulated to achieve the desired radiation pattern of low SLL and SBR.

4.4.1 16-elements Wired Dipole Array design

A half wavelength wired dipole considered as the array element in the problem is designed and simulated in CST. The total length of dipole is 50mm with gap of 0.25 mm between two arms of dipole. The design of wired dipole with its simulated radiation pattern is shown in figure 4.5 .

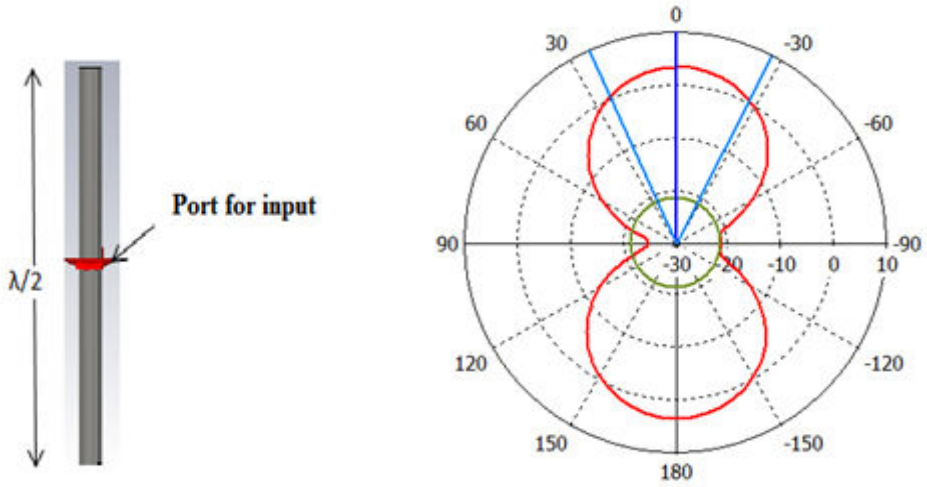

(a) (b)

Figure 4.5 (a) Geometry of wired dipole (d) Radiation pattern of wired dipole

Linear array consists of 16 half wavelength wired dipole antennas with λ/2 spacing (d) between the elements at 3GHz operating frequency (f_o) is shown in figure 4.6.

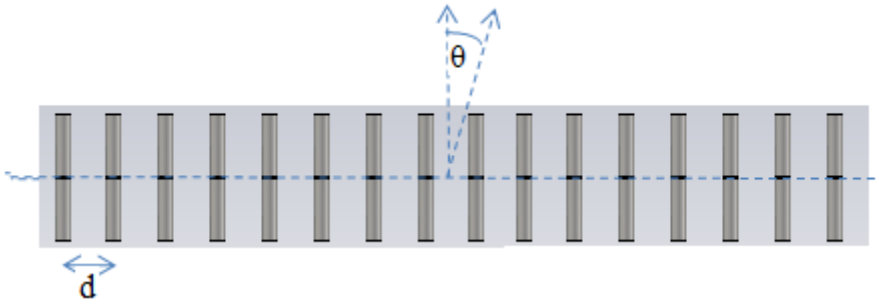

Figure 4.6 Geometry of an equally spaced 16-element linear array of wired dipoles

4.4.2 Design of 16-elements TMAA of Wired Dipoles for beam forming

Each element of the array is excited by a common excitation signal controlled by high speed PIN diode RF switches with 1MHz pulse repetition frequency fp(=1/Tp). The problem will synthesize radiation pattern with desired SLL and SBL. The fitness function is formed according to the design objective and is given as-

$$Fitness = \begin{cases} (SLL_o - SLL_d)^2_{f=f_0} + (SLL_o - SLL_d)^2_{f=f_o+f_p} \\ + (SLL_o - SLL_d)^2_{f=f_0-f_p} \quad if \quad FNBW \le 20^0 \\ 1000 \quad otherwise \end{cases} \tag{4.2}$$

SLL_d is the desired SLL while SLL_o is the obtained SLL.

PSO optimization technique is used to calculate the time sequences t_{on} and τ_n of all the elements of the TMAA to generate desired pattern at f_0 with specific SLL and FNBW. The PSO uses swarm size of 30 and parameters w= 0.5, c_1 = 2.0, and c_2 = 2.0. Each run of the algorithm is executed for 500 iterations where dynamic range of search space is bounded within (0,1). PSO fulfils the synthesis constraints on SLL at the convergence. The calculated time sequence of t_{on} and τ_n for the desired fitness function is shown in the figure 4.7. The designed TMAA is simulated using CST microwave studio to obtain the radiation patterns at centre frequency f_0 and first side bands $f_0 \pm$ fp using calculated time sequence. Figure 4.8 (a) shows the normalized radiation pattern at centre frequency. The SLL achieved is -23.8dB at 3GHz. Figure 4.8(b) is showing sideband levels of the designed TMAA. The maximum SBL at f_0+fp and f_0-fp is -31.72 dB and -29.59 dB respectively.

Figure 4.9 is showing the combined pattern at centre and sideband frequencies from where it is clear that sideband level is approximately -5dB lower than that of the power pattern obtained at centre frequency.

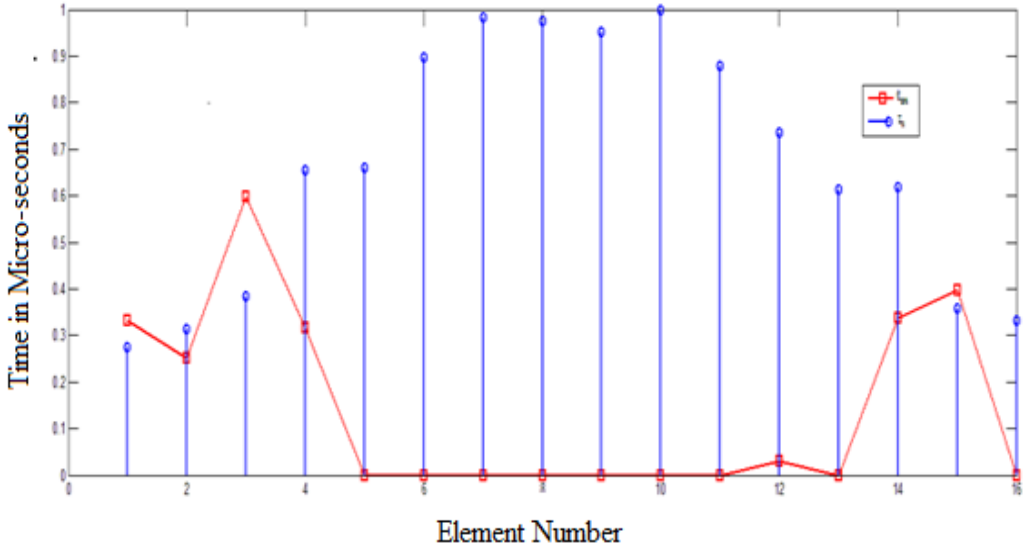

Figure 4.7 Optimized Switch-on time instant (t_{on}) and switch-on time duration (τ_n)

Table 4.3 shows the simulated results in terms of desired and obtained values of SLL, FNBW at centre frequency and relative level of sidebands respectively.

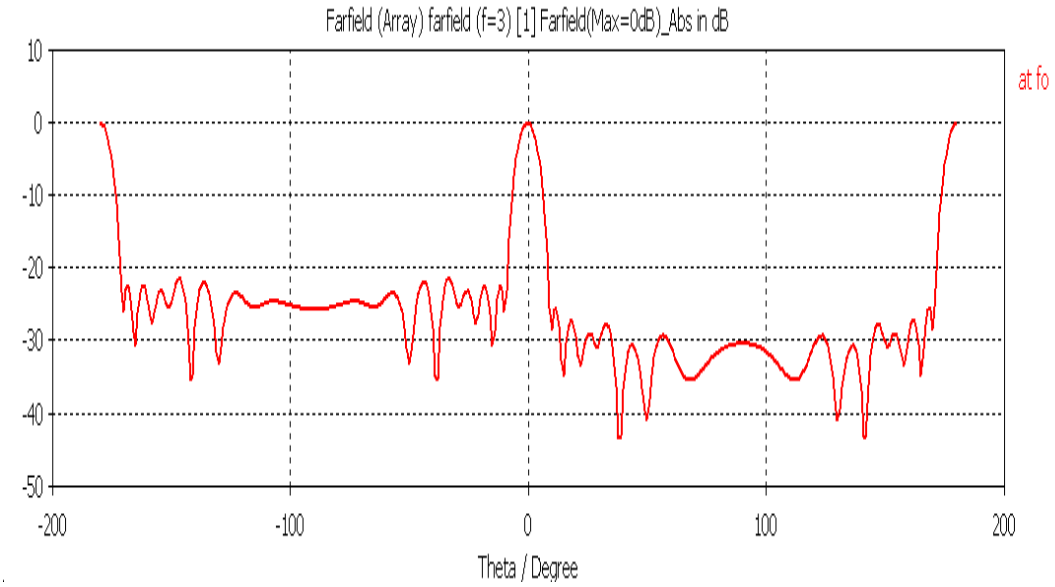

(a) Pattern at fo = 3GHz

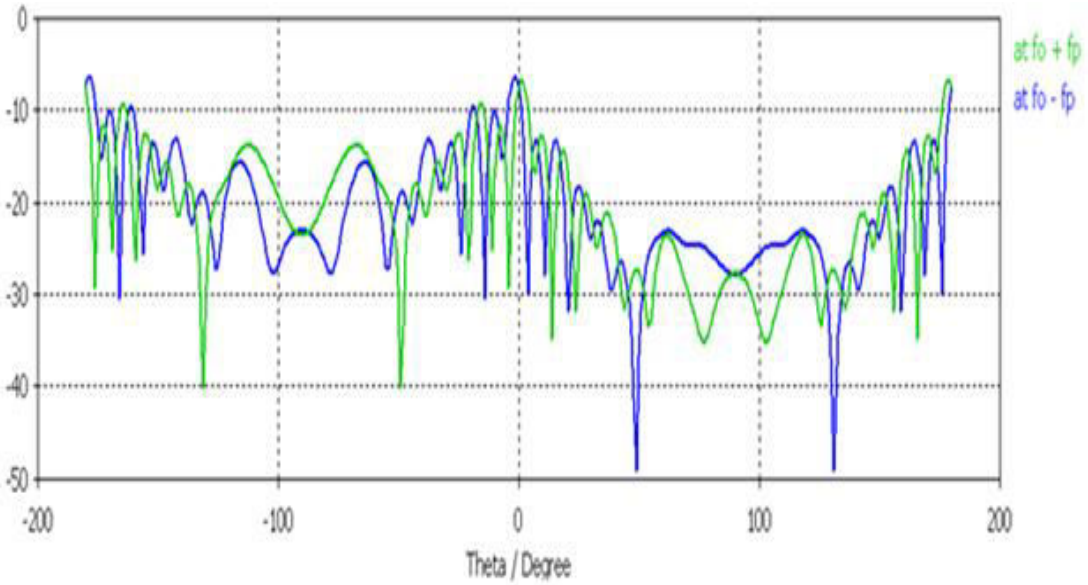

(b) Patterns at fo ± fp.

Figure 4.8 Simulated patterns (a) Pattern at fo = 3GHz. (b) Patterns at fo ± fp.

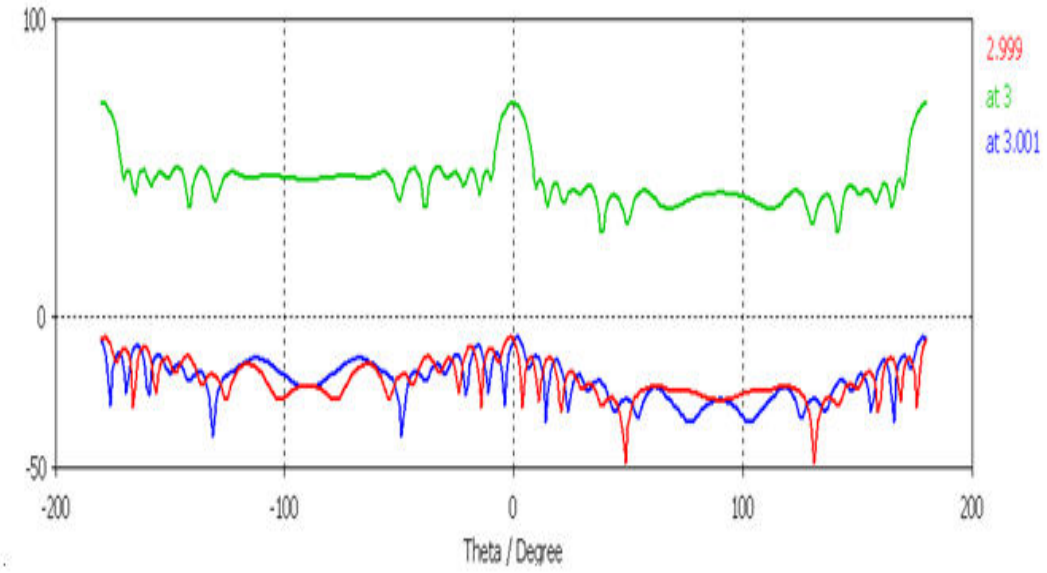

Figure 4.9 Combined Simulated patterns at f_o = 3GHz and at $f_o \pm f_p$

The same observations are also obtained by analytical method using MatLab 7 simulation software, which validates the correctness of the CST microwave studio model in this study. However, there is little disagreement between some simulated relative levels of sideband beams and analytical data due to the mutual coupling effect and errors of amplitude and phase excitations.

Table 4.3 Desired and obtained results for 16-element wired dipole TMAA

Design Parameters	Side Lobe Level (dB)		FNBW (degrees)	
	Desired	Obtained	Desired	Obtained
f_o=3GHz	-25	-23.8	$\leq 20^o$	19^o
f_o+f_p=3.001GHz	-30	-31.72	NA	
f_o-f_p=2.999GHz	-30	-29.59	NA	

4.5 Design of TMAA for Beam Scanning and Beam Shaping Without Phase Shifters Using ABC

To obtain shaped beam and scanned beam without applying external phase shifts between the elements, Linear array consists of 16 half wavelength printed dipole antennas with central frequency(f_o) 3GHz is considered with λ/2 spacing (d) between the elements. The elements of the array are controlled using high speed RF switches having 1MHz pulse repetition frequency fp.

The problem will synthesize for obtaining the cosecant squared and scanned beam pattern with specified SLL for a given FNBW at the centre frequency and minimization of SBR as well. The fitness function is formed according to the design objective as-

$$Fit(t_o,\tau)=c_1F_1+c_2F_2 \tag{4.3}$$

where c_1 and c_2 are the corresponding weighing factor of each term

$$F_1=\begin{cases}(SLL_o-SLL_d)^2 & if\ \ SLL_o > SLL_d \\ 0 & if\ SLL_o \leq SLL_d\end{cases} \tag{4.4}$$

$$F_2=\left\{\begin{bmatrix}w_1\\ w_2\end{bmatrix}\begin{bmatrix}A' & A''\end{bmatrix}\right. \tag{4.5}$$

Where

$$A' = \begin{cases} (FNBW_o - FNBW_d)^2 & if \;\; FNBW_o > FNBW_d \\ 0 & if \; FNBW_o \le FNBW_d \end{cases} \tag{4.6}$$

$$A'' = \begin{cases} (Ripple_o - Ripple_d)^2 & if \;\; Ripple_o > Ripple_d \\ 0 & if \; Ripple_o \le Ripple_d \end{cases} \tag{4.7}$$

$$\begin{bmatrix} w_1 & w_2 \end{bmatrix} = \begin{cases} \begin{bmatrix} 1 & 0 \end{bmatrix} & for \; Co\sec ant \\ \begin{bmatrix} 0 & 1 \end{bmatrix} & for \; Scanned \end{cases} \tag{4.8}$$

The switching time sequences $\{\tau_n : n = 1, 2,....,N\}$ and $\{t_{on} : n = 1; 2,....., N\}$ are considered as optimization parameters that are improved in iterations in order to minimize the fitness function.

To create the phase variation, each element in the array is uniformly excited by the complex continuous time exponential signal $e^{-j2\pi fpt}$ coupled with the RF switches as shown in figure 4.10.

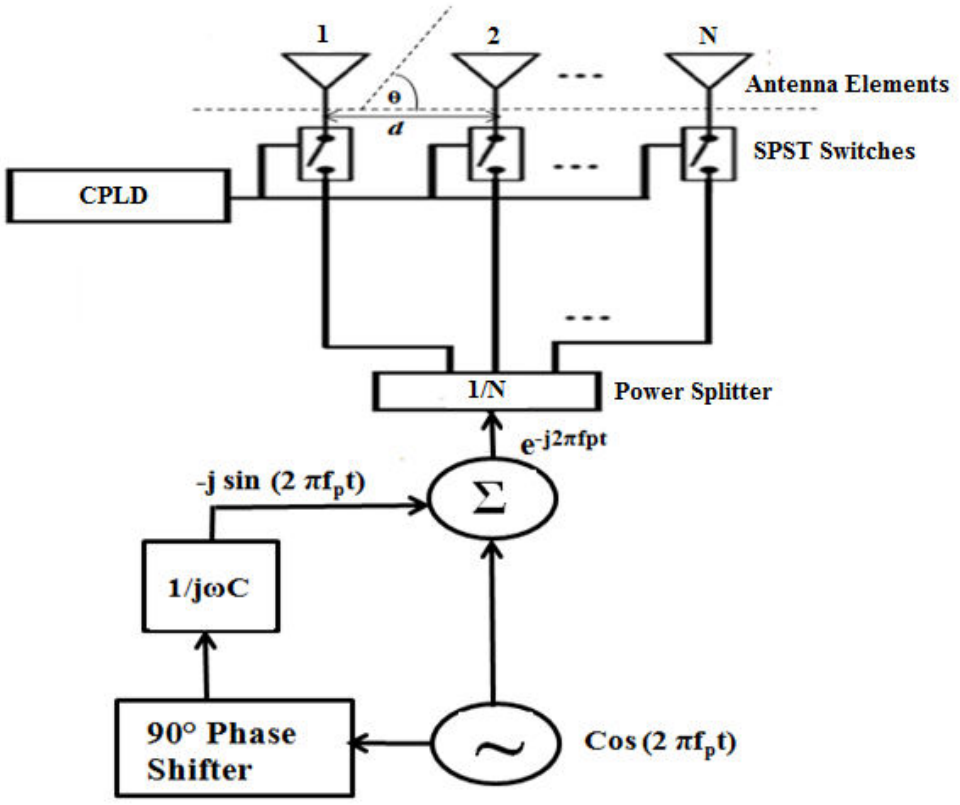

Figure 4.10 Design of TMAA with complex exponential input

The switching function of Eq. (3.13) becomes as:

$$S_n(t) = \begin{cases} 0 & KTp < t < KTp + t_{on} \\ e^{-j2\pi f_p t} & KTp + t_{on} \le t \le KTp + t_{on} + \tau_n \\ 0 & KTp + t_{on} + \tau_n < t < (K+1)Tp \end{cases} \quad (4.9)$$

According to the switching function as in Eq. (4.9), the complex amplitude coefficient of each element is modified. Thus the Eq. (3.15) becomes-

$$\beta_{mn} = E_n f_p \tau_n \frac{\sin(m\pi f_p \tau_n)}{m\pi f_p \tau_n} e^{-j(m+1)\pi f_p (2t_{0n}+\tau_n)} \quad (4.10)$$

At centre frequency i.e at m=0

$$\beta_{0n} = E_n f_p \tau_n e^{-j\pi f_p (2t_{0n}+\tau_n)} \quad (4.11)$$

Thus, Eq. (4.10) results in amplitude and phase distribution to the array elements that provide the desired beam pattern without phase shifters. It is clear from the Eq. (4.11) that there exists some phase difference at the centre frequency by using complex exponential signal at the input.

4.5.1 Generation of Cosecant square and scanned beam pattern

ABC is applied to find the time duration of the switching pulses in order to achieve the designing objective. To obtain cosecant-squared beam with its peak at θ = 0° that extends up to θ = 30° with the maximum acceptable ripple = ±1 dB, ABC is applied to carry out the optimization process by setting maximum SBL=-25 dB and maximum SLL =-20 dB at 3 GHz .The calculated time sequence is shown in figure 4.11 and the normalized excitation distribution for the array elements at centre frequency and first two sidebands are shown in figure 4.12.

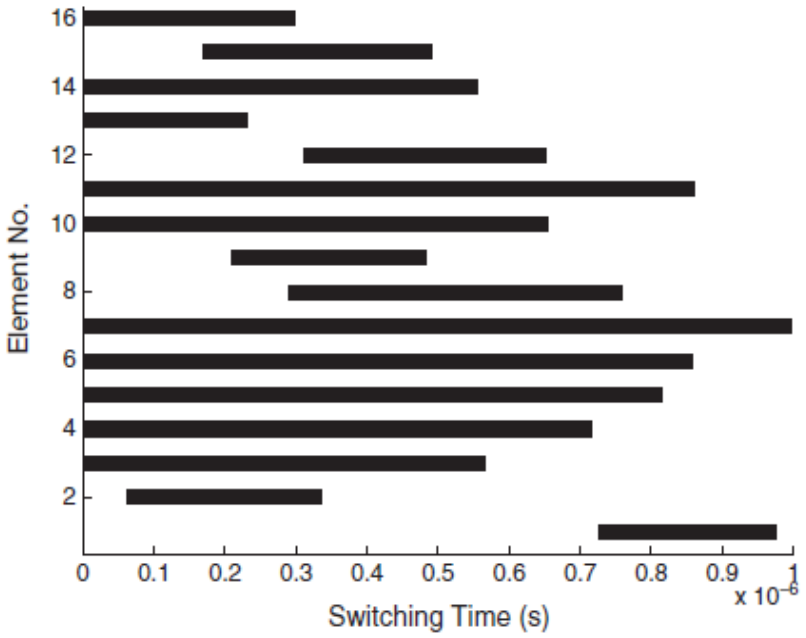

Figure 4.11 Switching timing Sequence for Cosecant pattern

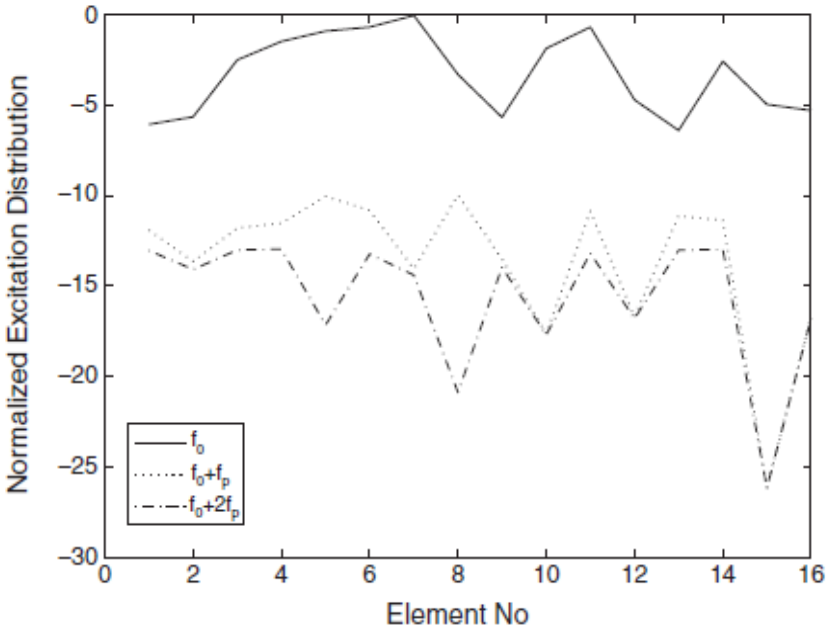

Figure 4.12 Normalized excitation distributions for cosecant pattern

In order to scan the main beam at -30°, ABC is used to carry out the optimization process by setting maximum SBL= -25 dB and maximum SLL = -17 dB at 3 GHz and the calculated time sequence providing the adequate phase difference between the each element is shown in figure 4.13 where as the figure 4.14 shows the normalized excitation distribution of each element at centre frequency and first two sidebands.

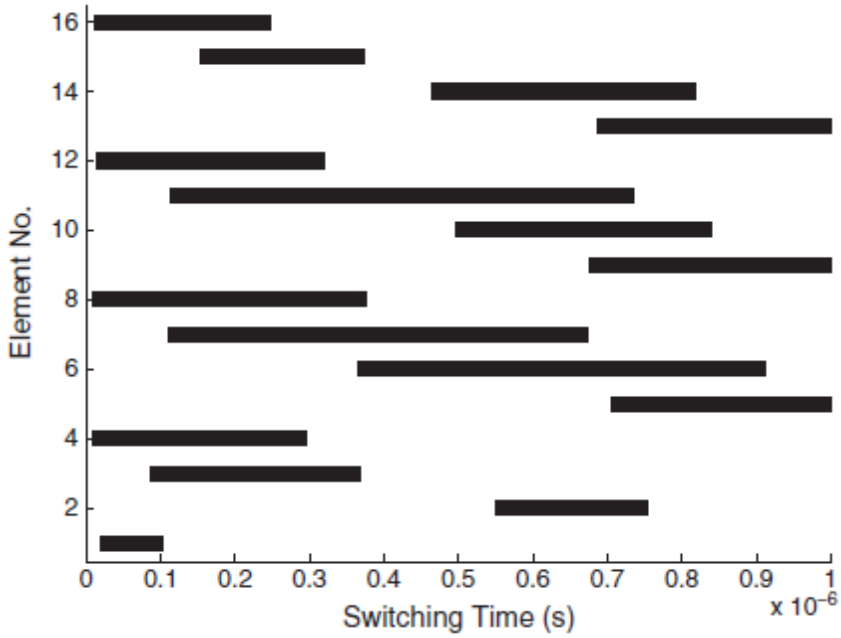

Figure 4.13 Switching timing Sequence for Scanned pattern

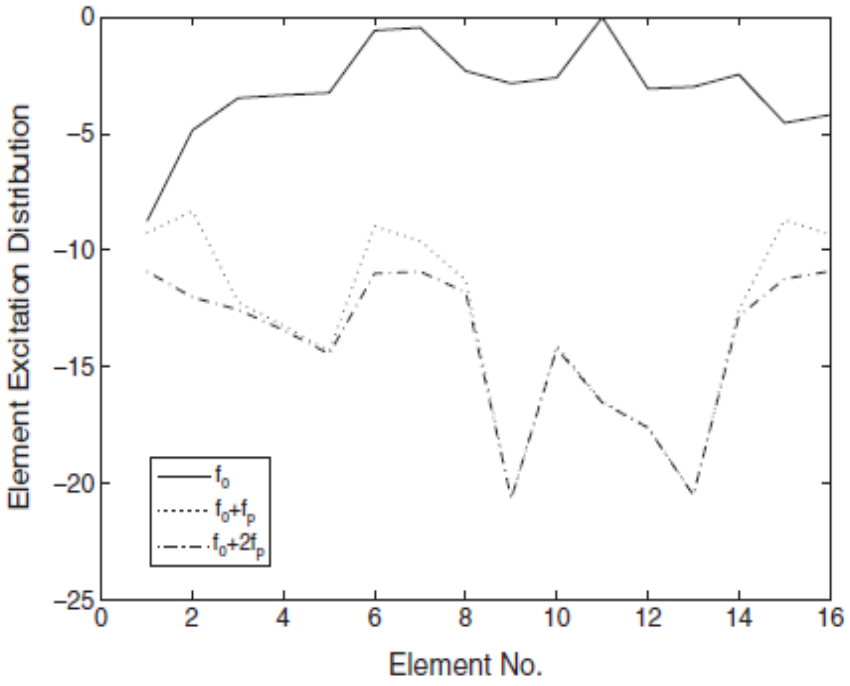

Figure 4.14 Normalized excitation distribution for scanned pattern

The convergence curves for both the cosecant and scanned pattern considering the best of 20 independent runs are shown in figure 4.15 and figure 4.16.

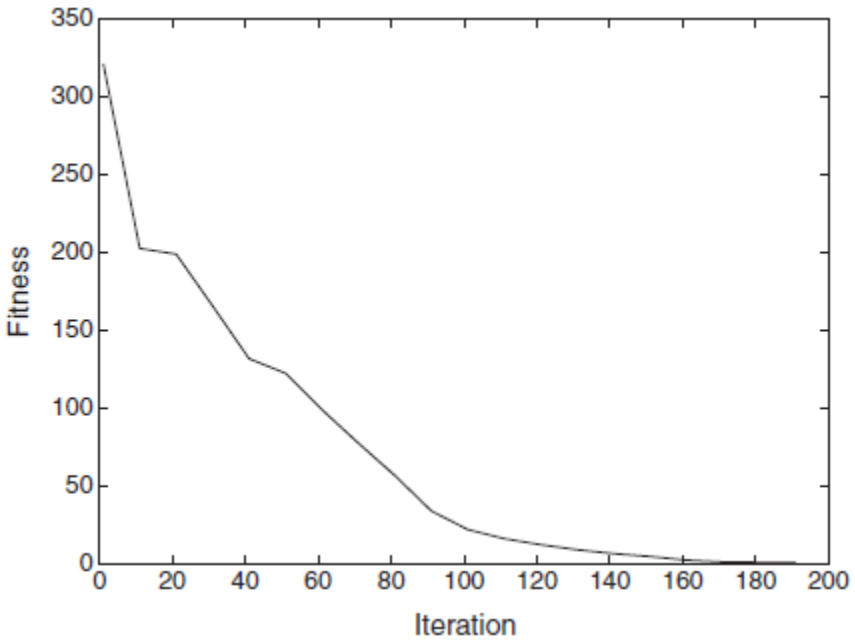

Figure 4.15 Fitness function to generate cosecant pattern using ABC

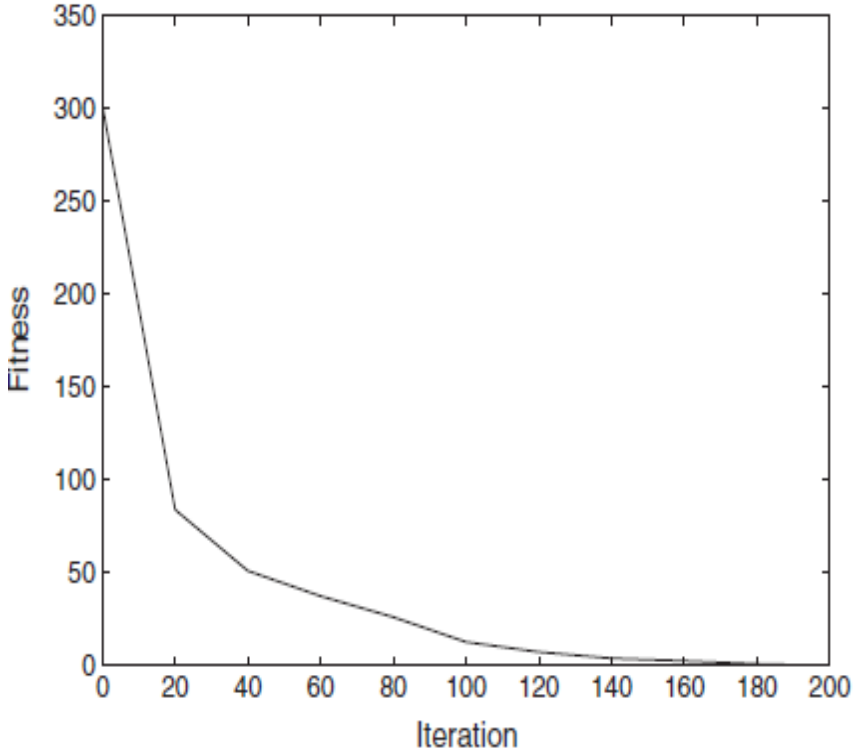

Figure 4.16 Fitness function to generate scanned pattern using ABC

The obtained normalized cosecant beam power patterns at the centre frequency and first two sidebands simulated using matlab and CST is shown in figure 4.17. It is observed that the synthesized pattern has one half-power point at θ = -4.8°, and the other half-power point is shifted to θ = 3.8°, and both drop to the null at θ = -11° and θ = 40° respectively.

Figure 4.18 shows that the maximum SBL of the power pattern at different frequencies decreases as number of sidebands increases to maintain the signal to noise interference ratio smaller. The dynamic efficiency of the designed TMAA is calculated as 65% using Eq. (3.26).

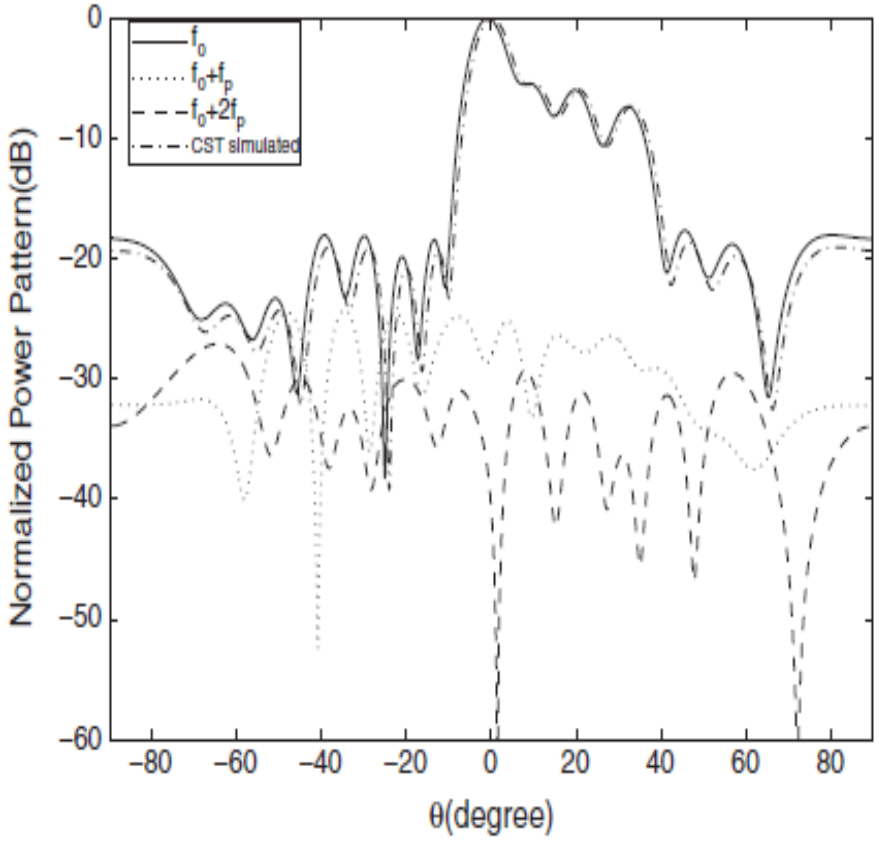

Figure 4.17 Normalized Cosecant beam pattern using TMAA

Calculated time sequences of figure 4.13 are used to obtain the scanned beam pattern as shown in figure4.19. The achieved pattern has FNBW = 21° with the first null on either side of the main beam at -40.9° and -19.9° respectively. The pattern is useful to receive any signal arriving at -30° angle from broad side.

As shown in figure 4.14 the maximum value of excitation distribution at sidebands is -10 dB less than that corresponding to m = 0 that effectively reduces the unwanted radiation at harmonic frequencies. The maximum SBL of each power pattern decreases progressively as m increases, which is shown in figure 4.20. The experiment shows that the calculated dynamic efficiency offered by the scanned time modulated linear array is 39%, which indicates that the total power radiated at the sidebands is more than the power radiated at

central frequency. Desired and obtained pattern specifications for both the patterns are listed in table4.4.

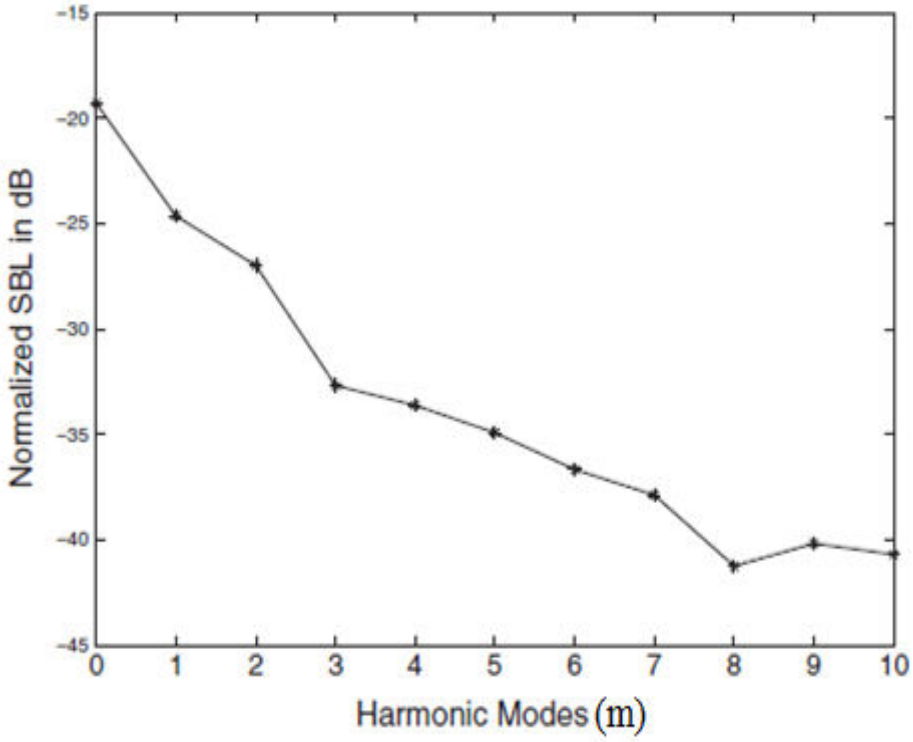

Figure 4.18 Maximum SBL for different harmonics for cosecant pattern

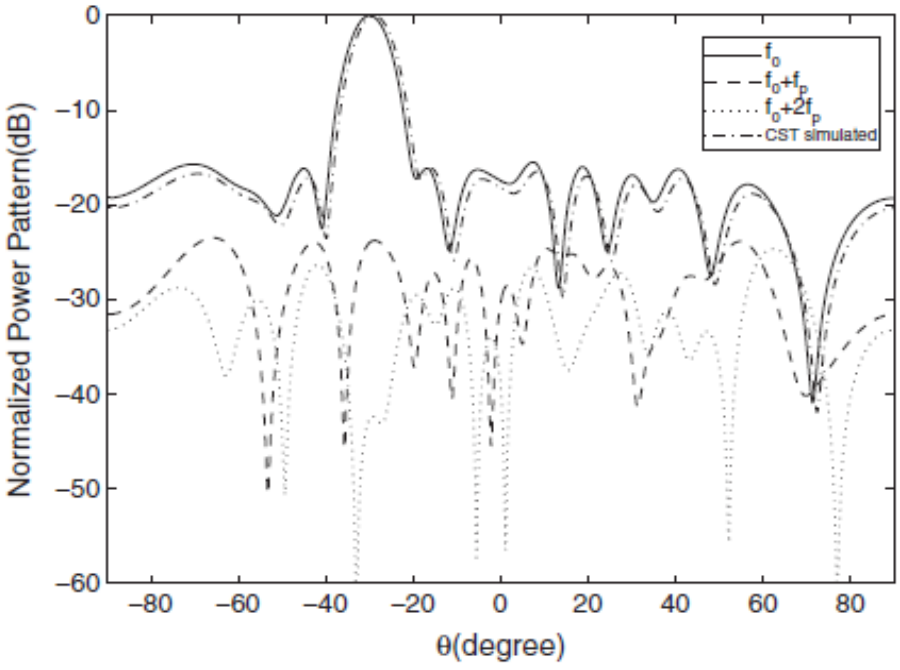

Figure 4.19 Normalized scanned beam pattern using TMAA

This type of antenna having cosecant squared pattern is useful for ground-based radars observing aircraft targets as well as airborne search radars observing ground targets when the target moves at constant altitude with an elevation or depression angle of 30° respectively.

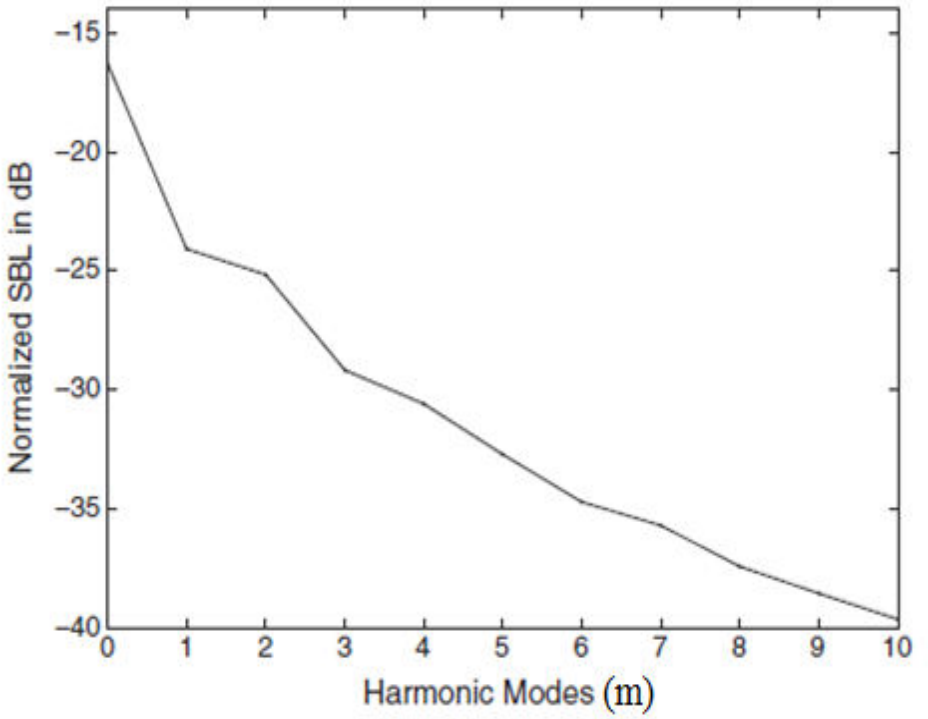

Figure 4.20 Maximum SBL for different harmonics for scanned pattern

Table 4.4 Desired and obtained results for cosecant square and scanned beam

Design Parameters	**Cosecant Square Beam Pattern**		**Scanned Beam Pattern**	
	Desired	**Obtained**	**Desired**	**Obtained**
SLL in dB	-20	-19.30	-17	-16.30
Maximum SBL in dB	-25	-24.65	-25	-24.15
Maximum Ripples (dB) For $0 \leq \theta \leq 30^{\circ}$	1	1.20	NA	NA
FNBW	NA	51°	21°	21°
Main Beam direction	NA	NA	-30°	-30°

4.6 Conclusion

TMAAs have been simulated for desired radiation performance. It is seen that the amplitude excitations of the conventional arrays with similar size is analogues to the switch on time duration of the uniformly excited TMAA to produce equivalent pattern at centre frequency. Modulation of the switch on time instant of the array introduces relative phase difference only at sidebands. The use of progressive phase difference between the elements to steer the main beam from broadside keeps the feeding network relatively simple. Scan beam offered broader FNBW compared to that of the broadside beam pattern with same SLL and similar number of array elements. Application of complex exponential excitation results in an unequal amplitude and phase distribution on the elements at the central frequency without phase shifters. It is found that the higher switching time duration enhances the dynamic efficiency of the system. The resulting beam-forming networks are very much useful in radar detection and information transmission at specific direction respectively. The suppression of the side bands at sidebands is adequate to reduce the side band radiation losses. ABC and PSO are found very effective to optimize the design problems. Simulation results are in well agreement with the theoretical results which confirms the proposed approach.

Chapter-5

Design and Fabrication of TMAAs for Pattern Synthesis

5.1 Introduction

Inspired by the designing flexibility and variety of beneficial properties including light weight, low profile, and low cost of the printed dipole antennas, the chapter presents synthesis of TMAAs consisted of printed dipoles for achieving patterns with different radiation characteristics. Printed dipole with microstrip balun is considered as array element and the ground plane of the dipole has been rigorously studied to improve radiation performance of the array. Proposed design structures are simulated using CST microwave studio. Experimental testing of the fabricated TMAAs has been done and results are compared with the simulated results.

5.2 Review

Use of TMAA as a versatile adequate radiation system for modern wireless applications has increased over the past decade. TMAAs find application in cognitive radio [123], secure communication [127]. Literature [122-127] presents the synthesis of TMAAs for obtaining different formations of radiation pattern. Printed antenna owing to variety of beneficial properties became explosively popular and widely investigated in articles [5-17]. Wideband printed antennas became popular in the modern wireless communication systems which utilize different communication technologies embedded in the same device, sharing the same antenna.

The chapter designs printed dipole antenna with modified ground structures. Parametric optimization of antenna elements has been studied. Antenna array is designed using microstrip balun and wilkinson power divider for implementing time modulated beam forming network.

5.3 Design of Printed Antenna with Microstrip Balun

Dipole requires balanced feeding such as parallel transmission line but microstrip feed lines utilized in printed antennas are of unbalance type. So a microstrip balun (unbalanced to balanced transformer) is needed along with the printed dipole. The geometry of a standard microstrip balun is shown in figure 5.1(a). The top and bottom layers are conducting strips on both sides of a dielectric substrate and are connected with metalized via hole. The input

is applied to top layer of microstrip line having characteristic impedance Z(M). The input signal reaches from point S of top layer to bottom layer through metalized via hole at point D. A quarter wavelength parallel dual line transmission line of characteristic impedance of Z(P) at the bottom layer is terminated to the balanced load of impedance Z(L). The current on the bottom transmission line and microstrip line are in opposite directions which produces balanced exciting to dipole. From point D, the equivalent circuit of the balun is observed as figure 5.1 (b) [126].

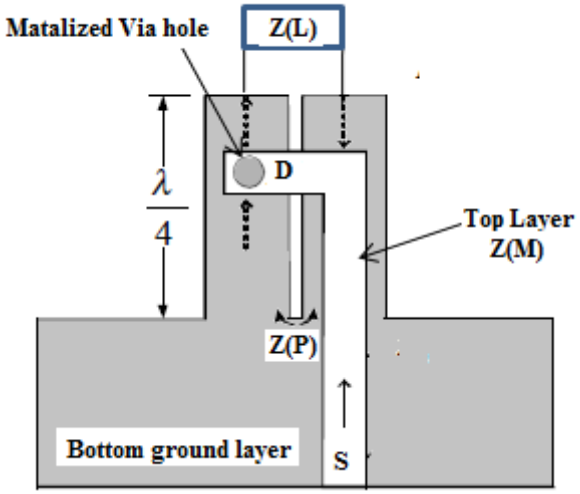

(a)

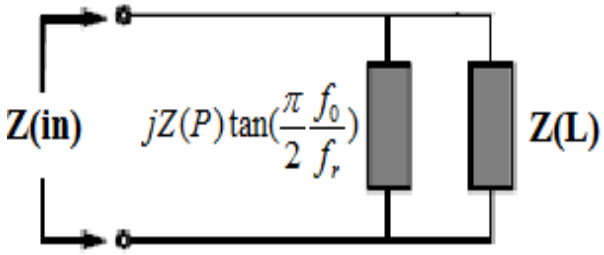

(b)

Figure 5.1 Printed microstrip Balun
(a) Structure (b) Equivalent Circuit

The input impedance of balun is given as:

$$Z(in) = \frac{jZ(L)Z(P)\tan(\frac{\pi}{2}\frac{f_0}{f_r})}{Z(L) + jZ(P)\tan(\frac{\pi}{2}\frac{f_0}{f_r})} \tag{5.1}$$

f_0 is the operating frequency and f_r is the resonating frequency. For Z(M)=Z(L) and (P)→∞, Z(in)=Z(M) for any value of f_0.

The standard configuration of printed dipole is shown in figure 5.2.

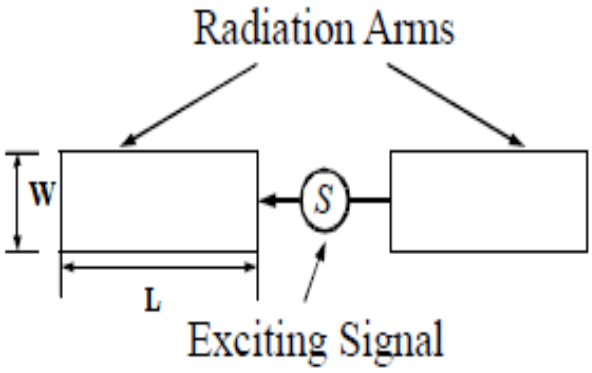

Figure 5.2 Configuration of printed dipole

The input impedance of the dipole is given by –

$$Z(dipole) = \frac{120(\ln 8L - \ln W - 1)}{\cosh(2\alpha L) - \cos(2\beta L)} \left\{ \left[\sinh(2\alpha L) - \frac{\alpha}{\beta}\sin(2\beta L) \right] - j\left[\frac{\alpha}{\beta}\sinh(2\alpha L) + \sin(2\beta L) \right] \right\} \tag{5.2}$$

Where α is the attenuation coefficient and β is the phase shifting coefficient of dipole surface current.

The thesis has considered a printed dipole operating at 2.45 GHz. The dimensions (L and W) of the printed dipoles with microstrip balun are suitably chosen so that Z(dipole) equals to Z(in) to provide good input impedance matching at 2.45GHz . Geometry of printed dipole with microstrip balun operated at 2.45 GHz frequency is shown in figure 5.3. The dimensions of the dipole are listed in table 5.1. The microstrip line connects the unbalanced

coaxial line to the printed dipole via metalized hole. The ground plane of the microstrip line and the dipole strips are in the same plane. The via-hole connection creates 180^0 phase shift between the two dipole strips. The dipole is fabricated on FR-4 laminated board with permittivity ε_r = 4.6 and height=1.6mm. The minima of the return loss curve of the designed printed dipole appears at -18.86dB as shown in figure5.4. The surface current distribution and radiation pattern of the dipole are shown in figure5.5.

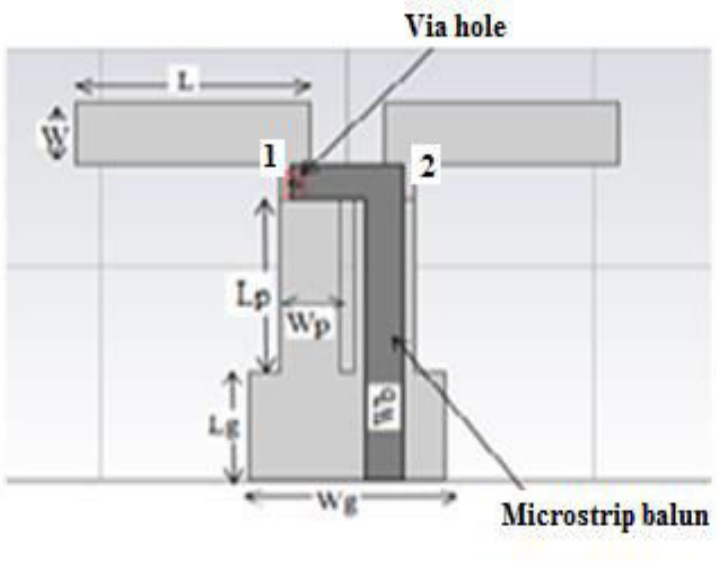

Figure 5.3 Structure of Printed dipole with microstrip balun

Table 5.1 Dimensions of printed dipole in λ

L	W	L_p	Wp	L_g	W_g	W_b	via hole radius
0.23	0.103	0.22	0.0086	0.17	0.25	0.05	0.005

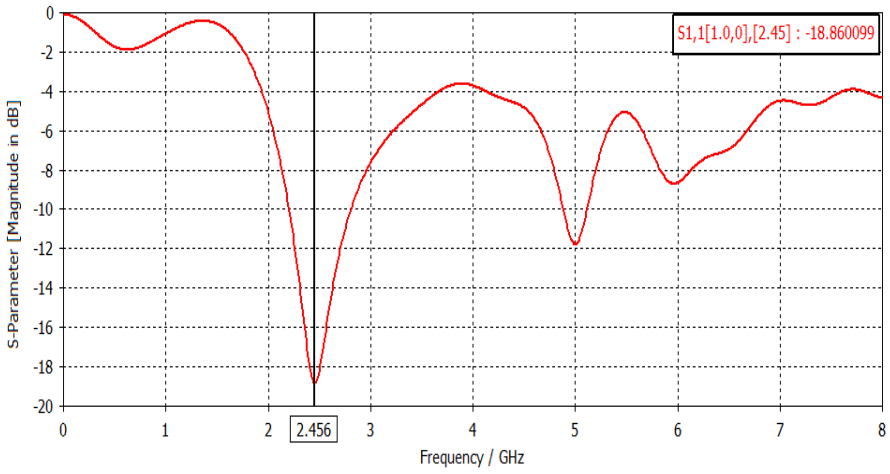

Figure 5.4 S_{11} of printed dipole with microstrip balun

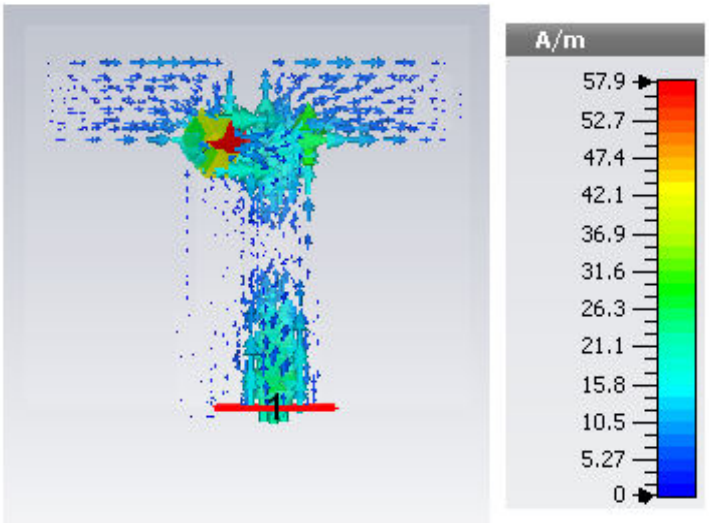

(a)

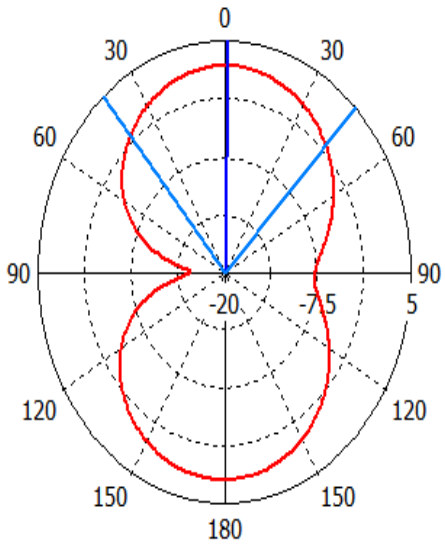

(b)

Figure 5.5 (a) Current distribution of Printed dipole

(b) Radiation pattern of Printed dipole

5.4 Design of TMAAs of Printed Dipole for Pattern synthesis

To demonstrate beam steering in TMAA, two examples are studied in the thesis. In first example TMAA is designed to operate at 2.45 GHz while the second example is designed to be operated at dual band, 2.45GHz and 5.8 GHz. A TMAA consisted of eight printed dipoles is also designed to meet the designing requirements.

5.4.1 Design of Power dividers

Antenna array is fed through a power divider. The Wilkinson power divider is considered in the thesis to feed the array. Figure 5.6 shows the equivalent transmission line circuit for a wilkinson power divider, where the power delivered to the two output ports is equal. The design of the wilkinson divider is composed of a transmission line that has been divided into a definite number of transmission lines, each one quarter-wavelength (λ/4) in length and λ is the operating wavelength.

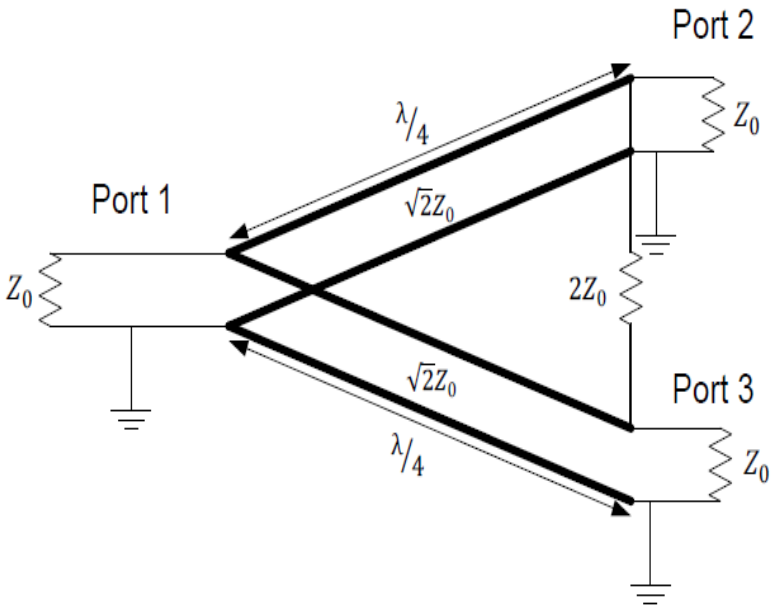

Figure 5.6 Two-way Wilkinson power divider

The impedance Z_0 of the power divider should match with the input impedance of the antenna elements. The printed Wilkinson power divider is designed to feed the 2-element antenna array. The geometry of printed power divider at 2.45 GHz is shown in figure 5.7. The dimensions of the power divider are listed in table 5.2.

The power divider is fabricated on FR4 substrate and is shown in figure 5.8. The S-parameters of power divider are shown in figure 5.9. It is observed from figure5.9 that the S_{11} of power divider is -27.45 dB at 2.45 GHz showing power is emerging well in the power divider through input port1. S_{21} and S_{31} are both equals to -3db ensuring that power is equally divided in two halves. The phase curves of S_{21} and S_{31} is shown in Figure 5.7(b) and it is seen that power is equally splitting without any phase difference between two output ports.

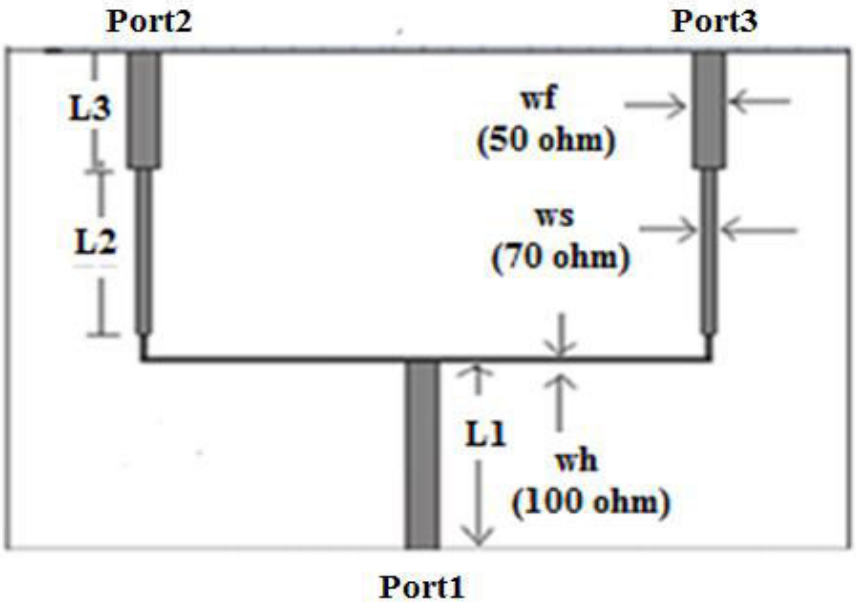

Figure 5.7 Geometry of printed power divider operated at 2.45 GHz

Table 5.2 Structural dimensions of power divider

PCB Substrate		Dimensions	
Thickness	1.6 mm	L1	8mm
ε_r	4.6	L2	12.33mm
tan δ	0.0018	L3	5mm
		Wf	1mm
		Ws	0.43mm
		Wh	0.15mm

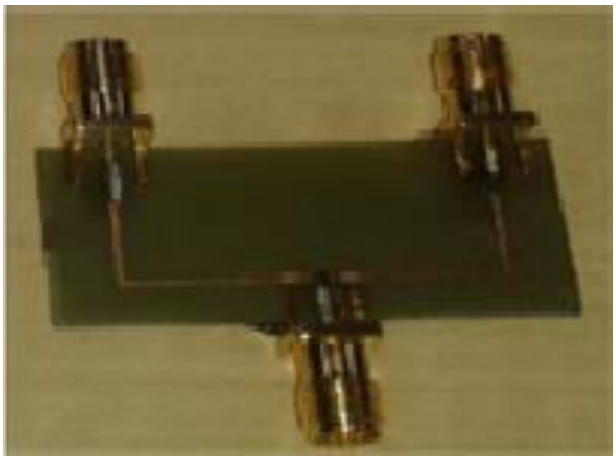

Figure 5.8 Fabricated 1:2 power divider

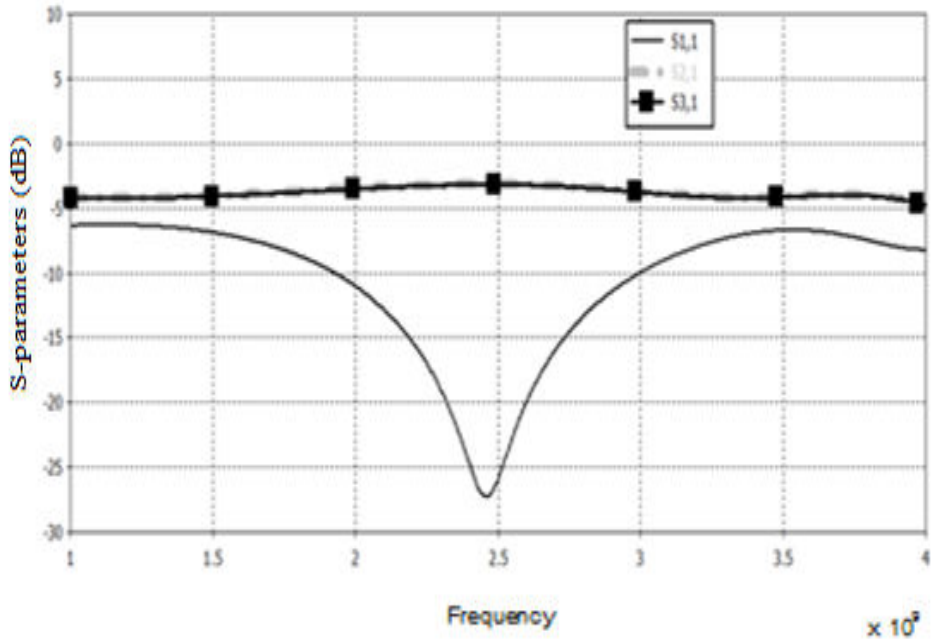

(a) Magnitude of S_{11},S_{21} and S_{31}

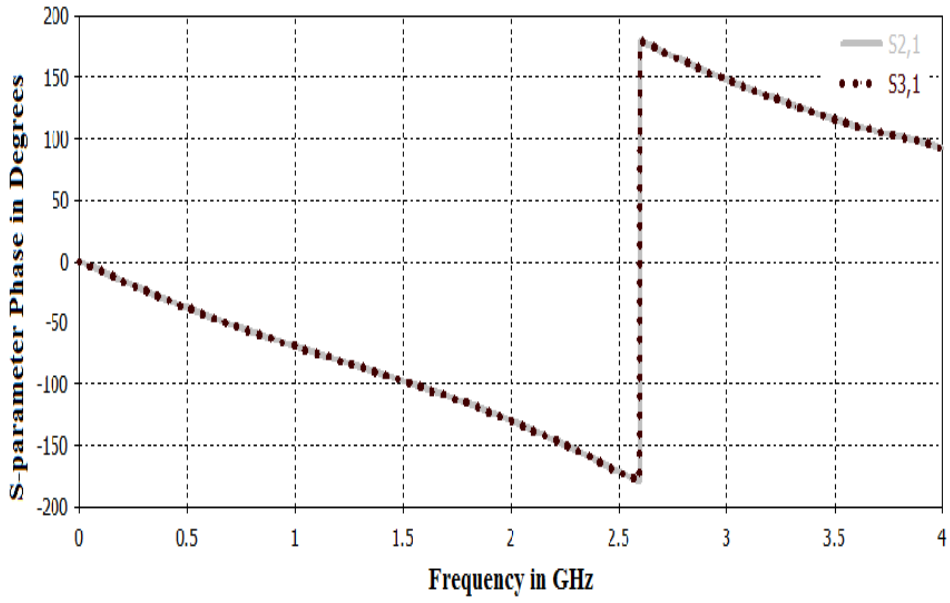

(b) Phase of $S_{11}$and S_{21}

Figure 5.9 S-parameters of Power divider (a) Magnitude of S_{11},S_{21} and S_{31} (b) Phase of $S_{11}$and S_{21}

The configuration of designed two way power divider is extended as shown in figure 5.10 for designing 1:8 power divider.

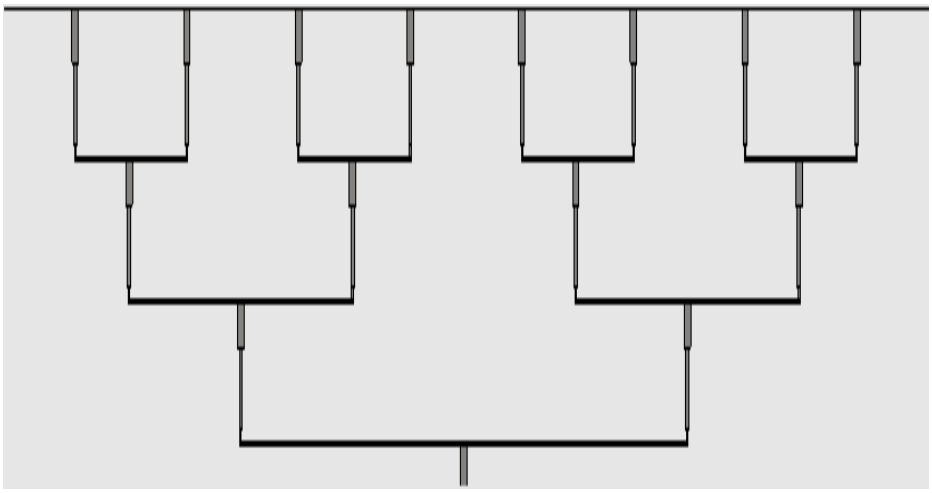

Figure 5.10 Layout of 1:8 Power divider

The 1:8 power divider is simulated using CST microwave studio. Scattering parameters of power divider are shown in figure.5.11 .It is observed that S_{11} of power divider is -15.70dB at operating frequency as shown in figure 5.11(a).The magnitudes of S-parameters shown in figure 5.8(b) are marginally deviated from -9dB ensuring almost equal power division at 2.45GHz.

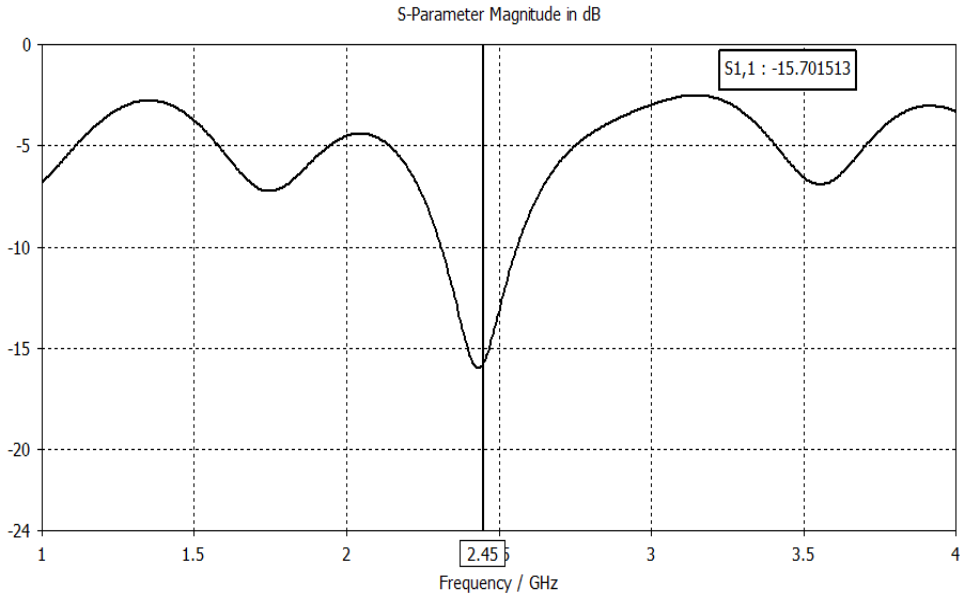

Figure 5.11(a)

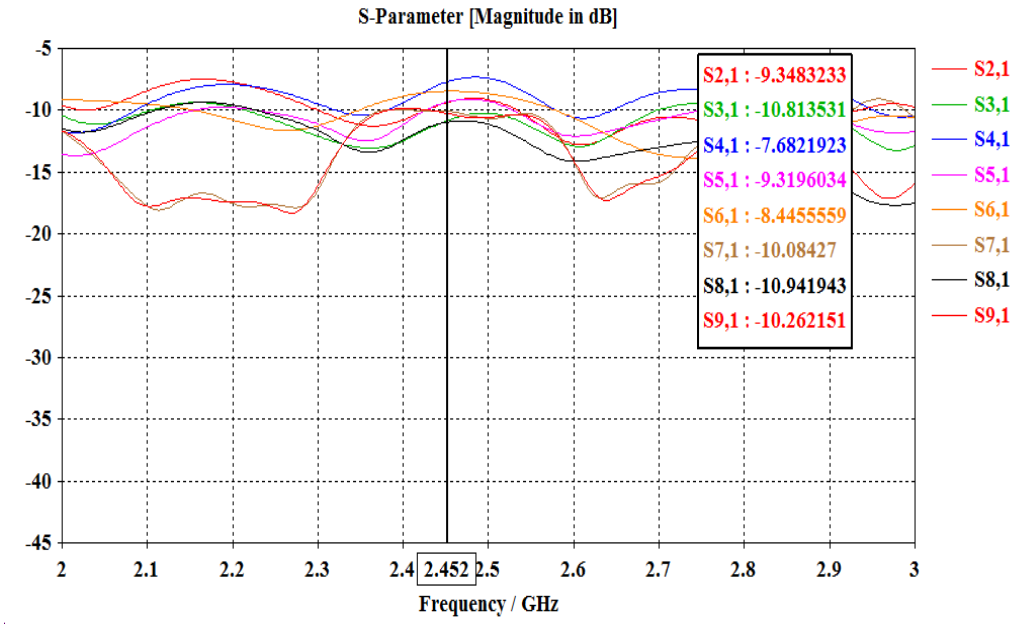

5.11(b)

Figure 5.11 Scattering parameter of Power divider
(a)S_{11} of Power divider
(b) S-parameters of Power divider

The dissertation has considered the design of wideband power divider to feed the dual band antenna array operating at 2.45GHz and 5.8 GHz. The layout of the wideband power divider is shown in figure 5.12. The size of the proposed power divider is 41mm x 30mm.

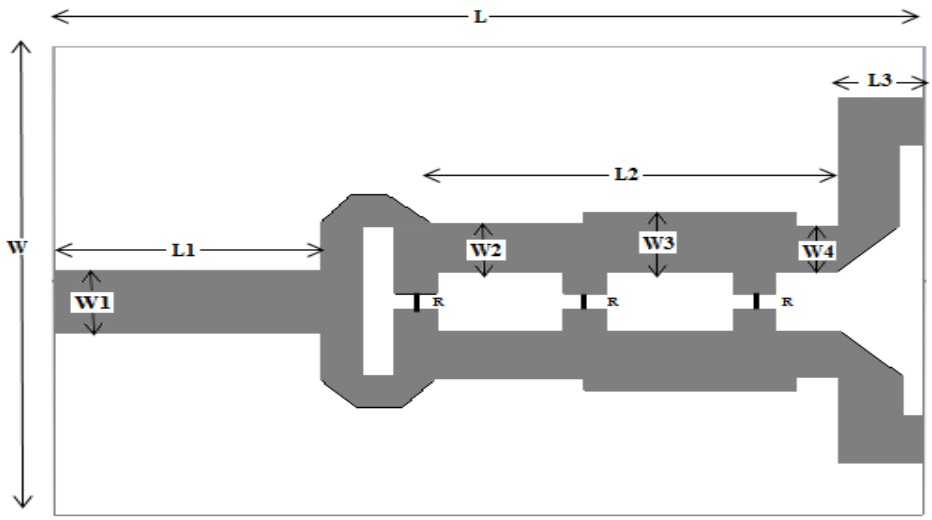

Figure 5.12 Layout of wideband power divider

The structure of front and the back side of the wideband power divider is taken identical which allows equal current distribution at both sides. Due to which this design of power divider can be used from both side. 100Ωresistors has been used to get all the ports matched to 50 Ω. The dimensions of the wideband power divider are shown in table 5.3. The fabricated wideband power divider is shown in figure 5.13.

Table 5.3 Dimensions of wideband power divider in mm

Parameter	L	W	L1	L2	L3	W1	W2	W3	W4
Dimensions	41	30	12.56	19	4	4	3.05	3.83	2.95

The S-parameters of the wideband power divider shown in figure5.14. It is seen that S_{11} is below -10dB from 2.1 GHz to 7GHz. figure 5.14 (b) shows that the magnitude of S_{21} and S_{31} are marginally deviated from -3dB ensuring almost equal power division at 2.45GHz. However it becomes almost -4.5dB at 5.8GHz. S_{21} and S_{31} are approximately at -3db which ensures that the power is equally divided in two halves. Figure 5.14(c) shows a small phase difference between port 2 and port 3 over the bandwidth and ensures almost equal power splitting. The designed wideband power divider operating for a wide range of frequencies from 2.1 GHz to 7 GHz will be used to feed the dual band antenna array in the thesis.

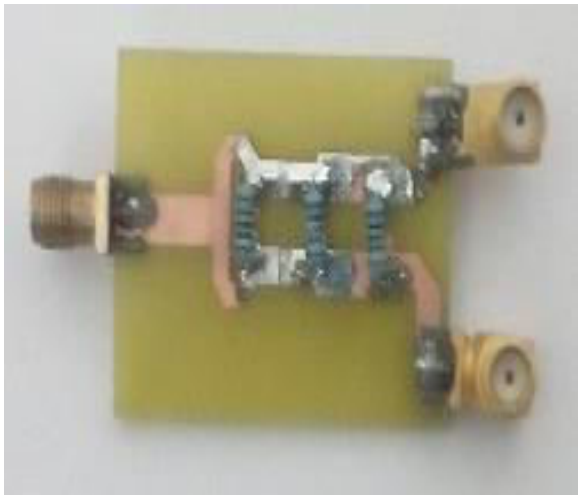

Figure 5.13 Fabricated wideband power divider

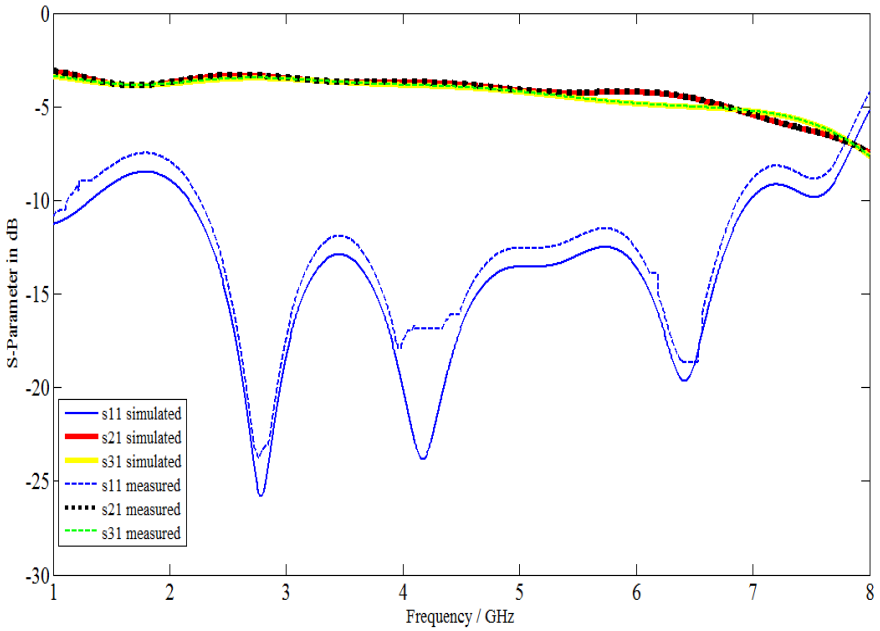

Figure 5.14(a)

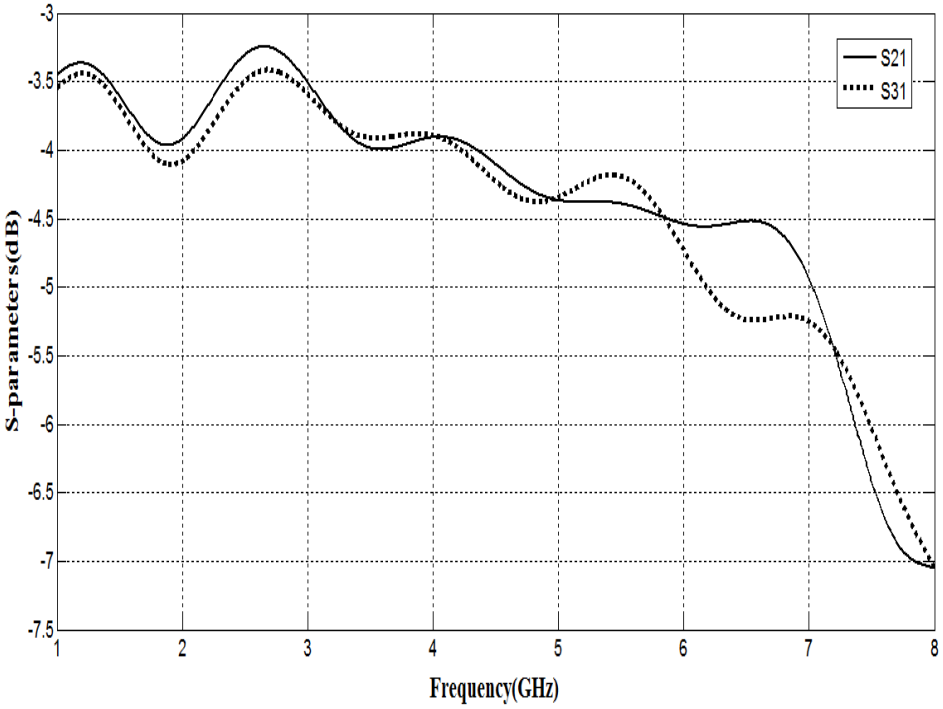

Figure 5.14 (b)

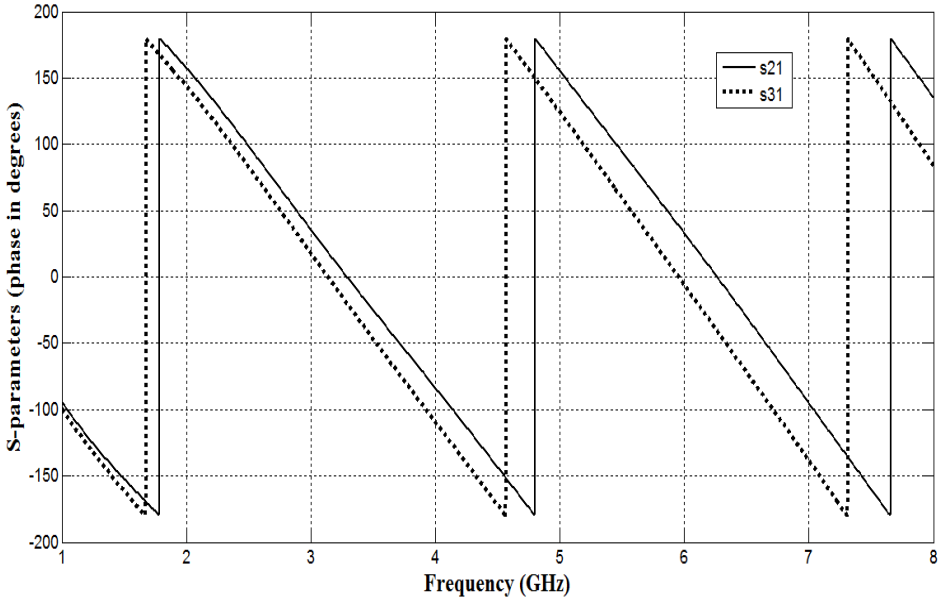

Figure 5.14 (c)

Figure 5.14 (a) Scattering parameters of wideband power divider
(b) Magnitude of simulated S_{21} and S_{31}
(c) Phase of simulated S_{21} and S_{31}

5.4.2 Design of Antenna arrays

At first, an antenna of two miniaturized microstrip fed printed dipoles with microstrip balun operating at 2.45 GHz is designed. The layout of the designed array is shown in figure 5.15.

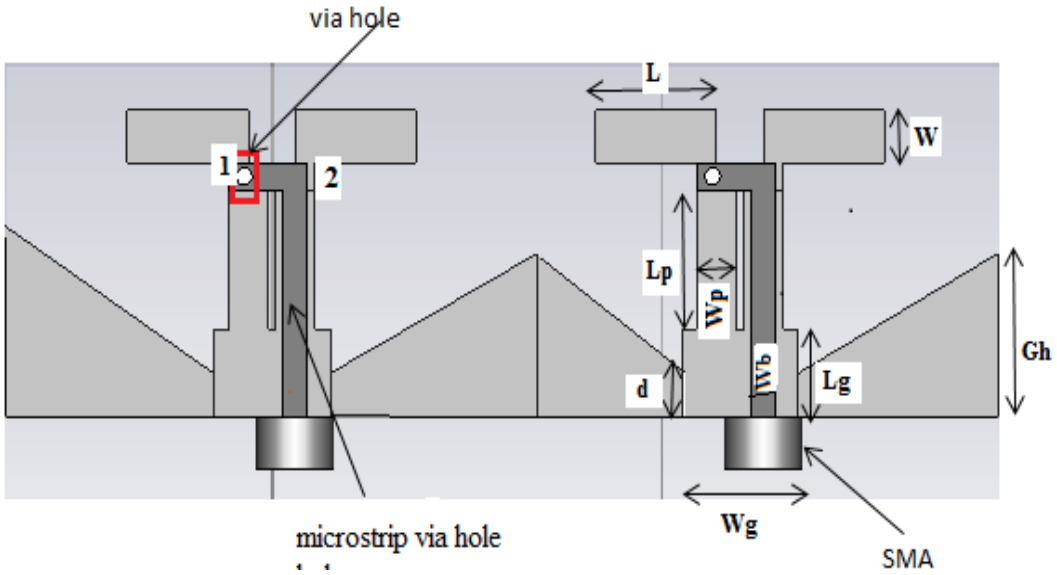

Figure 5.15 Schematic diagram of dipole array with V-shape ground

The shape of the ground is designed as V-shape which reflects the EM waves toward the feeding direction and broadens the antenna bandwidth performance. The dimensions of the antennas are listed in Table5.4. The array is fabricated on FR-4 laminated board of dimension 136mmX37mm with permittivity ε_r = 4.6 and height=1.6mm. The top view and bottom view of the fabricated printed dipole array with V-shape ground is shown in figure 5.16.

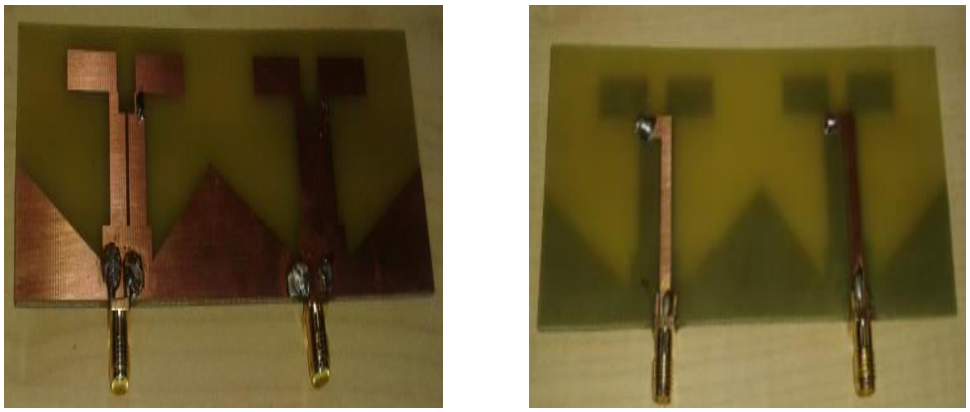

Bottom View
(a)

Top View
(b)

Figure 5.16 Fabricated dipole array with V-shape ground

Table 5.4 Structural parameters of printed dipole antenna

PCB Substrate	Thickness	1.6 mm
	ε_r	4.4
	tan δ	0.0018
Ground Plane	D	5 mm
	Gh	18.65 mm
	Lg	10 mm
	Wg	15 mm
	Lp	16 mm
	Wp	5 mm
Dipole Arm	L	16.7 mm
	W	6 mm
Microstrip Balun	Wb	3 mm
	via hole radius	1 mm

The array is fed through the 2:1 power divider shown figure 5.8. The simulated and measured S_{11} of the designed antenna array of V-shape ground are presented in figure 5.17 which shows that the antenna's configuration is matched at the 2.45 GHz. Measured S_{11}value and the corresponding bandwidth are tabulated in Table 5.5

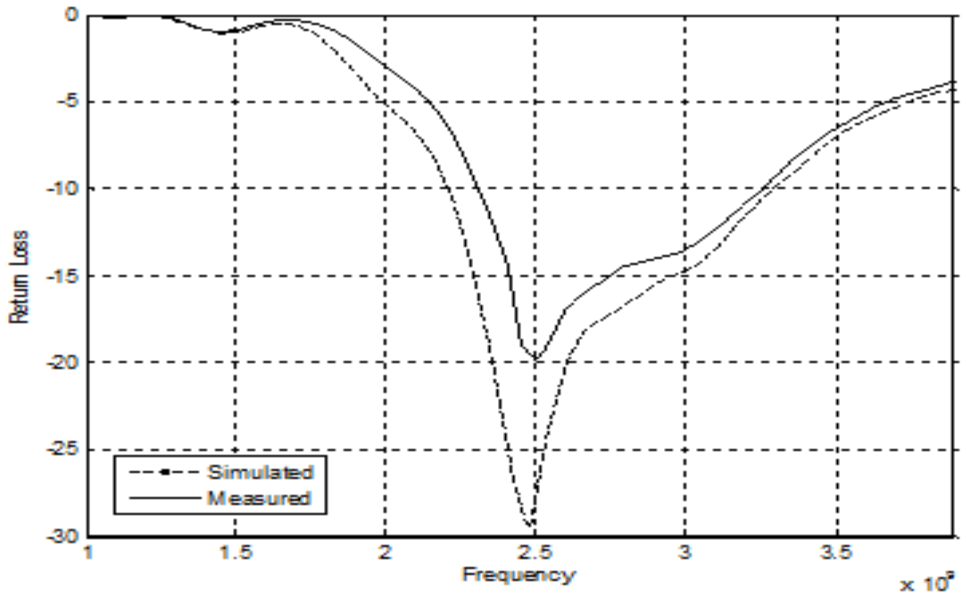

Figure 5.17 Return Loss (S_{11}) of dipole antenna array

The surface current distribution at 2.45 GHz on the microstrip line and the dipole strip is shown in figure5.18 which indicates biggest current density is on the arms of dipoles through microstrip via hole.

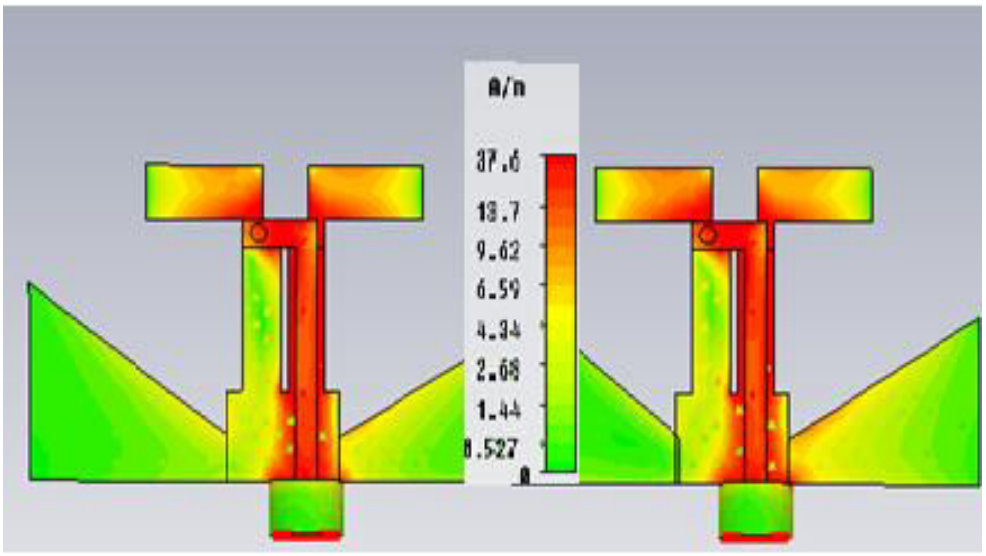

Figure 5.18 Simulated current distribution on microstrip line and dipole strip

Table 5.5 Results of printed dipole antenna array

Parameter	**Simulated value**	**Measured value**
S_{11}	-29dB	-20dB
Band width	990 MHz	954MHz

The V-shape of the ground structure is modified. Through extending and shaping the ground in U –shape, the coupling between the balun and the dipole is reduced and the antenna's impedance bandwidth and radiation are improved. The layout of the 2- elements printed dipole array with U-shape ground is shown in figure 5.19 utilizing the same FR4 substrate of dielectric constant of 4.6 with 1.6mm height. As shown in figure.5.19 the various parts of the dipole are chosen as L=16mm, L_p=13mm, L_g=10mm, W=6mm, W_p=5mm and W_g=15mm. The array has been simulated using CST Microwave EM simulator to characterize the antenna array performances.

The effects of the various dimensions of the ground plane i.e. the heights of the U shaped ground (**d** and $\mathbf{G_h}$) and the gap (**g**) between the two arms of the bottom ground layer are investigated in order to obtain optimized design parameters at two frequencies 2.45GHz and 5.8GHz.

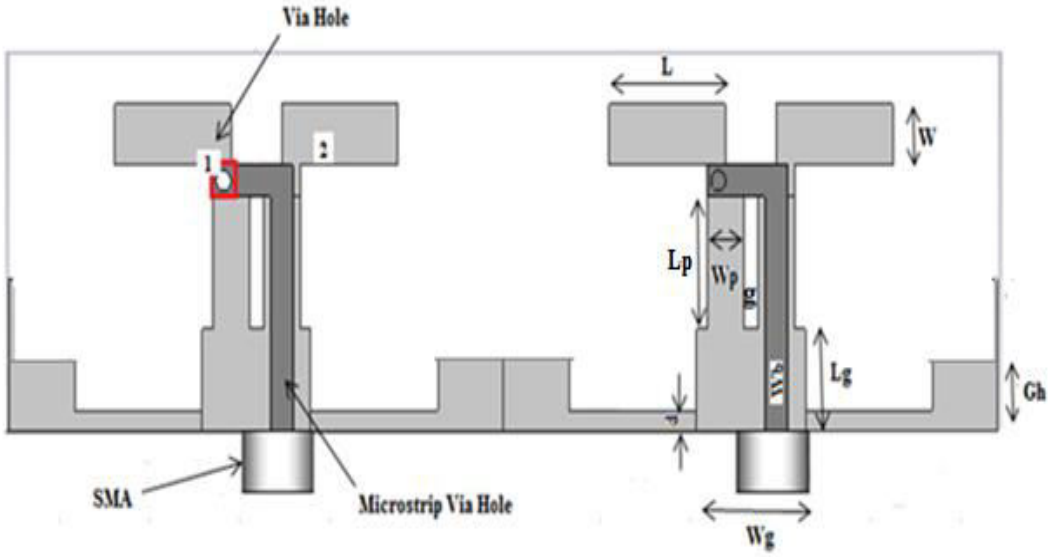

Figure 5.19 Layout of 2-Elements printed dipole array with U-shape Ground

At first G_h is fixed at 15mm and array is simulated for different values of **g** .The simulated return loss curves of the antenna array for different values of **g** is shown in figure 5.20.

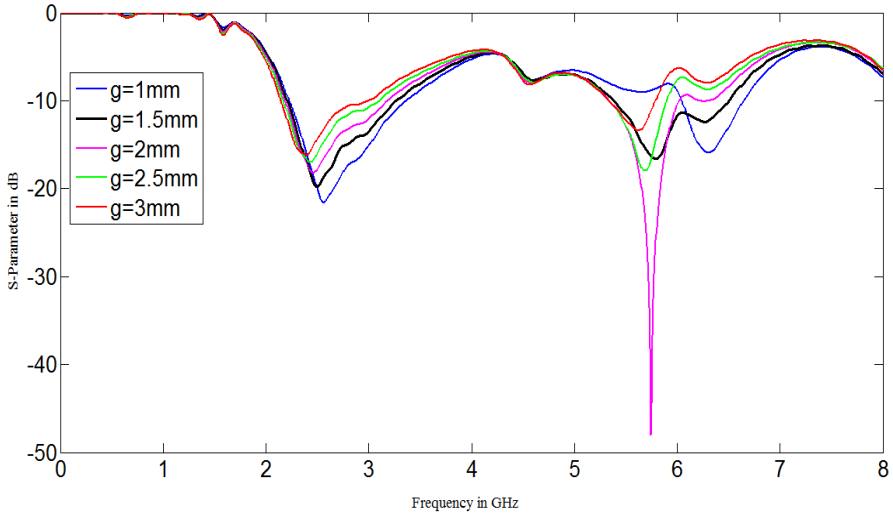

Figure 5.20 Return loss (S_{11}) curves of the antenna array for different values of g

The table 5.6 shows the S_{11} and bandwidth of the antenna array at both the resonance frequencies for different values of **g.** From figure 5.20 it is observed that as the g increases beyond 2mm the resonance frequencies decreases with increase in S_{11} and decrease in bandwidths at both the resonances. It is also observed that g=1.5mm offers maximum bandwidth of 1.01GHz at 2.45GHz and 1.12 GHz at 5.8 GHz respectively.

Table5.6 Effect of 'g'

Dimensions of 'g'	**Resonance Frequency**	**Return Loss (S_{11})**	**Bandwidth**
g=1mm	2.5GHz	-21.58dB	1.13GHz
	6.3GHz	-15.93dB	602MHz
g=1.5mm	2.45GHz	-19.81dB	1.01GHz
	5.8GHz	-16.57dB	1.12GHz
g=2mm	2.44GHz	-18.20dB	996MHz
	5.8GHz	-47.35dB	683.34MHz
g=2.5mm	2.4GHz	-17.01dB	937.24MHz
	5.7GHz	-17.94dB	561.67MHz
g=3mm	2.38GHz	-16.15dB	861.158MHz
	5.62GHz	-13.38dB	455.88MHz

we set g=1.5mm and G_h=15mm for studying the effects of other dimensions of ground. The smaller U-shape height **d** is varied to optimize the reflection coefficient and the bandwidth of the antenna. The simulated return loss curves of the antenna array for different values of **d** at g=1.5mm and G_h=15mm is shown in figure 5.21 and it is observed that as **d** increases the return loss curve improves but the bandwidth reduces at both the frequencies. Table 5.7

shows the S_{11} and bandwidth of the antenna array at both the resonance frequencies for different values of **d.**

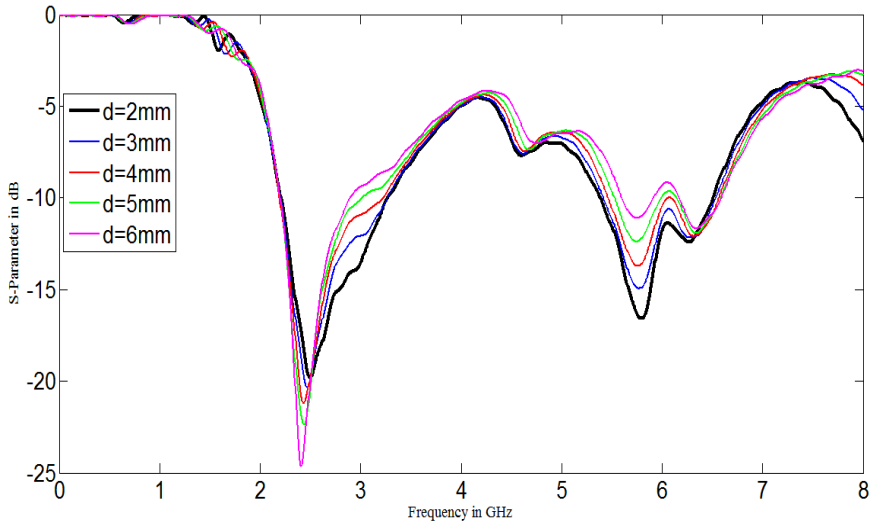

Figure 5.21 Return loss (S_{11}) of antenna array for different values of d

Table 5.7 Effect of 'd'

Dimensions of 'd'	**Resonance Frequency**	**Return Loss (S_{11})**	**Bandwidth**
d=2mm	2.45GHz	-19.80dB	1.06GHz
	5.8GHz	-16.578dB	1.12GHz
d=3mm	2.45GHz	-20.35dB	1.05GHz
	5.8GHz	-14.89dB	1.11GHz
d=4mm	2.43GHz	-21.16dB	1.03GHz
	5.77GHz	-13.68dB	594.59MHz
d=5mm	2.43GHz	-22.35dB	817.83MHz
	5.77GHz	-12.30dB	472.18MHz
d=6mm	2.4GHz	-24.47dB	696.61MHz
	5.7GHz	-11.09dB	315MHz

From the table 5.7 it is observed that at as the **d** increases both the resonance frequencies decreases with decrease in bandwidths. It is also observed that as **d** increases the, S_{11} improves at 2.45GHz and degrades at 5.8GHz.At d=2mm, a good trade off is obtained between return loss and frequency bandwidths at 2.45GHz and 5.8GHz frequencies.

Thus, we chose d=2mm and again vary G_h to study the S_{11} curves. Gh is investigated to get the optimum dimensions of the antenna array to operate at 2.45GHz and 5.8GHz. The simulated return loss curves of the antenna array for different values of G_h keeping

g=1.5mm and **d**=2mm is shown in figure 5.22. The S_{11} and bandwidth of the antenna array at both the resonance frequencies for different values of **Gh** is listed in table 5.8. It is observed from Table 5.8 that Gh=6mm is the optimum ground plane dimension that ensures the best tradeoff between return loss and bandwidth at both the frequencies.

Thus the optimum antenna dimensions achieved through rigorous simulation using CST microwave studio are listed in Table 5.9.

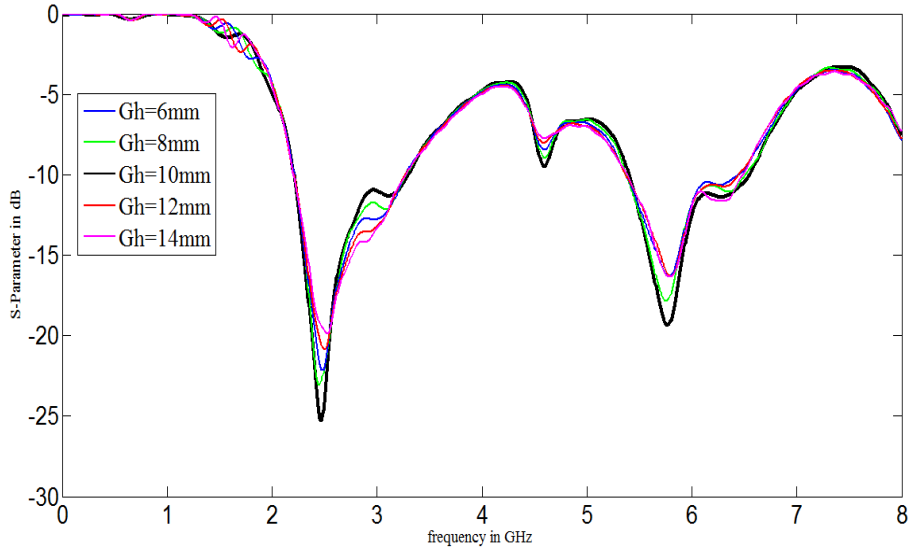

Figure 5.22 Return loss (S_{11}) of antenna array for different values of $\mathbf{G_h}$

The array is fabricated on FR-4 laminated board of dimension 136mmX37mm with permittivity ε_r = 4.6 and height=1.6mm. The top view and bottom view of the fabricated printed dipole array with U-shape ground is shown in figure 5.23.

Table 5.8 Effect of 'Gh'

Dimensions of 'Gh'	**Resonance Frequency**	**Return Loss (S_{11})**	**Bandwidth**
Gh=6mm	2.45GHz	-25.28dB	1.21GHz
	5.8GHz	-19.31dB	1.11GHz
Gh=8mm	2.45GHz	-23.05dB	1.07GHz
	5.76GHz	-17.84dB	1.13GHz
Gh=10mm	2.48GHz	-22.16dB	1.06GHz
	5.8GHz	-16.24dB	1.08GHz
Gh=12mm	2.48GHz	-20.70dB	1.06GHz
	5.8GHz	-16.28dB	1.08GHz
Gh=14mm	2.48GHz	-19.38dB	1.07GHz
	5.8GHz	-16.30dB	1.1GHz

Table.5.9 Structural parameters of dipole antenna

PCB Substrate	Thickness	1.6 mm
	ε_r	4.6
	tan δ	0.0018
Ground Plane	d	2mm
	G_h	6 mm
	L_g	10 mm
	W_g	15 mm
	L_p	13 mm
	W_p	5 mm
Dipole Arm	L	16 mm
	W	6 mm
	G	1.5mm
Microstrip Balun	W_b	3 mm
	via hole radius	1 mm

The designed array with U-shaped ground is excited by using wideband power divider shown in figure5.13. The simulated and measured S_{11} of the designed antenna array is presented in figure 5.24 from which it is evident that the antenna's configuration is matched at the 2.45GHz and 5.8GHz frequencies. Simulated and measured S_{11} value and the corresponding bandwidth are tabulated in Table 5.10.

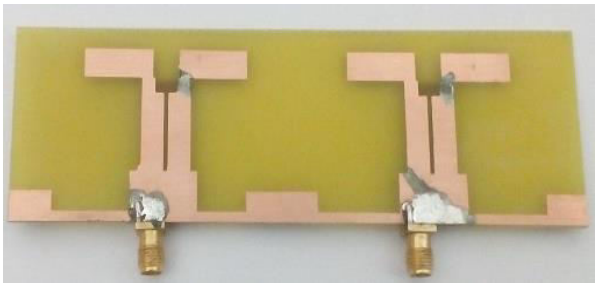

(a)

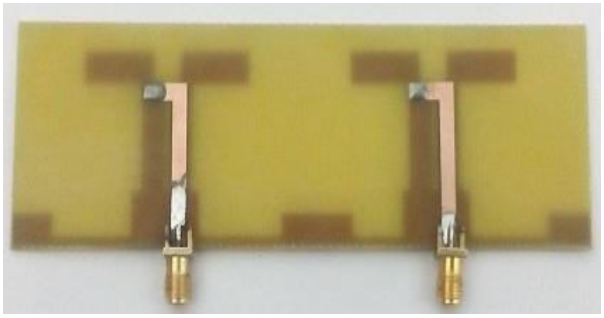

(b)

Figure 5.23 Printed Dipole Array with U-shape Ground
(a) Bottom view (b) Top view

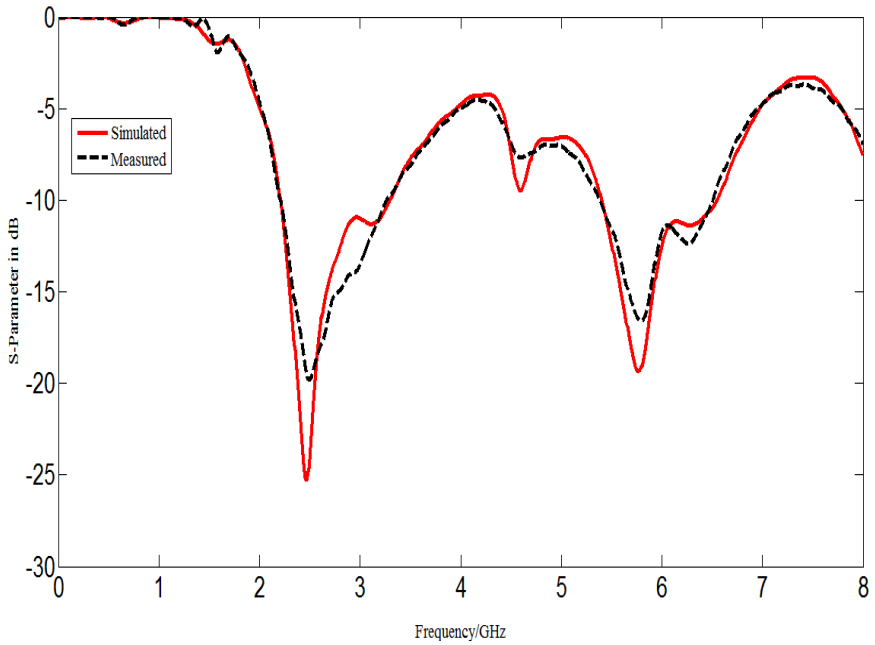

Figure 5.24 Return Loss (S_{11}) of dipole antenna array with U-shape ground

Table5.10 Simulated and measured $S_{11}$and bandwidth

Frequency	**Parameter**	**Simulated value**	**Measured value**
2.45 GHz	S_{11} Band width	-25.28dB 1.21GHz	-20.02dB 1.09GHz
5.8GHz	S_{11} Band width	-19.33dB 1.11GHz	-17.00dB 1.03GHz

The table5.10 shows that the measured return loss and bandwidths at both the frequencies are in good agreement with the simulated values. The current distribution of the designed array is shown in Figure. 5.25. In Figure. 5.25 (a) the current distribution at 2.45 GHz is shown which indicates biggest current density is on the arms of dipoles through microstrip via hole. As shown in Figure. 5.25 (b) lesser current density is at the arms of dipoles due to higher order resonance.

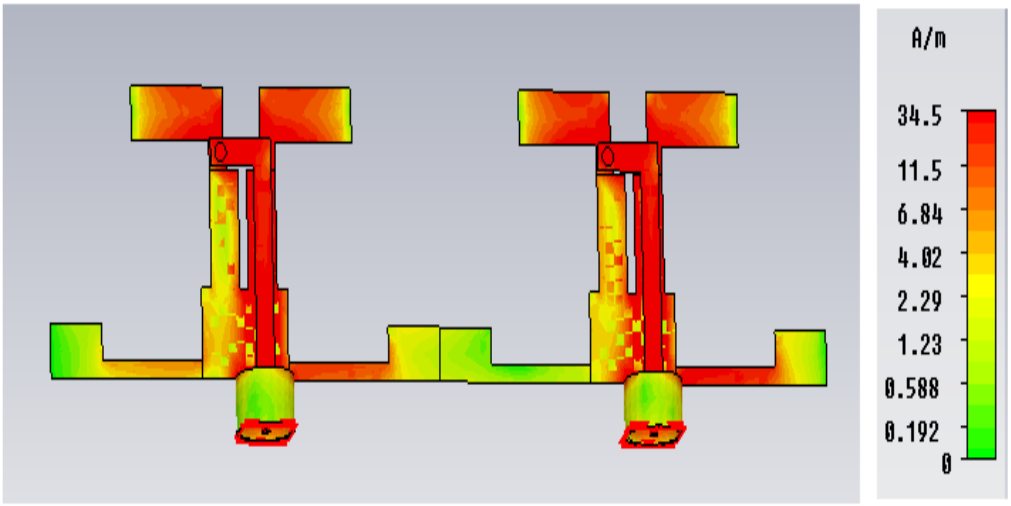

Figure 5.25 (a) Simulated current distribution on microstrip line and dipole strip at 2.45GHz

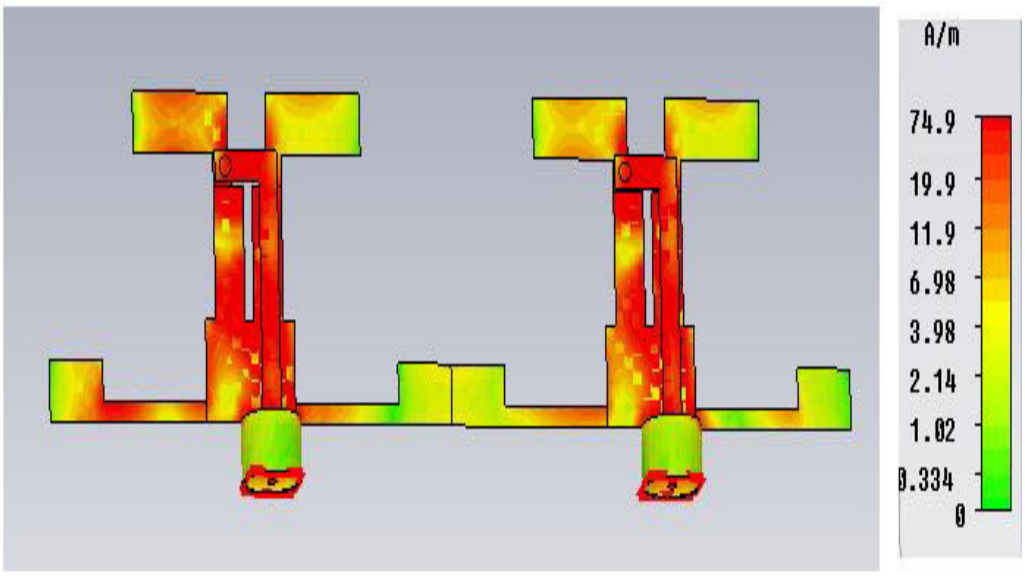

Figure 5.25 (b) Simulated current distribution on microstrip line and dipole strip at 5.8GHz

The thesis has also studied the antenna array of eight elements with integrated power divider on the same FR4 substrate is designed to operate at 2.45 GHz. The configuration of proposed 8-element array is shown in figure5.26 and the fabricated array is shown in figure5.27.

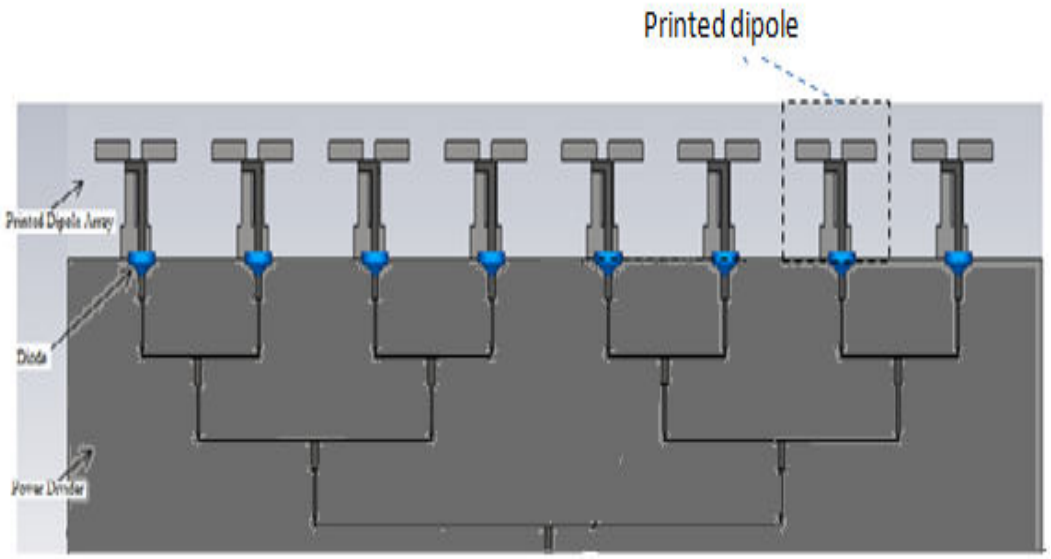

Figure 5.26 Layout of 8-element TMAA

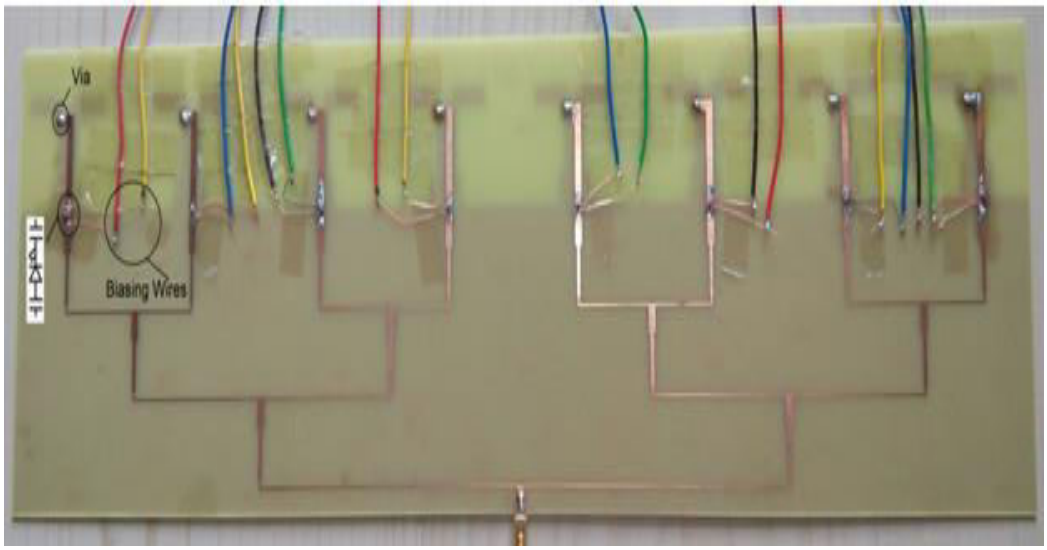

Figure 5.27 Fabricated 8-element TMAA

For controlling the ON/OFF behaviour of array elements, PIN diodes are inserted between the output of power divider and input of each element of the array. Figure 5.28 is showing the simulated and measured return loss of the proposed array which shows that the array is matched at 2.45 GHz operating frequency.

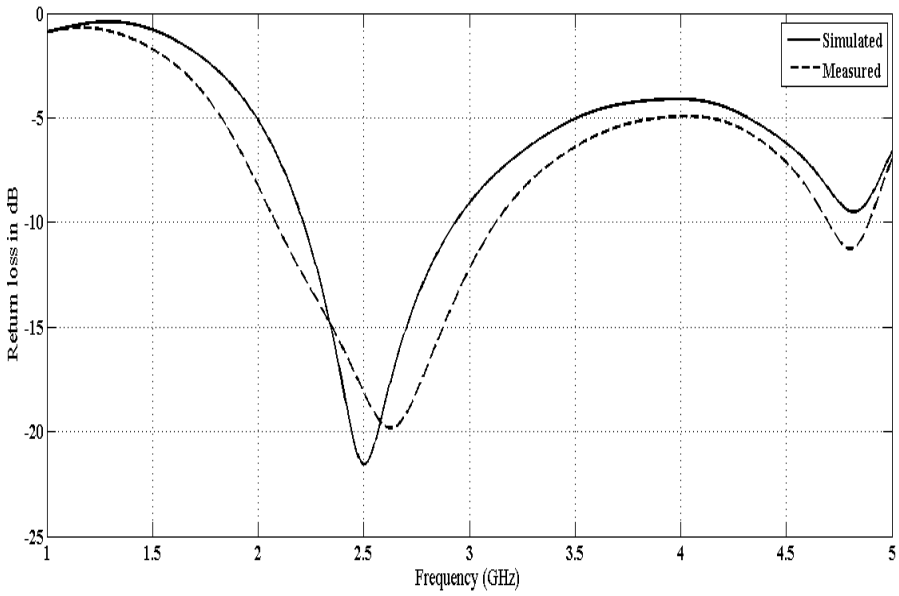

Figure 5.28 Return loss (S_{11}) of the 8-element TMAA

5.4.3 Design of TMAA for Beam Steering at 2.45GHz

At first, beam steering is presented at 2.45 GHz using TMAA of printed dipoles with V-shape ground. The elements of array coupled with high-speed RF switches are excited through power divider (fig.5.8). The RF switch consisting of PIN diode (BAR-63) is shown in figure 5.29.

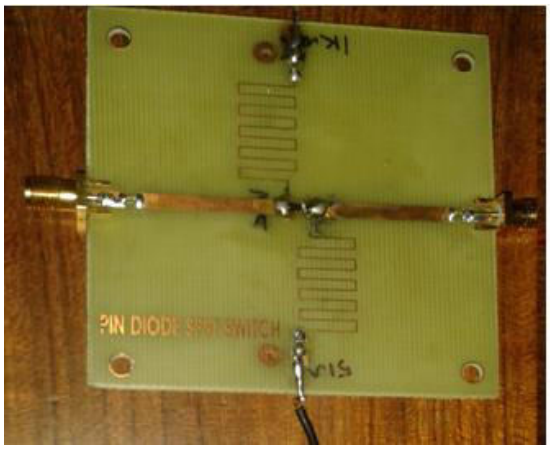

Figure 5.29 PIN diode RF switch

Both the antennas are excited with the common complex excitation signal using Eq. (4.11). It causes progressive phase differences between two elements. Relative phase difference between elements steers the beam at different angles. A CPLD used to generate the required

sequences to control the high-speed RF switches is shown in figure 5.30.Rectangular pulse train with amplitude 3V and repetition frequency 1MHz is applied for biasing through two bias ports of the PIN diode. Two capacitors of 10 nF are used on the balun to block the dc signal flowing back to the RF input. An inductor of 56 nH is connected between the dc bias source and PIN diode to block the RF leakage from it. A 100Ω resistor is used to limit the voltage across the diode as shown in figure 5.31.

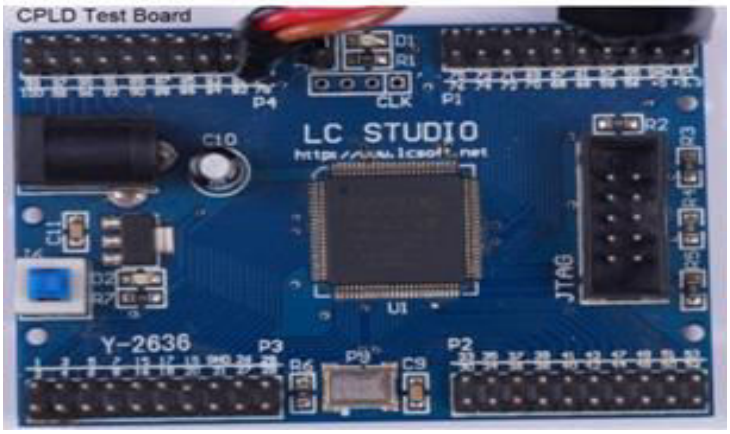

Figure 5.30 CPLD

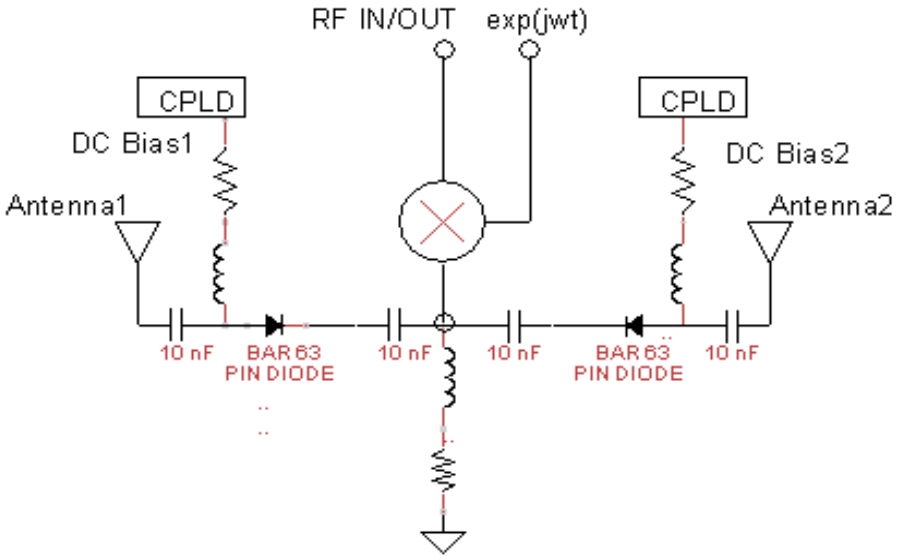

Figure 5.31 Dipole array with SPST PIN diode switch

The radiation pattern of the designed TMAA is measured and the measurement set-up is shown in figure 5.32. The radiation performance in E and H planes at two possible combinations of switches are shown in table 5.11. The radiation patterns are shown in figure 5.33. It is observed that the main lobe becomes sharper with improvement in gain when both the switches are ON i.e both the elements of TMAA are excited. The switches offer an isolation of 25 dB and an insertion loss of 0.6 dB.

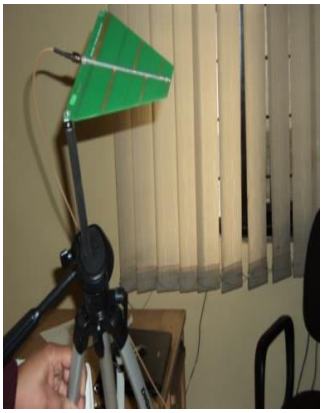

Log periodic antenna as transmitter

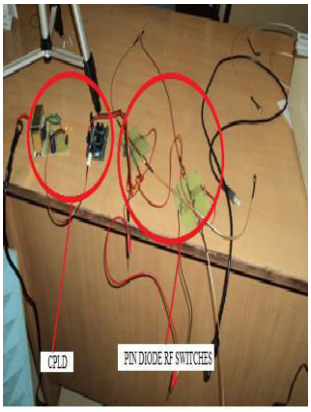

Feed Network

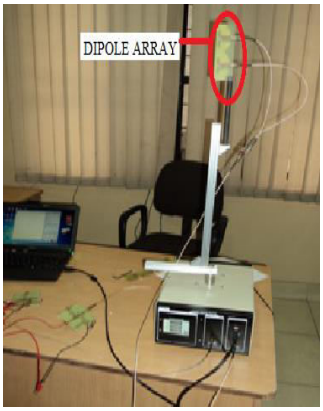

Dipole array as Receiver

Figure 5.32 Radiation measurements Setup

Table 5.11 Measurement performance of proposed TMAA

Switches	Measuring plane	Angular width	Gain
Both ON	E-plane	51.7°	6.3dB
	H-plane	184.6°	9.1dB
Only one ON	E-plane	102.6°	4.4dB
	H-plane	197.4°	6.1dB

After setting $t_{o1} = 0$ and $\tau_1 = \tau_2 = 0.5\mu s$ steering of beam in various directions is achieved by changing the t_{02} of RF switch as shown in table 5.12.

Radiation patterns of the designed antenna for different values of t_{o2} are shown in figure 5.34.

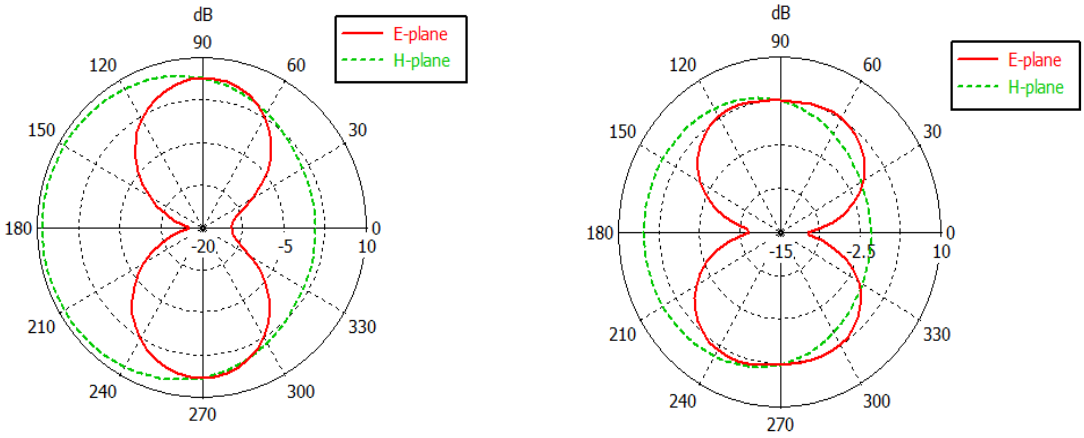

(a) (b)

Figure 5.33 Radiation pattern
(a) when both switches are ON
(b) when only one switch is ON

Table 5.12 Switch on instant and main beam direction

T_{o2} (μs)	**Phase Difference**	**Beam Steers**
0	0	0
0.125	$\pi/4$	-15
0.25	$\pi/2$	-25
0.375	$3\pi/4$	-30
0.5	π	-40

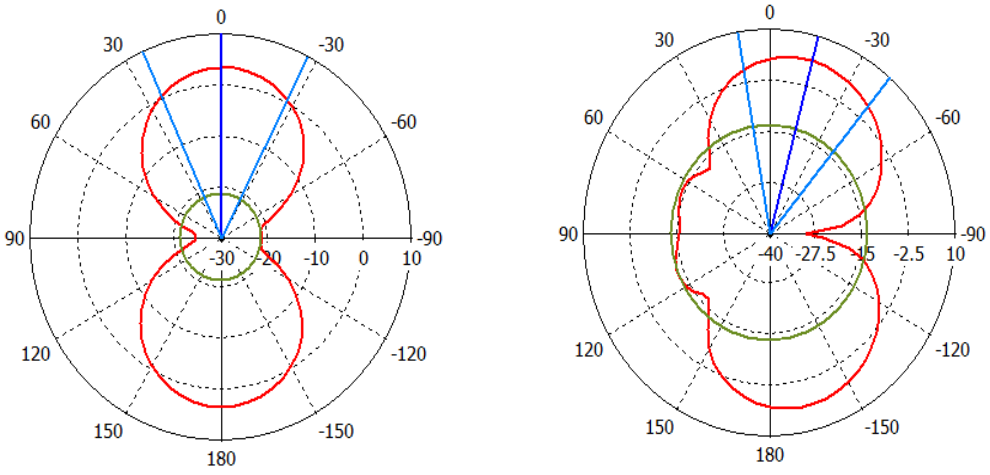

(a) **(b)**

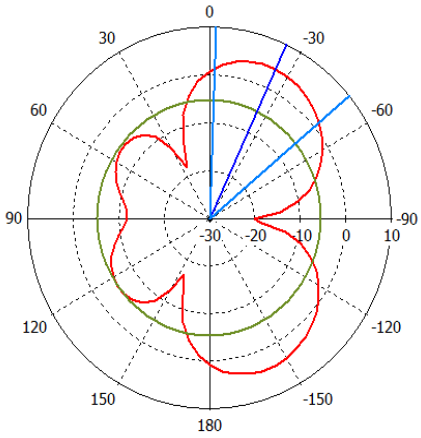

(c)

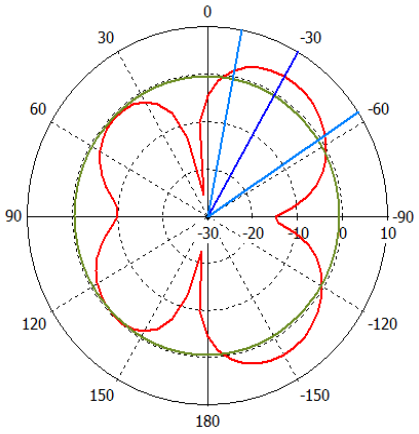

(d)

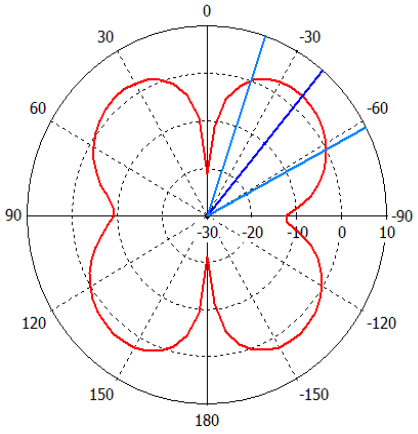

(e)

Figure 5.34 Radiation pattern at (a) t_{o2}=0 µsec (b) t_{o2}=0.125 µsec (c) t_{o2}=0.25 µsec (d) t_{o2}=0.375 µsec (e) t_{o2}=0.5 µsec

5.4.4 Synthesis of Dual Band TMAA

In this design of TMAA, Antenna array of 2-printed dipoles with U-shape ground (fig.5.23) coupled with RF switches (fig.5.29) are excited by wideband power divider (fig. 5.13). TMAA is synthesized to increase the dynamic efficiency of the array as well as to achieve beam steering at two resonance frequencies i.e. 2.45GHz and 5.8 GHz and their sidebands without using phase shifters.

The problem will find the switch-on time and switch-off time in each time step for each element in order to get the desired dynamic efficiency. To achieve the design goal the fitness function is formulated as

$$Fitness = k_1 SLL + k_2 (1/\eta) \qquad (5.3)$$

Where SLL and η are the SLL and dynamic efficiency of the array for optimized time sequences and k_1 and k_2 are two constants.

DE algorithm is applied as the global optimization method. To achieve $\eta \geq 98\%$, the time sequences are calculated as $\tau_1=0.6035, \tau_2=0.2548, t_{01}=0, t_{02}=0.1226$.

A continuous complex exponential signal is applied to excite the phase differences between dipoles. The radiation pattern is measured and the corresponding contour plots are shown in figure 5.35 and figure 5.36 at 2.45 GHz and 5.8 GHz respectively. The optimized radiation patterns are shown in figure 5.37 and figure 5.38 which show that the beam is steered at 30° at both the central frequencies as well as first positive sidebands. Though the sideband levels of harmonics of both the resonating frequencies have been reduced to increase the dynamic efficiency of the array ,the beams steered in different directions at sidebands may be utilized for other applications as well .Table 5.13 shows the desired and obtained values of SLL at centre frequency as well as first sidebands. The modulation of the switch-on time instant of the rectangular pulses varies the relative phase differences between elements. The radiation pattern is measured at both the resonating frequencies at different values of t_{02} and the beam steering characteristics of the designed system is clearly observed in figure 5.39 and figure 5.40.

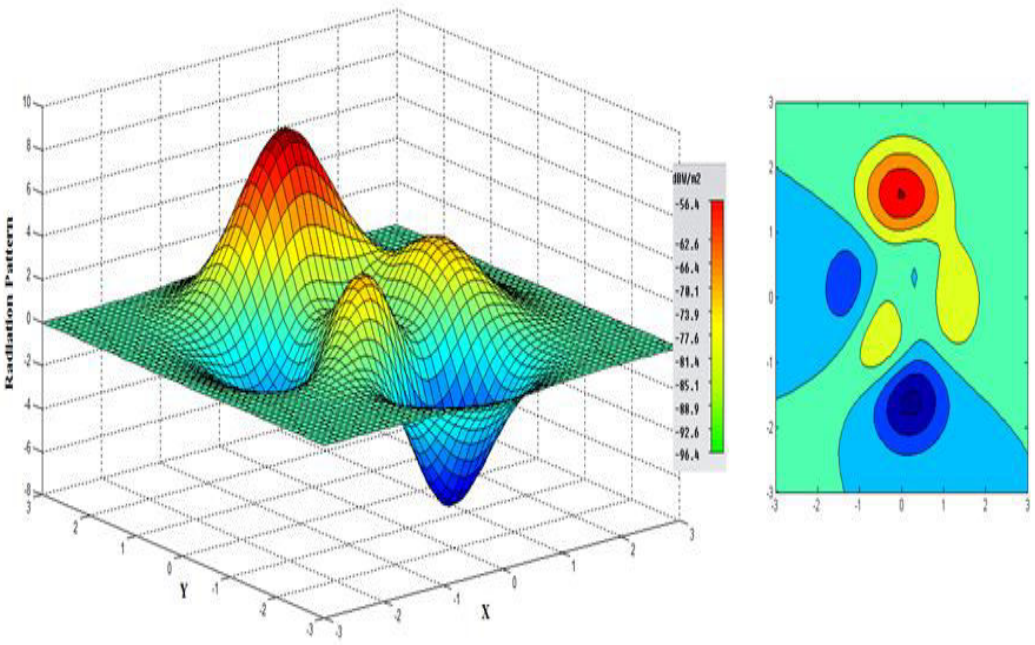

(a) 3-D Radiation Pattern Plot (b) Contour plot

Figure 5.35 Optimized radiation pattern at centre frequency 2.45 GHz

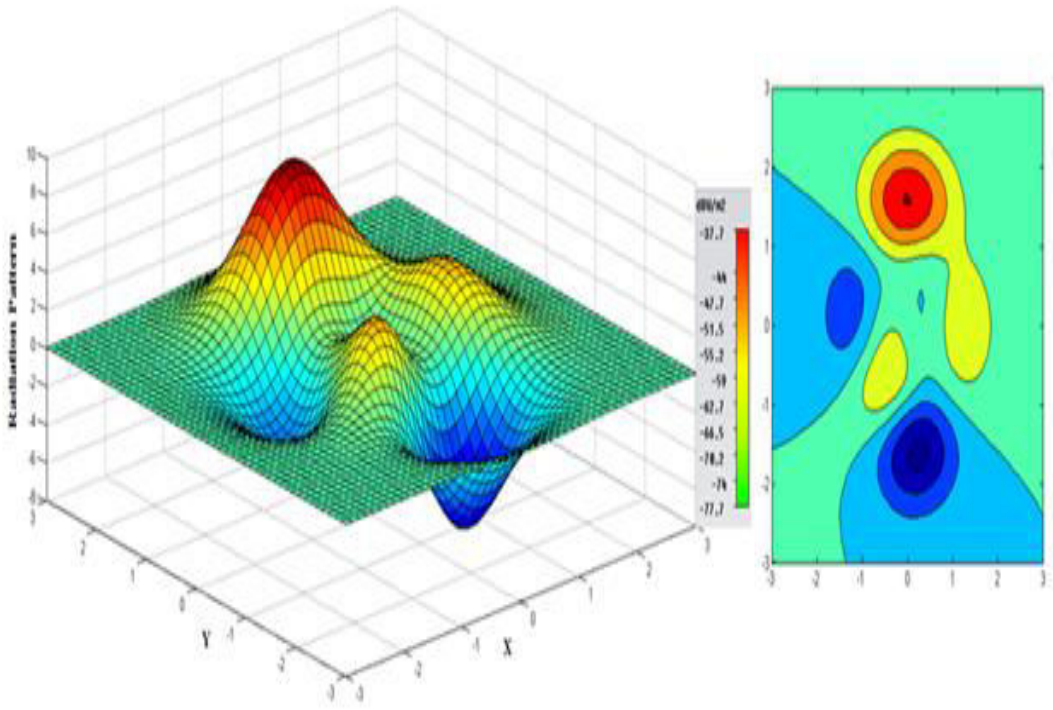

(a) 3-D Radiation Pattern Plot (b) Contour plot

Figure 5.36 Optimized radiation pattern at centre frequency 5.8 GHz

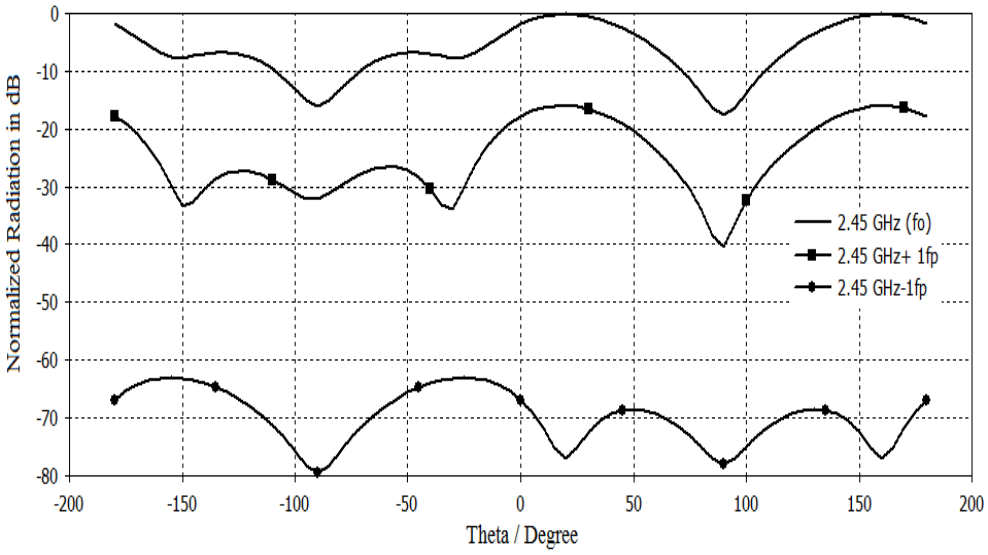

Figure 5.37 Radiation pattern at centre frequency 2.45 GHz andsidebands.

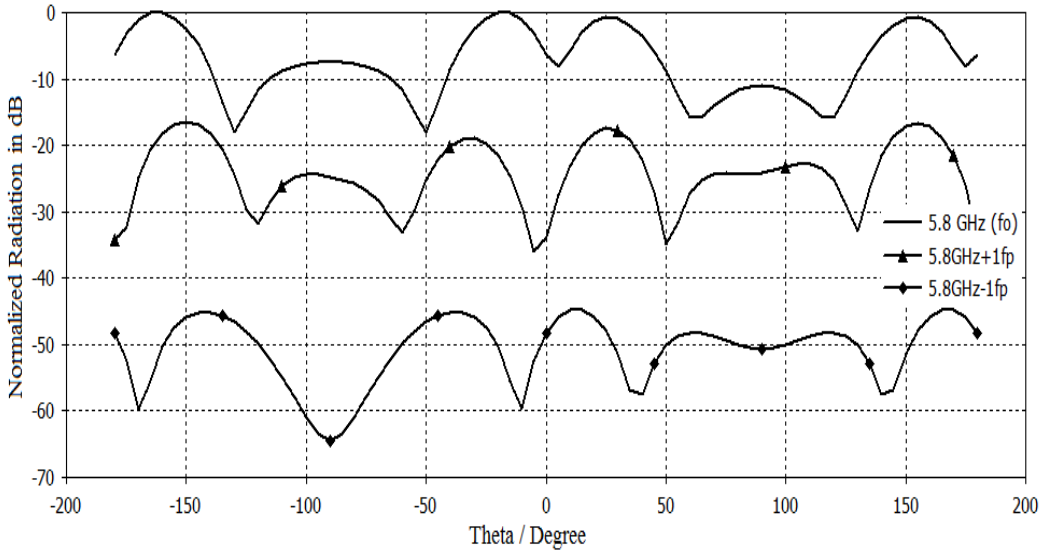

Figure 5.38 Radiation Pattern at Centre Frequency 5.8 Ghz andSidebands.

Table 5.13 Desired and obtained SLL

Design Parameter		**Side Lobe Level(dB)**	
		Desired	Obtained
2.45 GHz	f_0 (2.45GHz)	-8	-7.1
	f_0+f_p(2.451GHz)	≤ -25	-26.28
	f_0-f_p(2.449GHz)	≤ -45	-68.34
5.8GHz	f_0 (5.8GHz)	-8	-7.68
	f_0+f_p(5.801GHz)	≤ -25	-24.53
	f_0-f_p(5.799GHz)	≤ -45	-48.142

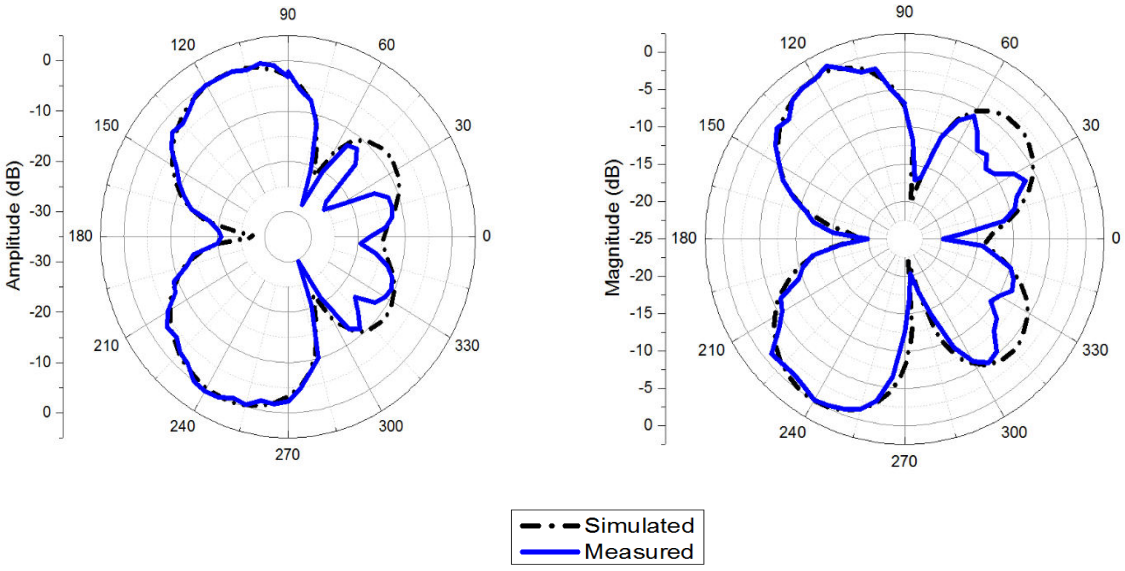

(a) (b)

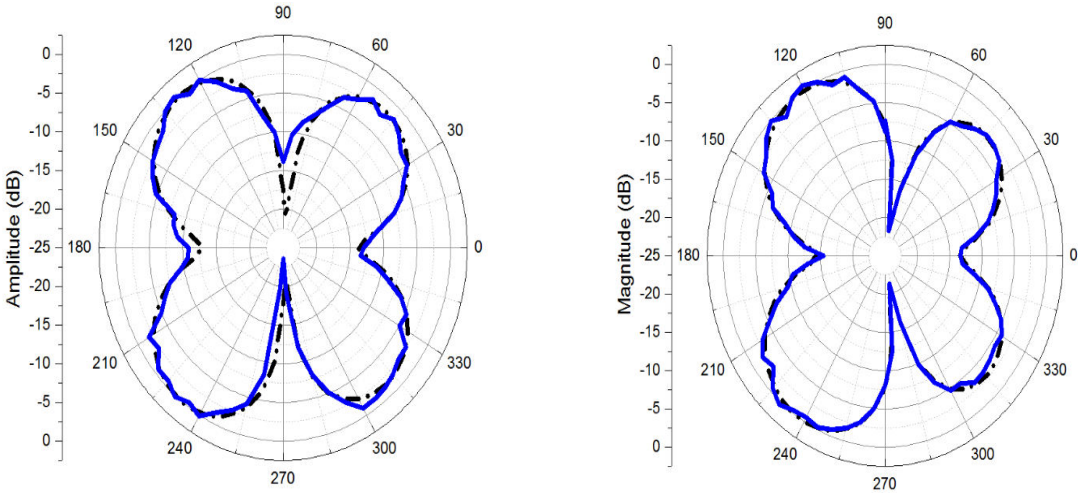

(c) (d)

Figure 5.39 Simulated and measured radiation patterns for different values of t_{02} At 2.45GHz (a) t_{02} =0 μ sec. (b) t_{02}=0.125 μ sec. (c) t_{02} =0.25 μ sec. (d)t_{02} =0.375 μ sec.

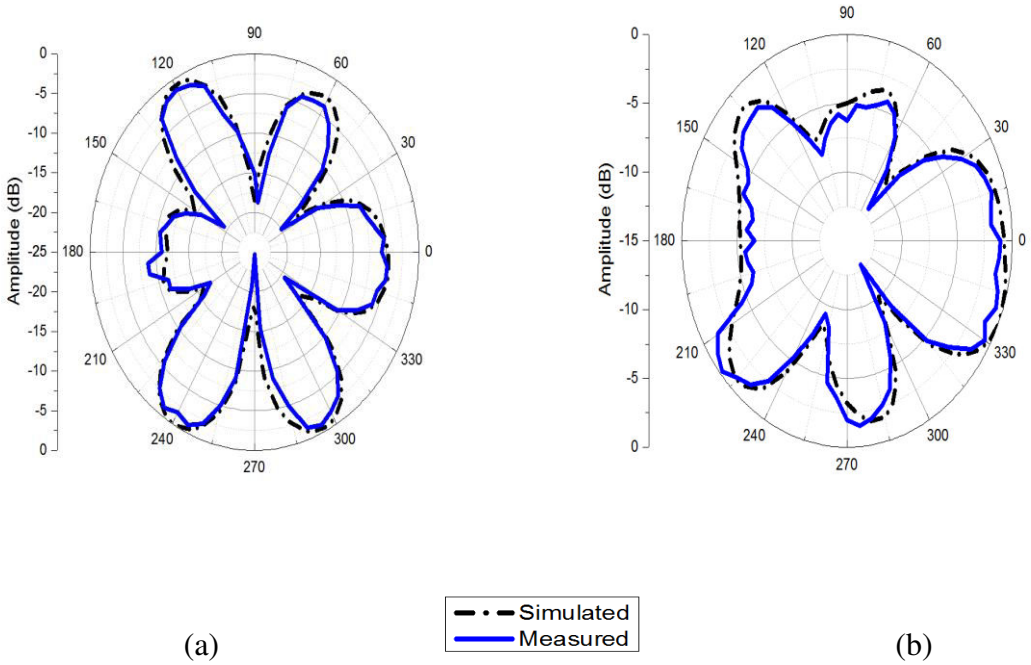

(a) (b)

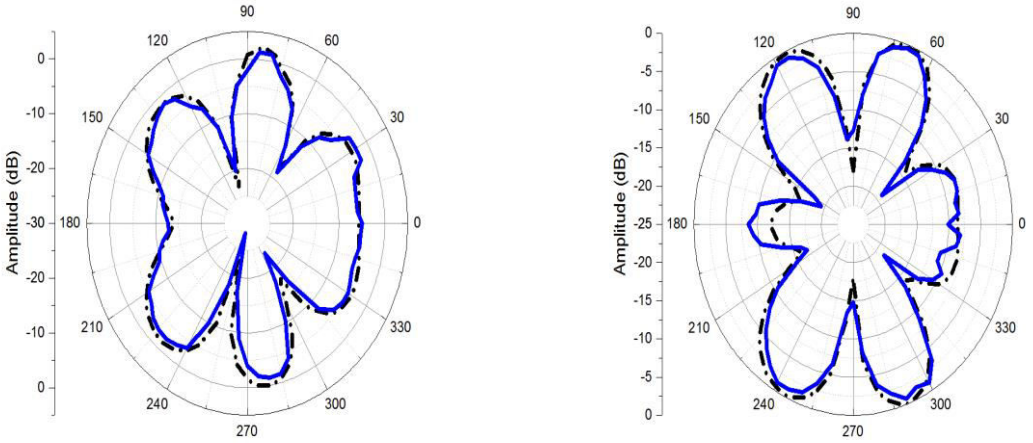

(c) (d)

Figure 5.40 Simulated and measured radiation pattern for different values of t_{02} at 5.8 GHz (a) t_{02} =0 μ sec. (b) t_{02}=0.125 μ sec. (c) t_{02} =0.25 μ sec. (d) t_{02} =0.375 μ sec.

5.4.5 Synthesis of 8-Element TMAA

The appropriate on time duration (τ_n) of RF switches connected to each element of TMAA for synthesizing the desired radiation pattern at 2.45GHz with specified SLL for a given HPBW condition will be calculated. To achieve the designing goal, the following fitness function is formulated:

$$Fit(\tau_n) = \begin{cases} (SLL_o - SLL_d)^2_{f=f_0} & if \quad HPBW_o \le HPBW_d \\ 1000 & otherwise \end{cases} \qquad (5.4)$$

SLL_d and SLL_o are desired and obtained SLL respectively while $HPBW_d$ and $HPBW_o$ are desired and obtained HPBW respectively. The switching time sequence { τ_n : n = 1, 2,....,8} is considered as optimization parameter that is improved in iterations in order to minimize the fitness function.

In order to achieve the desired radiation performance, The ECSS optimization is used to calculate the timing sequence which are shown in figure 5.41. A complex programmable logic device (CPLD) is used to generate the calculated timing pulses.

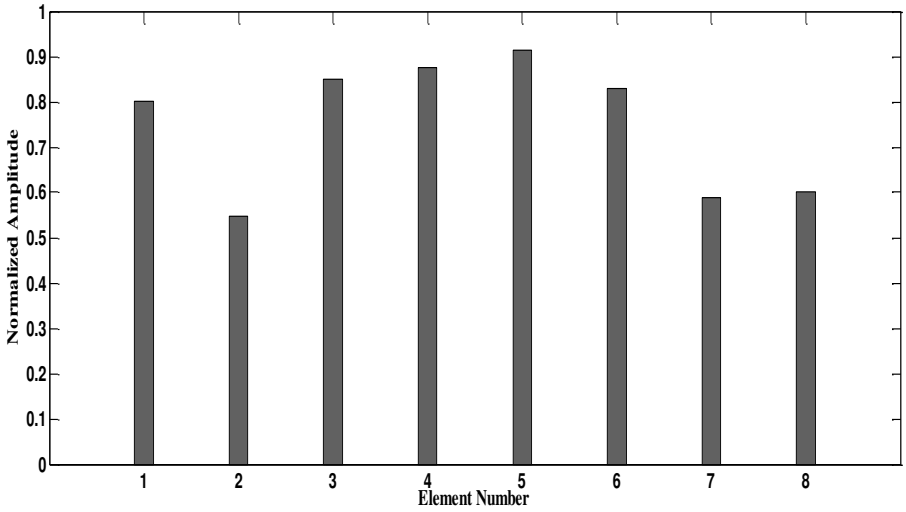

Figure 5.41 Optimized τ_n for each element for 8-element linear array

The optimized radiation patterns of the designed TMAA are shown in figure 5.42. The contour plot results in a plane with each point colored according to its field value. The contour plot is shown in figure 5.42(b) and it is observed that the proposed time modulated array provides coverage of circular geographical region marked by red color with maximum radiations while minimizing the radiations in other nearby regions.

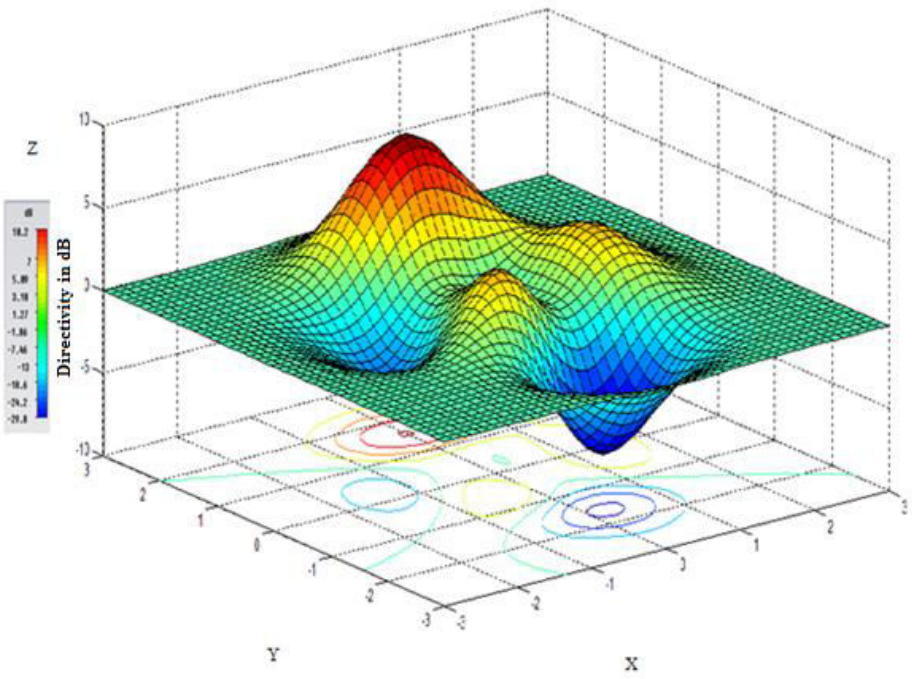

(a) 3-D Radiation Pattern

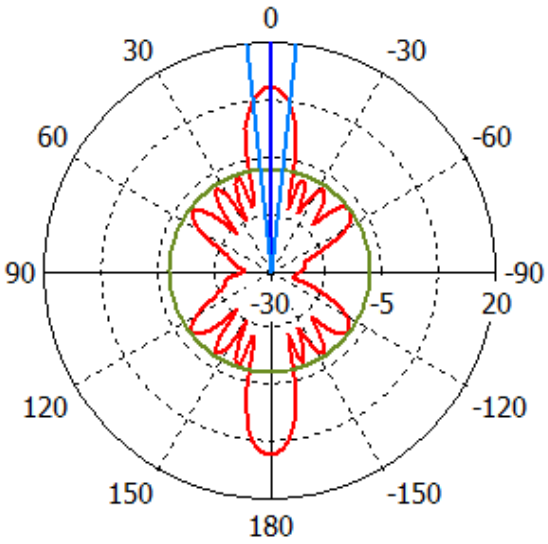

(b) Polar Plot

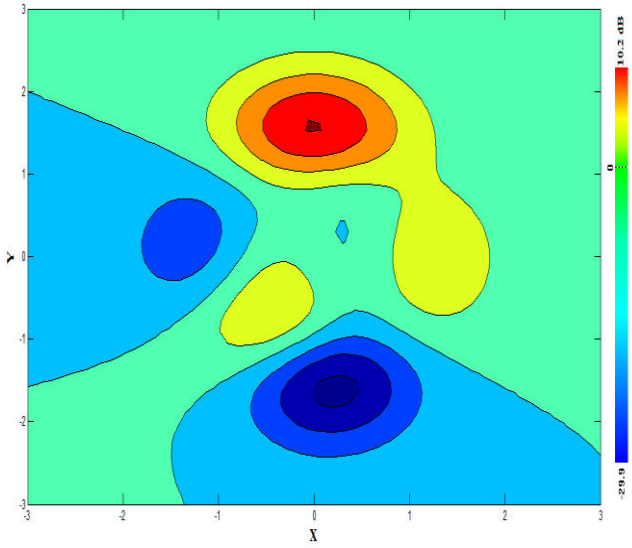

(c) Contour Plot

Figure 5.42 Optimized radiation patterns of 8-element TMAA
(a) 3-D Radiation pattern (b) Polar plot (c) Contour plot

Figure 5.43 shows the simulated and measured radiation pattern of the designed TMAA. The design specifications of TMAA and their corresponding simulated and measured results by using ECSS optimization technique are shown in table 5.14

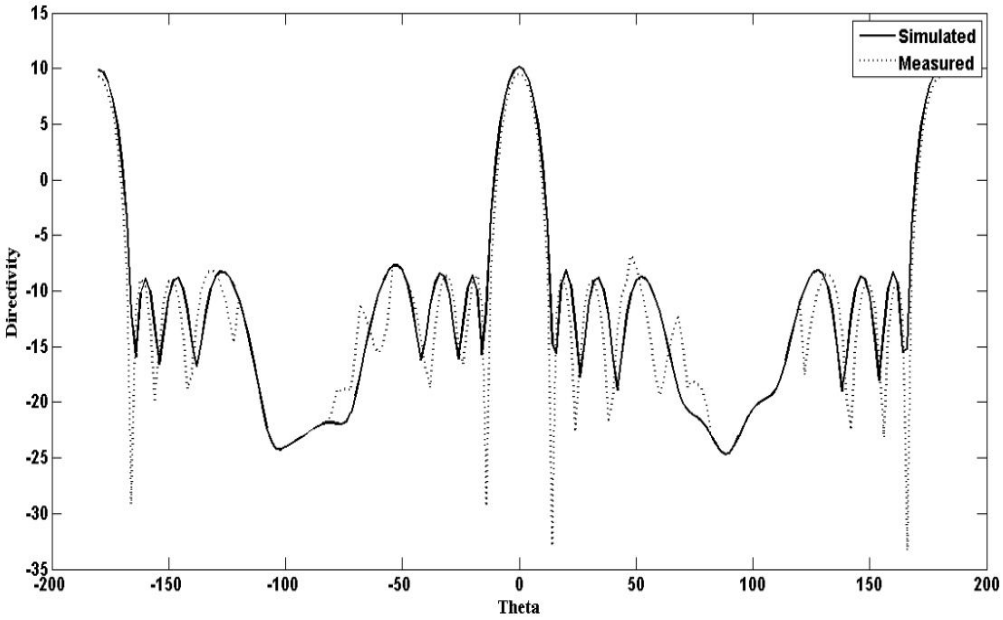

Figure 5.43 Simulated and measured radiation pattern of 8-element TMAA

Table 5.14 Design specifications and results of 8-element printed TMAA

Design parameter	**Desired**	**Obtained**	
		Simulated	**Measured**
SLL	-18dB	-17.9dB	-17 dB
HPBW	12°	12.5°	11.7°
Return Loss	NA	-20.59dB	-17.20dB
Directivity	NA	10.2dB	9.87 dB

5.5 Conclusion

In the chapter TMAAs using printed dipoles are discussed for various problems of pattern synthesis. The printed dipole design exhibits similar radiation performance as of wired dipoles. A power divider operating at 2.45GHz and a wideband power divider have been designed while discussing the scattering parameters. Parametric optimization of the array utilizing modified ground structure has been done to obtain wider impedance bandwidth at 2.45GHz and 5.8GHz. Hardware configuration of TMAAs has been discussed. Phase difference between the dipoles has been achieved without using phase shifters by exciting

the array with a complex exponential signal. DE has been successfully applied to increase the dynamic efficiency of the array pattern. The modulation of the switching sequences of the rectangular pulses controls the relative phase difference between elements and steers the beam in different directions at both the centre frequencies and their sidebands without phase shifter. Experimental validation confirms the effectiveness of the proposed technique over conventional phased array antenna. The implementation of ECSS in TMAA synthesis is found suitable.

Chapter-6

Conclusions and Future Scope

6.1 Conclusions

In the dissertation TMAAs have been studied for pattern synthesis, beam shaping and electronic beam steering utilizing the various optimization techniques.

The thesis begins with the discussion of antenna arrays. It is seen that the excitation distribution can be used to obtain different radiation patterns with various stringent radiation characteristics. However it is difficult to implement the precise excitation distribution. So TMAA is introduced to achieve the desired excitation distribution by controlling an additional parameter time of the RF switches connected to the array elements. PIN diode BAR-63 with additional biasing circuit is used as RF switch in the work. The switching timings of RF switches are easily and accurately controlled using micro-controller based circuit.

The dissertation has studied the mathematical analysis of TMAA. It is seen that the desired current excitation is modified by changing switch ON-time duration of antenna array elements. Suppression of power radiated at first sideband reduces the sideband radiations and increases the efficiency of the array.

Thesis simulates various examples of TMAAs for pattern synthesis using different optimization approaches. It designed 16-element TMAAs of half wave dipoles with fixed SLL and suppressed sidebands. ABC and PSO are used to compute the switching timings to obtain broadside and scanned beam pattern. The optimal selection of the switch on time sequence shapes the radiation pattern and application of progressive phase differences between the elements steers the main beam at different angle from broadside. It is seen that the scanned beam offers broader FNBW compared to that of the broadside beam pattern with same SLL. For both the cases SBL is approximately -7dB lower than that of the pattern at centre frequency.

The thesis has designed a 16-element TMAA of half wave dipoles to generate cosecant squared and scanned beam patterns without using phase shifters. Application of complex exponential excitation results in an unequal amplitude and phase distribution on the elements at the central frequency without phase shifters. ABC computes the switching

sequences to produce the cosecant and scanned patterns at fundamental frequency and suppress the SBR losses. It is observed that the higher switching time duration enhances the dynamic efficiency of the system. The designed cosecant squared antenna is useful for ground-based radars observing aircraft targets as well as airborne search radars observing ground targets when the target moves at constant altitude with a fixed elevation angle. Simulation results are in reasonable agreement with the theoretical results.

As the demand of printed antennas has been increasing due to the miniaturization of the communication devices, the thesis has designed TMAAs using printed dipoles. The subsequent design instances considered in the thesis: designed and analysed a printed dipole with microstrip balun. Beam steering is achieved without using phase shifters in a single and dual band TMAA. A TMAA consisted of 2-printed dipoles with V-shape ground is designed to be operated at 2.45 GHz frequency. A Wilkinson 1:2printed power divider is designed to feed the elements of the array. Application of complex exponential signal provides the phase difference between the dipoles. The switching timings of the SPST PIN diode RF switches connected to the array elements are modulated to have phase and amplitude variations. The phase difference among the antenna elements steers the beam in different directions accordingly.

The thesis investigated a 2-element dual band TMAA of printed dipoles operating at ISM bands: 2.45GHz and 5.8 GHz. Parametric optimization of the shape of ground plane of printed dipole is done rigorously to enhance bandwidth at both the resonating frequencies. A wideband power divider is designed to feed the elements of array. The designed power divider operates at wide range of frequencies from 2.1 GHz to 7GHz covering both the ISM bands. A common complex signal is applied to the array through SPST PIN diode RF switches using a wideband power divider. DE is used to calculate the switch on time to increase the dynamic efficiency of the array. Time sequence of RF switches is controlled using CPLD. The efficiency of the array achieved is quite satisfactory. The beam is steered in different direction at central frequencies as well as their sidebands. At both the frequencies, the beam steers at different angles for various instances of switch-on time of RF switch.

The thesis has synthesised 8-element TMAA of printed dipoles operating at 2.45 GHZ to obtain a radiation pattern with a specified SLL and SBL for a fixed HPBW. ECSS optimization is used to compute the timing sequence of the array. The study calculated the

directivity of the array at designing frequency. The designed TMAA overcomes the side lobe level limitation of uniformly excited arrays and large dynamic range ratio of amplitude excitation of non-uniformly excited arrays using same number of elements. The implementation of ECSS is found very efficient for antenna array synthesis.

The research work presented in the dissertation provides simple and low cost beam forming system using TMAA. The system produces radiation pattern with ultra-low SLL, cosecant beam and scanned beam with numerous design constraints. The radiation patterns are very much useful in the areas of radio broadcasting, space communication, radar, weather forecasting.

6.2 Future Scope

The design and analysis of TMAA presented in this thesis is interesting and offers the scope of further study in the following possible areas:

While designing TMAAs of large number of elements, it is very important to investigate the mutual coupling effects among the elements to approximate the performance of TMAA more accurately especially in radar applications. The mutual couping may be reduced by using defected ground planes or electromagnetic band gap structures (EBG).

Application of time modulation in antenna arrays to synthesize desired radiation characteristics excites the cross polarization components of the radiation pattern. A significant amount of power can be wasted in cross-polarized radiations. For highly directive antenna arrays the cross polarized components should be sufficiently small. The work in the thesis may be further extended to reduce the cross-polarization radiations to improve the polarization purity of TMAAs.

Unwanted side band maybe used for several other applications. Harmonic patterns may be exploited to configure a simple direction finding system with active null scanning capabilities. A simultaneous scan operation can be achieved where the beams at different sidebands are used to point at different directions.

The work may be extended to multiband planar TMAAs for cognitive radio and commercial applications.

Designing of more complex array geometries (square, rectangular, hexagonal, semicircular etc.) could be investigated for improved application.

More powerful global search algorithm with multiple conflicting design objectives may be investigated for synthesis of antenna array.

More complicated/complex beam shapes using other improved optimizing algorithms can be achieved. New pulse shaping schemes of time sequence may be investigated by dividing the entire time sequence into unequal steps to improve the radiation performance.

RF micro electromechanical system (MEMS) switches may be used in place of PIN diode RF switches used in the thesis as MEMS RF switch gives better performance than PIN diode RF switch in terms of bandwidth ,power consumption, insertion loss and isolation.

REFERENCES

[1] Balanis C. A., "Microstrip Antennas", Antenna Theory, Analysis and Design, Third Edition, John Wiley and Sons, pp.811-876, 2010.

[2] C. L. Dolph, "A Current Distribution for Broadside Arrays Which Optimizes the Relationship between Beam Width and Side-Lobe Level", *Proceedings of the IRE*, vol. 34, no. 6, pp. 335-348, 1946.

[3] T. T. Taylor, "Design of Line-Source Antennas for Narrow Beamwidth and Low Sidelobes", *Transactions of the IRE Professional Group on Antennas and Propagation*, vol. 3, no.1, pp.16–28, 1955.

[4] Gallergo A., Esposito F., Pallas M., "Dipole Antenna on a High Dielectric Substrate", *Proceedings of 1st European Microwave Conference*, pp. 387-390, 1969.

[5] Van de Capelle A., De Bruyne J., Verstraete M., Pues H., Vandensande J., "Microstrip Spiral Antennas", *International Symposium Antennas and Propagation Society*, vol. 17, pp. 383-386, 1979.

[6] I. J.Bahl and P. Bhartia, "Microstrip Antennas," Artech House, 2003.

[7] Gong B., Ren X.S., Zeng Y.Y., Su L.H. Zheng Q.R., "Compact Slot Antenna for Ultra-Wideband Applicatons", *IET microwave, Antennas and Propagations*, vol. 8, no. 3, pp. 200-205, 2014.

[8] Rafi G., Shafai L., "Broadband Microstrip Patch Antenna with V Slot", P*roceedings of IEEE Microwave, Antennas and Propagations*, vol.151, no.5, pp. 435-440, 2004.

[9] Deshmukh A.A., Ray K.P., "Compact Broadband Slotted Rectangular Microstrip Antenna", *IEEE Antennas and Wireless Propagation Letters*, vol. 8, pp. 1410-1413, 2009.

[10] Prapti Ganguly, David E. Senior, Patanjali V. Parimi, Amlan Chakrabarti, "Wearable RF Plethysmography Sensor Using a Slot Antenna", *2016 IEEE International Symposium on Antennas and Propagation (APSURSI)*, pp.1169-1170, DOI: 10.1109/APS.2016.7696292.

[11] Rowe W.S.T. Waterhouse, R.B., "Broadband CPW Fed Stacked Patch Antenna", *Electronics letters*, vol. 35, no. 9, pp. 681-682, 1999.

[12] Tingqiang W., Hua S., Liyun G., Huizhu C., "A Compact and Broadband Microstrip Stacked Patch Antenna with Circular Polarization for 2.45 GHz Mobile RFID Reader", *IEEE Antennas and Wireless Propagation Letters*, vol. 12, pp. 623-626, 2013.

[13] Jeen Sheen R., "Design of Aperture-Coupled Annular –Ring Microstrip Antennas for Circular Polarization", *IEEE Transactions on Antennas and Propagation*, vol. 53, no. 5, pp. 1779-1784, 2005.

[14] Meiguni J.S., Kamyab M., Hosseinbeig A., "Theory and Experiment of Spherical Aperture-Coupled Antennas", *IEEE Transactions on Antennas and Propagation*, vol. 61, no. 5, pp. 2379-2403, 2013.

[15] Majeed A.H., Abdullah A.S., Elmegri F., Sayidmarie K.H., Abd-Alhameed R.A., Noras J.M., "Aperture-Coupled Asymmetric Dielectric Resonators Antenna for Wideband Applications", *IEEE Antennas and Wireless Propagation Letters*, vol.13, pp. 927-930, 2014.

[16] Sung Y.J., "Bandwidth Enhancement of a Wide Slot using Fractal-Shaped Sierpinski", *IEEE Transactions on Antennas and Propagation*, vol.59, no. 8, pp. 3076-3079, 2011.

[17] Z. G. Fan, S. Qiao, J. T. Huangfu, L. X. Ran, "A Miniaturized Printed Dipole Antenna with V-Shaped Ground for 2.45 Ghz RFID Readers", *Progress In Electromagnetics Research*, vol.71, pp. 149–158, 2007.

[18] Subhradeep Chakraborty, Abhijyoti Ghosh, Sudipta Chattopadhyay, L. Lolit Kumar Singh, "Improved Cross Polarized Radiation and Wide Impedance Bandwidth from Rectangular Microstrip Antenna with Dumbbell Shaped Defected Patch Surface", *IEEE Antennas and Wireless Propagation Letters*, Doi 10.1109/Lawp.2015.2430881, 2015.

[19] Chandan K. Ghosh, Bappaditya Mandal, and Susanta K. Parui, "Mutual Coupling Reduction of a Dual-Frequency Microstrip Antenna Array by Using U-Shaped DGS and Inverted U-Shaped Microstrip Resonator", *Progress In Electromagnetics Research*, vol. 48, pp. 61-68, 2014.

[20] Dimitris Bertsimas, Jhon Tsitsiklis, “Simulated Annealing”, *Statistical Science*, vol.8, no.1, pp.10-15,1993

[21] Kirkpatrick, S., Gelatt, C. D., Vecchi, M. P., "Optimization by Simulated Annealing", *Science, New Series*, vol. 220, no. 4598, pp. 671-680, 1983.

[22] Ingber. L., Rosen. B., “Genetic Algorithms and Very Fast Simulated Re-annealing: A Comparison”, *J. Mathematical and Computer Modeling*, vol. 16, no.11, pp. 87–100, 1992.

[23] Ingber. L., “Simulated Annealing: Practice Versus Theory”, *J. Mathematical and Computer Modeling*, vol. 18, no. 11, pp. 29–57, 1993.

[24] Hajek. B., “Cooling Schedules for Optimal Annealing”, *Math. Oper. Res*., vol.13, pp.311-329, 1988.

[25] Holland JH, “Adaptation in Natural and Artificial Systems”, *University of Michigan Press*, Ann Arbor, 1975.

[26] Goldberg DE, “Genetic Algorithms in Search, Optimization and Machine Learning”, *Addison-Wesley, Reading*, MA, 1975.

[27] J. Kennedy, R. C. Eberhart, “Particle Swarm Optimization”, *Proceedings of IEEE International Conference on Neural Networks,* pp. 1942–1948, 1995.

[28] W. T. Li, X. W. Shi, Y. Q. Hei, “An Improved Particle Swarm Optimization Algorithm for Pattern Synthesis of Phased Arrays,” *Progress In Electromagnetics Research*, vol. 82, pp.319–332, 2008.

[29] Z. D. Zaharis, D. G. Kampitaki, P. I. Lazaridis, A. I. Papastergiou, A. T. Hatzigaidas, P. B. Gallion, "Improving the Radiation Characteristics of a Base Station Antenna Array using a Particle Swarm Optimizer", *Microwave Opt Technol Lett* 49, pp.1690-1698, 2007.

[30] N. Jin, Y. Rahmat-Samii, “Advances in Particle Swarm Optimization for Antenna Designs: Real-number, Binary, Single- objective and Multiobjective Implementations,” *IEEE Transactions on Antennas and Propagation* , vol. 55, no. 3, pp.556-567, 2007.

[31] Jang-Ho Seo, Chang-Hwan Im, Chang-Geun Heo, Jae-Kwang Kim, Hyun-Kyo Jung, Cheol-Gyun Lee., "Multimodal Function Optimization Based on Particle Swarm Optimization", *IEEE Transactions on Magnetics*, vol. 42, no.4, pp.1095-1098, 2006.

[32] Shutao Li, Mingkui Tan, Ivor W. Tsang, James Tin-Yau Kwok, "A Hybrid PSO-BFGS Strategy for Global Optimization of Multimodal Functions", *IEEE Transactions On Systems, Man, And Cybernetics—Part B: Cybernetics*, vol. 41, no. 4, pp. 1003-1014, 2011.

[33] Zhi-Hui Zhan, Jun Zhang, Yun Li , Yu-Hui Shi, "Orthogonal Learning Particle Swarm Optimization", *IEEE Transactions on Evolutionary Computation*, vol. 15, no. 6, pp. 832-847, 2011.

[34] Arezoo Modiri, Kamran Kiasaleh, "Modification of Real-Number and Binary PSO Algorithms for Accelerated Convergence", *IEEE Transactions on Antennas and Propagation*, vol. 59, no. 1, pp. 214-224, 2011.

[35] YAN Zhe-Ping, DENG Chao, Zhou Jia-Jia, Chi Dong-Nan , "A Novel Two-Subpopulation Particle Swarm Optimization", *World Congress On Intelligent Control and Automation, Beijing, China*, pp. 4113-4117, July 6-8, 2012.

[36] Feng Luan, Jong-Ho Choi, And Hyun-Kyo Jung, "A Particle Swarm Optimization Algorithm With Novel Expected Fitness Evaluation For Robust Optimization Problems", *IEEE Transactions on Magnetics*, vol. 48, no. 2, pp. 331-334, 2012.

[37] Fengrui Zhang1, Jianshu Cao, Zhenhui Xu, "An Improved Particle Swarm Optimization Particle Filtering Algorithm", *Proceedings of 2013 International Conference on Communications, Circuits and Systems (ICCCAS)*, vol.2, pp. 173-177,2013, DOI. 10.1109/ICCCAS.2013.6765312.

[38] Y. Volkan Pehlivanoglu, "A New Particle Swarm Optimization Method Enhanced With A Periodic Mutation Strategy And Neural Networks", *IEEE Transactions on Evolutionary Computation*, vol. 17, no. 3, pp. 436-452, 2013.

[39] Mengqi Hu, Teresa Wu, Jeffery D. Weir, "An Adaptive Particle Swarm Optimization With Multiple Adaptive Methods", *IEEE Transactions on Evolutionary Computation*, vol. 17, no. 5, pp. 705-720, 2013.

[40] Wei-Neng Chen, Jun Zhang, Ying Lin, Ni Chen, Zhi-Hui Zhan , Henry Shu-Hung Chung, Yun Li, Yu-Hui Shi, "Particle Swarm Optimization With an Aging Leader and Challengers", *IEEE Transactions on Evolutionary Computation*, vol. 17, no. 2, pp. 241-258, 2013.

[41] A. Naha, A.K. Deb, "Particle Swarm Optimisation With Kalman Correction" *Electronics Letters* , vol. 49, no. 7, 2013.

[42] Yan-Liang Li, Wei Shao, Long You, Bing-Zhong Wang, "An Improved PSO Algorithm and Its Application to UWB Antenna Design", *IEEE Antennas and Wireless Propagation Letters*, vol. 12, pp. 1236-1239, 2013.

[43] Bing Zhang, Lina Zhuang, Lianru Gao, Wenfei Luo, Qiong Ran, Qian Du, "PSO-EM: A Hyperspectral Unmixing Algorithm Based On Normal Compositional Model", *IEEE Transactions on Geo science And Remote Sensing*, vol. 52, no. 12, pp. 7782-7792, 2014.

[44] Zhigang Ren, Aimin Zhang, Changyun Wen, Zuren Feng, "A Scatter Learning Particle Swarm Optimization Algorithm For Multimodal Problems", *IEEE Transactions on Cybernetics*, vol. 44, no. 7, pp. 1127-1140, 2014.

[45] Elisa Carrubba, Axel Junge, Filippo Marliani, Agostino Monorchio, "Particle Swarm Optimization For Multiple Dipole Modeling of Space Equipment", *IEEE Transactions on Magnetics*, vol. 50, no. 12, 2014.

[46] R. Storn, K. V. Price, J. Lampinen, "Differential Evolution–A Practical Approach to Global Optimization", *Springer-Verlag*, 2005.

[47] S. Das, A. Abraham, U.K. Chakraborty, A. Konar", Differential Evolution Using a Neighborhood-Based Mutation Operator," *IEEE Transactions on Evolutionary Computation*, vol. 13, no. 3, pp.526-553, 2009.

[48] Nyambayar Baatar, Minh-Trien Pham, Chang-Seop Koh, "Multiguiders and Nondominate Ranking Differential Evolution Algorithm for Multiobjective Global Optimization of Electromagnetic Problems", *IEEE Transactions on Magnetics*, vol. 49, no. 5, pp. 2105-2108, 2013.

[49] Saber M. Elsayed, Ruhul A. Sarker, Daryl L. Essam, "An Improved Self-Adaptive Differential Evolution Algorithm for Optimization Problems", *IEEE Transactions on Industrial Informatics*, vol. 9, no. 1, pp. 89-99, 2013.

[50] Nyambayar Baatar, Dianhai Zhang, and Chang-Seop Koh, "An Improved Differential Evolution Algorithm Adopting -Best Mutation Strategy for Global Optimization of Electromagnetic Devices", *IEEE Transactions on Magnetics*, vol. 49, no. 5, pp. 2097-2100, 2013.

[51] Aniruddha Basak, Swagatam Das, Kay Chen Tan, "Multimodal Optimization Using a Biobjective Differential Evolution Algorithm Enhanced With Mean Distance-Based Selection", *IEEE Transactions on Evolutionary Computation*, vol. 17, no. 5, pp. 666-685, 2013.

[52] Jing Yang, Wen-Tao Li, Xiao-Wei Shi, Li Xin, Jian-Feng Yu, "A Hybrid ABC-DE Algorithm and Its Application for Time-Modulated Arrays Pattern Synthesis", *IEEE Transactions on Antennas and Propagation*, vol. 61, no. 11, pp. 5485-5495, 2013.

[53] Fenggan Zhang, Weimin Jia, Minli Yao, "Linear Aperiodic Array Synthesis using Differential Evolution Algorithm", *IEEE Antennas and Wireless Propagation Letters*, vol. 12, pp. 797-800, 2013.

[54] Wenyin Gong, Zhihua Cai, "Differential Evolution With Ranking-Based Mutation Operators", *IEEE Transactions on Cybernetics*, vol. 43, no. 6, pp. 2066 -2081, 2013.

[55] Swagatam Das, Ankush Mandal, Rohan Mukherjee, "An Adaptive Differential Evolution Algorithm for Global Optimization in Dynamic Environments", *IEEE Transactions on Cybernetics*, vol. 44, no. 6, pp. 966-978, 2014.

[56] Yang Ding, Yong-Chang Jiao, Li Zhang, Biao Li, "Solving Port Selection Problem in Multiple Beam Antenna Satellite Communication System by Using Differential Evolution Algorithm", *IEEE Transactions on Antennas and Propagation*, vol. 62, no. 10, pp. 5357-5361, 2014.

[57] Nyambayar Baatar, Kwang-Young Jeong, Chang-Seop Koh, "Adaptive Parameter Controlling Non-Dominated Ranking Differential Evolution for Multi-Objective

Optimization of Electromagnetic Problems", *IEEE Transactions On Magnetics*, vol. 50, no. 2, 2014.

[58] Bin Xia, Nyambayar Baatar, Ziyan Ren, Chang-Seop Koh, "A Numerically Efficient Multi-Objective Optimization Algorithm: Combination of Dynamic Taylor Kriging and Differential Evolution", *IEEE Transactions on Magnetics*, vol. 51, no. 3, 2015.

[59] Mahanti, Gautam Kumar, Narendra Nath Pathak, and Prabhat K. Mahanti. "Synthesis of Thinned Linear Antenna Arrays with Fixed Sidelobe Level using Real-Coded Genetic Algorithm." *Progress In Electromagnetics Research*, vol. 75, pp. 319-328, 2007.

[60] S Pal, B Qu, S Das, PN Suganthan, "Linear Antenna Array Synthesis With Constrained Multi-Objective Differential Evolution", *Progress In Electromagnetics Research B* ,Vol.21, 87-111,2010.

[61] A Chowdhury, R Giri, A Ghosh, S Das, A Abraham, V Snasel, "Linear Antenna Array Synthesis Using Fitness-Adaptive Differential Evolution Algorithm", *Proceedings of Evolutionary Computation (CEC), 2010 IEEE Congress* , 2010

[62] Gopi Ram, Durbadal Mandal, Rajib Kar and Sakti Prasad Ghoshal , "Optimized Hyper Beam forming of Receiving Linear Antenna Arrays Using Firefly Algorithm", *International Journal of Microwave and Wireless Technologies*, vol. 6, no.2, pp. 181-194, 2013

[63] Gopi Ram, Durbadal Mandal, Rajib Kar, Sakti Prasad Ghoshal, "Optimized Hyper Beam forming of Linear Antenna Arrays Using Collective Animal Behaviour ", *The Scientific World Journal* , DOI. 10.1155/2013/982017, 2013.

[64] Karaboga D, Basturk B., "A Powerful and Efficient Algorithm for Numerical Function Optimization: Artificial Bee Colony (ABC) Algorithm", *J. Global Optim.*, vol. 39, pp.459–471, 2007.

[65] Karaboga D, Basturk B., "On the Performance of Artificial Bee Colony (ABC) Algorithm", *Appl. Soft Comput.*, vol. 8, no. 1, pp. 687–697, 2008.

[66] Akay B, Karaboga D, "Solving Integer Programming Problems by using Artificial Bee Colony Algorithm", *In AI (ASTERISK) IA, University Modena Reggio*, vol. 5883, pp. 355–364, 2009.

[67] Ho SL, Yang S, "An Artificial Bee Colony Algorithm for Inverse Problems", *Int. J. Appl. Electrom.* , vol. 31, no. 3, pp.181–192, 2009.

[68] Rashedi A, Kavian YS, Ghassemlooy Z, "Artificial Bee Colony Model for Routing and Wavelength Assignment Problem", *Proceedings of International Conference on Transparent Optical Networks*, DOI. 10.1109/ ICTON.2011.5970870, 2011.

[69] Delican Y, Vural R, Yildirim T., "Artificial Bee Colony Optimization Based CMOS Inverter Design Considering Propagation Delays", *International Workshop on Symbolic and Numerical Methods. Modeling and Applications to Circuit Design*, pp. 1–5. DOI. 10.1109/SM2ACD. 2010.5672326, 2010.

[70] Akdagli A, Bicer MB, Ermis S, " A Novel Expression for Resonant Length Obtained by Using Artificial Bee Colony Algorithm in Calculating Resonant Frequency of C-Shaped Compact Microstrip Antennas", *Turk. J. Electr. Eng. Co.*, vol. 19, no. 4, pp. 597–606, 2011.

[71] Toktas A, Bicer MB, Akdagli A, Kayabasi A, "Simple Formulas for Calculating Resonant Frequencies of C and H Shaped Compact Microstrip by Using Artificial Bee Colony Algorithm", *J. Electromagn. Wave*, vol. 25, no.11–12, pp. 1718–1729.2011.

[72] Rao RV, Pawar PJ., "Parameter Optimization of a Multi-Pass Milling Process Using Non-Traditional Optimization Algorithms", *Appl. Soft Comput.*, vol. 10, no. 2, pp. 445–456, 2010.

[73] Taspinar N, Karaboga D, Yildirim M, Akay B., "Partial Transmit Sequences Based on Artificial Bee Colony Algorithm for Peak-to-Average Power Ratio Reduction in Multicarrier Code Division Multiple Access Systems", *IET Commun.*, vol. 5, no. 8, pp. 1155–1162, 2011.

[74] Ruchi, Arnab Nandi, Banani Basu, "Synthesis Of Broadside And Scanned Beam Pattern With Time Modulated Antenna Array Using Artificial Bees Colony Algorithm",

proceedings of International Microwave and RF Conference, DOI. 10.1109/IMaRC.2013.6777745, 2013.

[75] A. Kaveh, S. Talatahari, "A Novel Heuristic Optimization Method: Charged System Search", *Acta Mech*, vol. 213, pp. 267–289, 2010.

[76] A. Kaveh, S. Talatahari, "An Enhanced Charged System Search for Configuration Optimization Using the Concept of Fields of Forces", *Struct. Multidisc. Optim.*, vol. 43, pp. 339–351, 2011.

[77] Shanks HE, Bickmore RW, "Four-Dimensional Electromagnetic Radiators", *Can. J. Phys.*, vol.37, pp. 263–275, 1959.

[78] Kummer WH, Villeneuve AT, Fong TS, Terrio FG., "Ultra-Low Sidelobes from Time-Modulated Arrays, *IEEE Transaction on Antennas and Propagation* , vol. 11, no. 6, pp. 633–639, 1963.

[79] Shiwen Yang, Yeow Beng Gan, Anyong Qing, "Sideband Suppression in Time-Modulated Linear Arrays by the Differential Evolution Algorithm", *IEEE Antennas and Wireless Propagation Letters*, vol. 1, pp. 173-175, 2002.

[80] Shiwen Yang, Zaiping Nie, Feng Yang, "Synthesis of Low Sidelobe Planar Antenna Arrays with Time Modulation", *Proceedings of APMC 2005 Asia-Pacific Conference,* vol.3, 2005.

[81] Shiwen Yang, Yeow-Beng Gan, Peng Khiang Tan, "Linear Antenna Arrays with Bidirectional Phase Center Motion", *IEEE Transactions on Antennas and Propagation*, vol. 53, no. 5, pp. 1829-1835, 2005.

[82] Tennant, B. Chambers, "A Two-Element Time-Modulated Array with Direction-Finding Properties", *IEEE Antennas and Wireless Propagation Letters*, vol. 6, pp. 64-65, 2007.

[83] Xiaowen Zhu, Shiwen Yang, Zaiping Nie, "Full-Wave Simulation of Time Modulated Linear Antenna Arrays in Frequency Domain", *IEEE Transactions on Antennas and Propagation*, vol. 56, no. 5, pp. 1479-1482, 2008.

[84] J. C. Brégains, J. Fondevila-Gómez, G. Franceschetti, F. Ares, "Signal Radiation and Power Losses of Time-Modulated Arrays", *IEEE Transactions on Antennas and Propagation*, vol. 56, no. 6, pp. 1799-1804, 2008.

[85] S. W. Yang, Y. K. Chen, Z. P. Nie, "Simulation of Time Modulated Linear Antenna Arrays Using The FDTD Method", *Progress in Electromagnetics Research*, vol. 98, pp. 175-190, 2009.

[86] Gang Li, Shiwen Yang, and Zaiping Nie, "A Study on the Application of Time Modulated Antenna Arrays to Airborne Pulsed Doppler Radar", *IEEE Transactions on Antennas and Propagation*, vol. 57, no. 5, pp. 1578-1582, 2009.

[87] G. Li, S. Yang, Y. Chen, and Z. Nie, "A Novel Electronic Beam Steering Technique in Time Modulated Antenna Arrays", *Progress in Electromagnetics Research*, vol. 97, pp. 391-405, 2009.

[88] L. Manica, P. Rocca, L. Poli, A. Massa, "Almost Time-Independent Performance in Time-Modulated Linear Arrays", *IEEE Antennas and Wireless Propagation Letters*, vol. 8, pp. 843-846, 2009.

[89] Gang LI, Shiwen YANG, Ming HUANG, Zaiping NIE, "Shaped Patterns Synthesis in Time-Modulated Antenna Arrays With Static Uniform Amplitude and Phase Excitations", *Front. Electr. Electron. Eng. China*, vol. 5, no.2, pp. 179-184, 2010.

[90] Lorenzo Poli, Paolo Rocca, Luca Manica, Andrea Massa, "Handling Sideband Radiations in Time-Modulated Arrays Through Particle Swarm Optimization", *IEEE Transactions on Antennas and Propagation*, vol. 58, no. 4, pp. 1408-1411, 2010.

[91] Banani Basu, G. K. Mahanti, "Beam Reconfigureuration of Linear Array of Parallel Dipole Antennas Through Switching With Real Excitation Voltage Distribution", *Ann. Telecommun.*, vol.67, pp. 285-293, 2012.

[92] S. Pal, S. Das, A. Basak, "Design of Time-Modulated Linear Arrays with A Multi-Objective Optimization Approach", *Progress in Electromagnetics Research B*, vol. 23, pp. 83-107, 2010.

[93] Y. Tong, A. Tennant, "Simultaneous Control of Sidelobe Level and Harmonic Beam Steering in Time-Modulated Linear Arrays", *Electronics letters*, vol. 46, no. 3, 2010.

[94] B. Basu, G. K. Mahanti, "Fire Fly and Artificial Bees Colony Algorithm for Synthesis of Scanned and Broad-Side Linear Array Antenna", *Progress In Electromagnetics Research B*, vol. 32, pp. 169-190, 2011.

[95] L. Poli, P. Rocca, L. Manica, A. Massa, "Pattern Synthesis in Time Modulated Linear Arrays through Pulse Shifting" , *Technical Report #DISI-11-074, 2011.*

[96] Yizhen Tong, Alan Tennant, "Reduced Sideband Levels in Time-Modulated Arrays Using Half-Power Sub-Arraying Techniques", *IEEE Transactions on Antennas and Propagation*, vol. 59, no. 1, pp. 301-303, 2011.

[97] Jin Shi, Jian Wang, Kai Xu, Jian-Xin Chen, Wei Liu "A Balanced-to-Balanced Power Divider with Wide Bandwidth" *IEEE Microwave and Wireless Components Letters*, vol. 25, no. 9, pp. 573-575, 2015.

[98] Muhammad Z. B. M. Nor, Sharul K. A. Rahim, Mursyidul I. B. Sabran, Mohd S. B. A. Rani, "Wideband Planar Wilkinson Power Divider Using Double-Sided Parallel-Strip Line Technique ",*Progress in Electromagnetics Research C*, vol. 36, pp. 181-193, 2013.

[99] Lorenzo Poli, Paolo Rocca, Giacomo Oliveri, Andrea Massa, "Harmonic Beam forming in Time-Modulated Linear Arrays", *IEEE Transactions on Antennas and Propagation*, vol. 59, no. 7, pp. 2538-2545, 2011.

[100] Ertugrul Aksoy, Erkan Afacan, "Calculation of Sideband Power Radiation in Time-Modulated Arrays With Asymmetrically Positioned Pulses", *IEEE Antennas and Wireless Propagation Letters*, vol. 11, pp. 133-136, 2012.

[101] Quanjiang Zhu, Shiwen Yang, Li Zheng, Zaiping Nie, "Design of A Low Side lobe Time Modulated Linear Array with Uniform Amplitude and Sub-Sectional Optimized Time Steps", *IEEE Transactions on Antennas and Propagation*, vol. 60, no. 9, pp. 4436-4439 , 2012.

[102] Quanjiang Zhu, Shiwen Yang,, Ruilin Yao, Zaiping Nie, "Gain Improvement in Time-Modulated Linear Arrays Using SPDT Switches", *IEEE Antennas and Wireless Propagation Letters*, vol. 11, pp. 994-997, 2012.

[103] Jyoti Prasad Bandyopadhyay, "Semiconductor Devices", ISBN-9789325974128, Vikas Publishing, 2014.

[104] Paolo Rocca, Lorenzo Poli, Giacomo Oliveri, Andrea Massa, Member, "Adaptive Nulling in Time-Varying Scenarios Through Time-Modulated Linear Arrays", *IEEE Antennas and Wireless Propagation Letters*, vol. 11, pp. 101-104, 2012.

[105] Y. Tong, A. Tennant. "A Two-Channel Time-Modulated Linear Array with Adaptive Beamforming," *IEEE Transactions on Antennas and Propagation*, vol. 60, no. 1, pp. 141–147, 2012.

[106] Tong Y, Tennant A. "Sideband Level Suppression in Time-Modulated Linear Arrays using Modified Switching Sequences and Fixed Bandwith Elements", *Electron. Lett*.," vol. 48, no. 1, pp.10–11, 2012.

[107] P. Rocca, L. Poli, A. Massa, "Instantaneous Directivity Optimisation in Time-Modulated Array Receivers", *IET Microwave and Antennas Propagation*, vol. 6, no. 14, pp. 1590–1597, 2012.

[108] P. Rocca, L. Poli, L. Manica, A. Massa, "Synthesis of Monopulse Time-Modulated Planar Arrays With Controlled Sideband Radiation", *IET Radar, Sonar and Navigation*., vol. 6, no. 6, pp. 432–442, 2012.

[109] Kerim Guney, Suad Basbug, "Null Synthesis of Time-Modulated Circular Antenna Arrays Using an Improved Differential Evolution Algorithm", *IEEE Antennas and Wireless Propagation Letters,* vol.12, pp. 817-820, 2013.

[110] Jing Yang, Wen-Tao Li, Xiao-Wei Shi, Li Xin, Jian-Feng Yu, "A Hybrid ABC-DE Algorithm and Its Application for Time-Modulated Arrays Pattern Synthesis", *IEEE Transactions on Antennas and Propagation*, vol. 61, no. 11, pp. 5485-5495, 2013.

[111] Chong He, Xianling Liang, Zhaojin Li, Junping Geng, Ronghong Jin , "Direction Finding by Time Modulated Array with Harmonic Characteristic Analysis", *IEEE Antennas and Wireless Propagation Letters,* DOI. 10.1109/LAWP.2014.2373432.

[112] L. Poli, P. Rocca, L. Manica, A. Massa, "Time Modulated Planar Arrays—Analysis and Optimisation of the Sideband Radiations," *IET Microwave and Antennas Propagation*, vol. 4, no. 9, pp. 1165–1171, 2010.

[113] E. Aksoy, E. Afacan, "Generalized Representation of Sideband Radiation Power Calculation in Arbitrarily Distributed Time-Modulated Planar And Linear Arrays," *Proceedings of Progr. Electromagnetics Research Symp.*, Suzhou, China, Pp. 368–371, 2011.

[114] E.T. Bekele, L. Poli, P. Rocca, M. D'Urso, A. Massa. "Pulse-Shaping Strategy for Time Modulated Arrays-Analysis and Design", *IEEE Transactions on Antennas and Propagation*, vol. 61, no. 7, pp. 3525–3537, 2013.

[115] D. Masotti, P. Francia, A. Costanzo, V. Rizzoli, "Rigorous Electromagnetic/Circuit-Level Analysis of Time-Modulated Linear Arrays", *IEEE Transactions on Antennas and Propagation*, vol. 61, no. 11, pp. 5465- 5474 , 2013.

[116] William C. Barott, Braham Himed "Time-Modulated Array Pattern for Sidelobe Blanking in Spectrometry and Radar", *IEEE Antennas and Wireless Propagation Letters*, vol. 13, pp. 1015-1018, 2014.

[117] J. Euziere, R. Guinvarc'h, B. Uguen, R. Gillard, "Optimization of Sparse Time-Modulated Array by Genetic Algorithm for Radar Applications," *IEEE Antennas and Wireless Propagation Letters*, vol. 13, pp. 161–164, 2014.

[118] Ertugrul Aksoy, Erkan Afaca, "An Inequality for the Calculation of Relative Maximum Sideband Level in Time-Modulated Linear and Planar Arrays", *IEEE Transactions on Antennas and Propagation*, vol. 62, no. 6, pp. 3392-3397, 2014.

[119] Lorenzo Poli, Paolo Rocca, Giacomo Oliveri, Andrea Massa, "Failure Correction in Time-Modulated Linear Arrays", *IET Radar, Sonar and Navigation*, vol. 8, no.3, pp. 195-201, 2014.

[120] Chong He, Xianling Liang, Bin Zhou, Junping Geng, Ronghong Jin,"Space-Division Multiple Access Based on Time-Modulated Array", *IEEE Antennas And Wireless Propagation Letters*, vol.14, pp. 610-613, 2015.

[121] Paolo Rocca, Quanjiang Zhu, Ephrem T. Bekele, Shiwen Yang, Andrea Massa,"4-D Arrays as Enabling Technology for Cognitive Radio Systems", *IEEE Transactions on Antennas and Propagation*, vol. 62, no.3, pp. 1102-1116 , 2014.

[122] Kerim Guney, Suad Basbug, "Null Synthesis of Time-Modulated Circular Antenna Arrays Using an Improved Differential Evolution Algorithm", *IEEE Antennas And Wireless Propagation Letters*, vol.12, pp. 817-820, 2013.

[123] G. Bogdan, P. R. Bajurko, Y. Yashchyshyn, "Null-Steering in Two-Element Time Modulated Linear Antenna Array Through Pulse-Delay Approach," *Proceedings of 20th International Conference of Microwave Radar Wireless Commun. (MIKON'14)*, pp. 15–18, 2014.

[124] Chong He, Xianling Liang, Zhaojin Li, Junping Geng, Ronghong Jin, "Direction Finding by Time-Modulated Array with Harmonic Characteristic Analysis", *IEEE Antennas And Wireless Propagation Letters*, vol.14, pp. 642-645, 2015.

[125] Q. Zhu, S. Yang, R. Yao, Z. Nie, "Direction Modulation Based on 4D Antenna Arrays", *IEEE Transactions on Antennas and Propagation*, vol. 62, no.2, pp. 621–628, 2014.

[126] Fan, Z. G., L. X. Ran, K. S Chen, "Novel Printed Dipole Antenna with Reflecting Structure of V-Shaped Ground Plane," *Journal Of Zhejiang University (Engineering Science)*, vol. 39, no. 9, pp. 1292–1295, 2005.